Materials Research, Vol. 12, No. 1, 1-39, 2009

Review Article

Nanocomposites: Synthesis, Structure, Properties and New Application Opportunities

Pedro Henrique Cury Camargo, Kestur Gundappa Satyanarayana, Fernando Wypych*

Departamento de Química, Centro Politécnico, Universidade Federal do Paraná, Jardim das Américas, 81531-990 Curitiba - PR, Brazil

Received: November 24, 2008; Revised: February 10, 2009

Nanocomposites, a high performance material exhibit unusual property combinations and unique design possibilities. With an estimated annual growth rate of about 25% and fastest demand to be in engineering plastics and elastomers, their potential is so striking that they are useful in several areas ranging from packaging to biomedical applications. In this unified overview the three types of matrix nanocomposites are presented underlining the need for these materials, their processing methods and some recent results on structure, properties and potential applications, perspectives including need for such materials in future space mission and other interesting applications together with market and safety aspects. Possible uses of natural materials such as clay based minerals, chrysotile and lignocellulosic fibers are highlighted. Being environmentally friendly, applications of nanocomposites offer new technology and business opportunities for several sectors of the aerospace, automotive, electronics and biotechnology industries.

Keywords: *composites, layered compounds, polymers, metals, ceramics*

1. Introduction

Nanocomposites are composites in which at least one of the phases shows dimensions in the nanometre range (1 nm = 10^{-9} m)[1]. Nanocomposite materials have emerged as suitable alternatives to overcome limitations of microcomposites and monolithics, while posing preparation challenges related to the control of elemental composition and stoichiometry in the nanocluster phase. They are reported to be the materials of 21st century in the view of possessing design uniqueness and property combinations that are not found in conventional composites. The general understanding of these properties is yet to be reached[2], even though the first inference on them was reported as early as 1992[3].

The number of published papers containing words such as nanoscience, nanotechnology, nanomaterials, etc., doubled in 1.6 years[4] in the late 1990s. Also, a literature survey made by the authors reveals that about 13.420 papers (of which 4028 contain the keywords nanocomposite and polymer in Web of Science-ISI: updated on 10 February 2009) have been published on nanocomposites in the last two decade (1988-2008). Similarly, patents with complete document on nanocomposites account for about 4663 during the same period as per Scirus (www.scirus.com). Additionally, specific conferences and special issues of some journals have been devoted exclusively to the emerging science and technology of nanomaterials.

It has been reported that changes in particle properties can be observed when the particle size is less than a particular level, called 'the critical size' (Table 1)[5]. Additionally, as dimensions reach the nanometre level, interactions at phase interfaces become largely improved, and this is important to enhance materials properties. In this context, the surface area/volume ratio of reinforcement materials employed in the preparation of nanocomposites is crucial to the understanding of their structure–property relationships. Further, discovery of carbon nanotubes (CNTs) in 1991[6] and their subsequent use to fabricate composites exhibiting some of the unique CNT related mechanical, thermal and electrical properties[7-9] added a new and interesting dimension to this area. The possibility of spinning CNTs into composite products and textiles[10] made further inroads for the processing and applications of CNT-containing nanomaterials. Nowadays, nanocomposites offer new technology and business opportunities for all sectors of industry, in addition to being environmentally friendly[11].

As in the case of microcomposites, nanocomposite materials can be classified, according to their matrix materials, in three different categories as shown in Table 2.

Ceramic Matrix Nanocomposites (CMNC);
Metal Matrix Nanocomposites (MMNC) and
Polymer Matrix Nanocomposites (PMNC).

Nanocomposite systems, including those reinforced with CNTs, have been extensively studied since the 1990s and, accordingly, there has been a steady and continuous increase in the number of publications on the subject, including reviews from time to time[2,12-35]. In spite of this growth, the majority of the reviews describe the current status of only one type of nanocomposite. Thus, there are only two reviews on CMNC[16,32] and three on CNT-reinforced nanocomposites[17,20,27] and a quite large number on PMNC[16,18,19,21,28-35]. In the case of PMNC, reviews deal with processing aspects, including those on layered silicates[18,26], conducting and biodegradable polymer-based systems[19,34,35], fibre reinforced[17,20] and structure/morphology/property aspects[16,35], as well as with applications and perspectives, including key opportunities and challenges in the development of structural and functional fibre nanocomposites[18,26,29].

Conducting polymer-based composites are novel materials with less than a decade of history. It is believed[19] that the total control of the whole conducting polymer-based composite system and the optimisation of their physical properties (such as electrical conductivity and colloidal stability) are yet to be achieved, while both their commercial availability in the near future and a big leap forward for materials science are expected with their appropriate utilization. In the case of biodegradable polymer-based nanocomposites, recent developments in preparation, characterization and properties, including crystallization behaviour and melt rheology, of both the matrix and the layered (montmorillonite) nanocomposites have been discussed[34,35]. Similarly, an emphasis on toughness and interfacial bonding between CNTs and polymer matrices is critically discussed[27] to underline the stress transfer

*e-mail: kgs_satya@yahoo.co.in

Table 1. Feature sizes for significant changes in properties reported in nanocomposite systems [reproduced from reference 5 with the kind permission of the author and the Japan Society of Powder and Powder Metallurgy].

Properties	Feature size (nm) at which changes might be expected
Catalytic activity	<5
Making hard magnetic materials soft	<20
Producing refractive index changes	<50
Producing super paramagnetism and others electromagnetic phenomena	<100
Producing strengthening and toughening	<100
Modifying hardness and plasticity	<100

Table 2. Different types of nanocomposites.

Class	Examples
Metal	Fe-Cr/Al_2O_3, Ni/Al_2O_3, Co/Cr, Fe/MgO, Al/CNT, Mg/CNT
Ceramic	Al_2O_3/SiO_2, SiO_2/Ni, Al_2O_3/TiO_2, Al_2O_3/SiC, Al_2O_3/CNT
Polymer	Thermoplastic/thermoset polymer/layered silicates, polyester/TiO_2, polymer/CNT, polymer/layered double hydroxides.

from the matrix and the potential of these composites for possible macro scale CNT-polymer production. Here, problems encountered so far are considered, and hints given regarding a critical volume fraction of CNTs to get appropriate strengthening (as observed in microcomposites); possible failure mechanisms in such composites are also presented. Finally, to the best of our knowledge, and in view of the very limited work on metal-based nanocomposites including the ones with CNT reinforcements, no review is available to-date on this system.

Considering these facts and also the absence of a more general review comprising the three different kinds of nanocomposites (metal-, ceramic- and polymer-based), this paper gives an overview of them, including those with incorporation of CNTs. However, while doing so only a few relevant publications[2,4,7-9,11,14-308] are considered here. The main features, current status and recent developments in the area are provided, focussing on the preparation methods, structure, properties and applications of these systems to avoid repetition. Also, the potential uses of nanocomposites and the opportunities they provide, along with perspectives for the future and market and safety aspects are also presented. Nanocomposite coating is not covered, in order to keep the focus of the review.

1.1. Potentials and opportunities in nanocomposites

Before going into details regarding processing, structure, properties and applications of the three types of nanocomposites, let us look at the potentials of these systems and the general opportunities they provide. Ceramics have good wear resistance and high thermal and chemical stability. However, they are brittle. In this context, the low toughness of ceramics has remained a stumbling block for their wider use in industry. In order to overcome this limitation, ceramic-matrix nanocomposites have been receiving attention, primarily due to the significant enhancement on mechanical properties which can be achieved. For example, the incorporation of energy-dissipating components such as whiskers, fibres, platelets or particles in the ceramic matrix may lead to increased fracture toughness[309-311]. The reinforcements deflect the crack and/or provide bridging elements, hindering further opening of the crack. In addition, the incorporated phase undergoes phase transition in conjunction with the volume expansion initiated by the stress field of a propagating crack, contributing for the toughening and strengthening processes, even in nanocomposites[36].

The potential of ceramic matrix nanocomposites (CMNC), mainly the Al_2O_3/SiC system, was revealed by the pioneering work of Niihara[37,38]. Most studies reported so far have confirmed the noticeable strengthening of the Al_2O_3 matrix after addition of a low (i.e. ~10%) volume fraction of SiC particles of suitable size and hot pressing of the resulting mixture. Some studies have explained this toughening mechanism based on the crack-bridging role of the nanosized reinforcements[39]. Consequently, the incorporation of high strength nanofibres into ceramic matrices has allowed the preparation of advanced nanocomposites with high toughness and superior failure characteristics compared to the sudden failures of ceramic materials[40].

Metal matrix nanocomposites (MMNC) refer to materials consisting of a ductile metal or alloy matrix in which some nanosized reinforcement material is implanted. These materials combine metal and ceramic features, i.e., ductility and toughness with high strength and modulus. Thus, metal matrix nanocomposites are suitable for production of materials with high strength in shear/compression processes and high service temperature capabilities. They show an extraordinary potential for application in many areas, such as aerospace and automotive industries and development of structural materials[41]. Both MMNC and CMNC with CNT nanocomposites hold promise, but also pose challenges for real success.

Polymer materials are widely used in industry due to their ease of production, lightweight and often ductile nature. However, they have some disadvantages, such as low modulus and strength compared to metals and ceramics. In this context, a very effective approach to improve mechanical properties is to add fibres, whiskers, platelets or particles as reinforcements to the polymer matrix. For example, polymers have been filled with several inorganic compounds, either synthetic or natural, in order to increase heat and impact resistance, flame retardancy and mechanical strength, and to decrease electrical conductivity and gas permeability with respect to oxygen and water vapour[25]. Furthermore, metal and ceramic reinforcements offer striking routes to certain unique magnetic, electronic, optical or catalytic properties coming from inorganic nanoparticles, which add to other polymer properties such as processibility and film forming capability[42]. Using this approach, polymers can be improved while keeping their lightweight and ductile nature[31,43-47]. Another important aspect is that nanoscale reinforcements have an exceptional potential to generate new phenomena, which leads to special properties in these materials as will be seen later. It may be pointed out that the reinforcing efficiency of these composites, even at low volume fractions, is comparable to 40-50% for fibres in microcomposites[34].

Addition of reinforcements to a wide variety of polymer resins produces a dramatic improvement in their biodegradability. This underlines a good example of polymer matrix nanocomposites [PMNC] as promising systems[24] for ecofriendly applications. Besides, future space mission concepts involve large ultra lightweight spacecrafts termed "Gossamer"[48]. The materials required for such spacecrafts should possess and maintain a specific combination of properties for over a long period (10-30 years) in relatively harsh environments such as 173 to 373 K for satellites and cycling temperatures of 1273 K for re-entry vehicles, exposure to atomic O_2 and solar radiation. Some of the Gossamer spacecraft devices are movable mechanical parts such as gears and gyroscopes, and others include solar arrays/sails, antennae and drives, sunshields, rovers, radars, solar concentrators, and reflector arrays. It is reported[48] that these parts will have to be fabricated from flexible, appropriate materials, which can be folded or packaged into small volumes, similarly to those available in conventional launch vehicles, and should possess many of the common mission concepts. This is needed since the structure consisting of ultra lightweight parts would

be deployed mechanically or by inflation into a large ultra-lightweight functioning spacecraft once it achieves the required orbit. It is imperative that the above mentioned characteristics should be available in one single material. Metal oxide-incorporated polymer nanocomposites seem to meet these requirements. It is expected that such spacecrafts offer a significant cost advantage compared to on-orbit construction, and the large size can enable some unique missions. Similarly, rocket propellants are prepared from a polymer-Al/Al_2O_3 nanocomposite to improve ballistic performance[306]. In addition, recent information on nanomaterials, nanoindustries and a host of possible A to Z applications of polymer nanocomposites have been reported[312].

On the other hand, even after a decade of research[27], CNTs have not fully realized their potentials as nanoscopic reinforcements[313-334] in polymer matrices. Thus great challenges and opportunities are still expected for the system. These are based on the following:

a) CNTs with small number of defects per unit length possess[27] 500 times more surface area per gram on the basis of equivalent volume fraction of a typical carbon fiber, high aspect ratio (~1000), very high tensile properties and electrical and thermal conductivities (more details are given in the next section).

b) Research on CNT-related areas has been most active, with publications doubling within six months[335]. Even the patenting activity in this area has been impressive, with about 3,000 applications filed from 2001 to June 2006 as per the literature survey.

c) Because of their hollow nature, CNTs can be opened and filled with a variety of materials including biological molecules[335], generating technological opportunities. Added to this, the challenges in obtaining homogeneous dispersions and strong interfacial interactions, which can be better done by surface grafting/functionalizations, make the use of CNTs in composites more intriguing[49].

d) Various applications of CNTs in composites have been reported extensively [30,33,313-334].

e) The possibility of spinning polymers to obtain textiles[10] certainly constitutes a great promise for their extended use in a variety of applications, particularly in the electronic and thermal management sectors.

f) Nanoreinforcements with biodegradable polymers have a high potential for the design of environmentally friendly 'green materials' for future applications.

On the whole, opportunities and rewards appear to be great with nanocomposites and hence there is a tremendous worldwide interest in these materials.

2. Processing of Nanocomposites

2.1. Raw materials

As with microcomposites, CMNC matrix materials include Al_2O_3, SiC, SiN, etc., while metal matrices employed in MMNC are mainly Al, Mg, Pb, Sn, W and Fe, and a whole range of polymers, e.g. vinyl polymers, condensation polymers, polyolefins, speciality polymers (including a variety of biodegradable molecules) are used in PMNC. In general, it is the reinforcement that is in the nanorange size in these materials. Both synthetic and natural crystalline reinforcements have been used, such as Fe and other metal powders, clays, silica, TiO_2 and other metal oxides, although clays and layered silicates are the most common[176]. This is so due to their availability with very low particle sizes and well-known intercalation chemistry[18,50,51], in addition to generating improved properties even when they are used at very low concentrations[252]. Most of these reinforcements are prepared by known techniques: chemical, mechanical (e.g. ball milling), vapour deposition, etc.; details of these may be found in many of the references given in the following sections.

Similarly, CNTs are prepared mostly by chemical/vapour deposition methods and details are available elsewhere[319-327]. A bibliometric analysis of CNTs made in 2000[335] revealed that about 49% of the patents filed between 1992-1999 were related to the processing of CNTs and about 14% to their structure, properties and models. CNTs consist of graphene cylinders and are available in two varieties, as single walled (SWCNT) and multi walled (MWCNT), with about 70% yield in the case of SWCNT[317]. While SWCNTs are single graphene cylinders, MWCNTs consist of two or more concentric cylindrical sheets of graphene around a central hollow core. Both types exhibit physical characteristics of solids, either metallic or semiconducting in nature, with microcrystallinity and very high aspect ratios of 10^3.

Surface modifications of reinforcements are carried out to give homogeneous distribution with less agglomeration, and to improve interfacial bonding between the matrix and the nanosized reinforcements. Details on these can be found in the references given for each type of nanocomposites in later Sections. In the case of CNTs, use of surfactants, oxidation or chemical functionalization of surfaces are some of the techniques employed[27]. Chemical methods may be more effective, particularly for polymer and ceramic matrices. Physical blending and in situ polymerization are used for improving dispersion in the case of CNT-reinforced polymer composites, while alignment of CNTs could be achieved by techniques such as ex-situ techniques (filtration, template and plasma-enhanced chemical vapour deposition, force field-inducements, etc.)[33].

Table 3a. Processing methods for ceramic nanocomposites.

Method	System	Procedure	Ref.
Powder Process	Al_2O_3/SiC	i) Selection of raw materials [mostly powders - small average size, uniformity and high purity]; ii) Mixing by wet ball milling or attrition milling techniques in organic or aqueous media; iii) Drying by heating, using lamps and/or ovens, or by freeze-drying; iv) consolidation of the solid material by either hot pressing or gas pressure sintering or slip casting or injection moulding and pressure filtration.	38, 53
Polymer Precursor Process	Al_2O_3/SiC, SiN/SiC	Mixing a Si-polymeric precursor with the matrix material → Pyrolysis of the mixture using a microwave oven, generating the reinforcing particles.	16, 54-57
Sol-Gel Process	SiO_2/Ni, ZnO/Co, TiO_2/Fe_2O_3, La_2O_3/TiO_2, Al_2O_3/SiC, TiO_2/Al_2O_3, Al_2O_3/SiO_2, Al_2O_3/SiO_2/ ZrO_2, TiO_2/Fe_2 TiO_5, $NdAlO_3$/Al_2O_3	Hydrolysis and polycondensation reactions of an (in)organic molecular precursor dissolved in organic media. Reactions lead to the formation of three-dimensional polymers containing metal-oxygen bonds (sol or gel) → drying to get a solid material and further consolidation by thermal treatment.	58-73

2.2. Processing methods

Despite their nano dimensions, most of the processing techniques of the three types of nanocomposites remain almost the same as in microcomposites. This is also true even for CNT-reinforced composites. Details on these techniques are given below.

2.2.1. Ceramic Matrix Nanocomposites (CMNC)

Many methods have been described for the preparation of ceramic matrix nanocomposites [20,38,53-112]. The most common methodologies, as used for microcomposites, are Conventional powder method; Polymer precursor route; Spray pyrolysis; Vapour techniques (CVD and PVD) and Chemical methods, which include the sol-gel process, colloidal and precipitation approaches and the template synthesis. While Table 3a lists systems prepared by some of these methods, Table 3b shows their advantages and limitations. Scheme 1a depicts the conventional powder method and Scheme 1b illustrates the polymer precursor route used in the synthesis of an Al_2O_3/SiC nanocomposite.

A large variety of parameters affecting the sol-gel process, such as type of solvent, timing, pH, precursor, water/metal ratio, etc., allow a versatile control of structural and chemical properties of the final oxide materials[61]. Regarding the processing of carbon nanotubes (CNT)-reinforced ceramic nanocomposites, many approaches have been described[20,74-112]. Several of these are listed in Table 3c.

Table 3b. Advantages and limitations of ceramic nanocomposite processing methods.

Method	Advantages	Limitations	Ref.
Powder Process	Simple	Low formation rate, high temperature, agglomeration, poor phase dispersion, formation of secondary phases in the product.	38, 53
Polymer Precursor Process	Possibility of preparing finer particles; better reinforcement dispersion	Inhomogeneous and phase-segregated materials due to agglomeration and dispersion of ultra-fine particles	16, 54-57
Sol-Gel Process	Simple, low processing temperature; versatile; high chemical homogeneity; rigorous stoichiometry control; high purity products; formation of three dimensional polymers containing metal-oxygen bonds. Single or multiple matrices. Applicable specifically for the production of composite materials with liquids or with viscous fluids that are derived from alkoxides.	Greater shrinkage and lower amount of voids, compared to the mixing method.	58-73

Table 3c. Processing methods for ceramic-CNT nanocomposites.

Process	System	Procedure	Ref.
Hot pressing	SiO_2/CNT, SiC/CNT	Dispersion of CNTs and SiO_2 glass powders into ethanol, stirring and ultrasonic treatment, drying and hot pressure sintering in pure N_2 atmosphere. Mixing of nanoparticles of SiC and carbon nanotubes	20, 74
CVD or Spray pyrolysis	Al_2O_3/CNT	Preparation of the alumina matrix by anodizing growth of CNTs into its porous walls. CNTs grow into hexagonal array of straight pores extending from the substrate to the matrix surface.	75, 77
Catalytic decomposition	Al_2O_3/CNT	Use of acetylene over Al_2O_3 powder impregnated with iron catalysts.	76
Solvothermal process	Fe_3O_4/CNT	Dispersion of CNTs in EDA (ethylenediamine) using ultrasonic treatment; addition of an iron(III)-urea complex; heating in a Teflon-lined autoclave maintained at 200 °C for 50 hours, followed by cooling to room temperature.	78

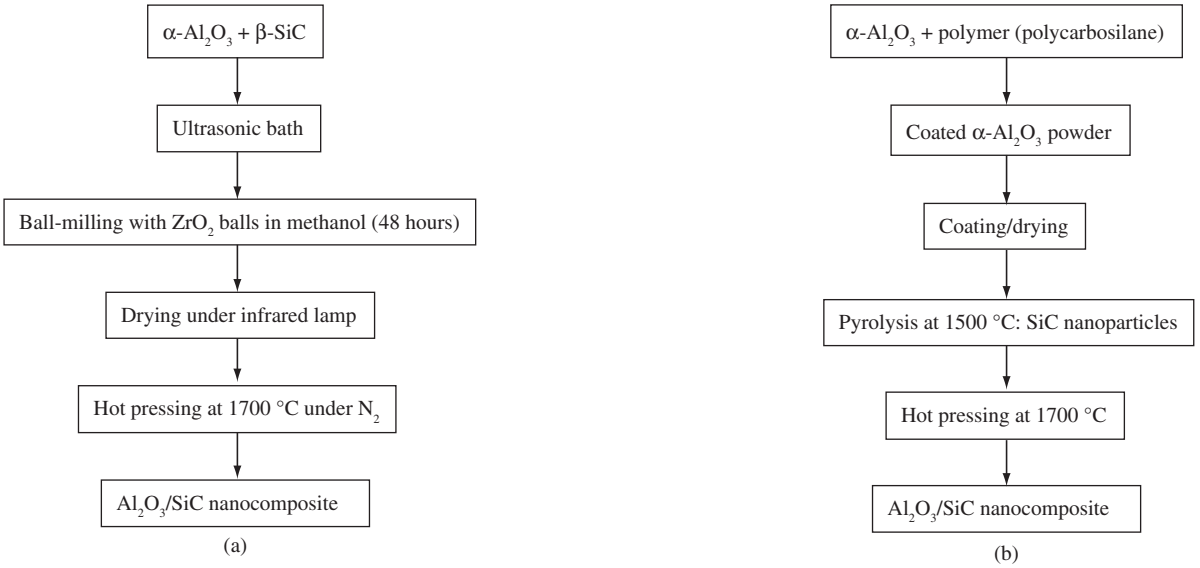

Scheme 1. a) Conventional Powder Processing, and b) Polymer Precursor route.

2.2.2. Metal Matrix Nanocomposites (MMNC)

The most common techniques for the processing of metal matrix nanocomposites are[113-150] Spray pyrolysis; Liquid metal infiltration; Rapid solidification; Vapour techniques (PVD, CVD); Electrodeposition and Chemical methods, which include colloidal and sol-gel processes. Table 4a lists various systems prepared by these methods and Table 4b shows their advantages and limitations. Only two reports are found, for example, on Fe-based nanocomposites prepared by solidification techniques. The first one, by Branagan[121], is called "devitrified nanocomposite steel". This was obtained by quenching the metallic glass obtained from a Fe-based alloy, followed by devitrifying the glass precursor through heat treatment above its crystallization temperature. This resulted in a material showing a crystalline multi-phase microstructure. The formation of nanophases was explained by the high nucleation frequency within the limited time for growth of grains before impingement. In order to explain the very high hardness of these Fe-based nanocomposites, Branagan and Tang studied[122] novel nanostructures obtained in bulk Fe alloys by designing alloy compositions with different amounts of W and C to get maximum solubility. Difficulties have been encountered in preparing composites with very fine particles due to their induced agglomeration and non-homogeneous distribution. Use of ultrasound helped to improve the wettability between the matrix and the particles.

A number of CNT-reinforced MMCs have been synthesised by different techniques[87,135-141] since the first report in 2002[137]. Some of these techniques are listed in Table 4c.

2.2.3. Polymer Matrix Nanocomposites (PMNC)

Many methods have been described for the preparation of polymer nanocomposites, including layered materials and those containing CNTs [151-308]. The most important ones are i) Intercalation of the polymer or pre-polymer from solution; ii) In-situ intercalative polymerization; iii) Melt intercalation (Figure 1); iv) Direct mixture of polymer and particulates; v) Template synthesis; vi) In-situ polymerization; and vii) Sol-gel process. Publications dealing with various methods for the incorporation of nanodispersoids into conducting polymers are also available[19,201,234]; the most prominent one is probably the incorporation of inorganic building blocks in organic polymers.

Table 5a shows the procedures adopted in some of these processes, while their advantages and limitations are listed in Table 5b.

Intercalative processes employed for the preparation of polymer-based nanocomposites, including those containing layered silicates, are shown in Scheme 2. It may be noted that, in this method, a range of nanocomposites with structures from intercalated to exfoliated can be obtained, depending on the degree of penetration of the polymer chains into the silicate galleries. As a result, this procedure has become standard for the preparation of polymer-layered silicate combinations.

The preparation of CNT-reinforced polymer nanocomposites is generally performed by different methods, including direct mixing, solution mixing, melt-mixing and in-situ polymerisation. These, as applicable to various systems[187,202], are listed in Table 5c.

Table 4a. Processing methods for metal-based nanocomposite systems.

Process	System	Procedure	Ref.
Spray Pyrolysis	Fe/MgO, W/Cu	i) Dissolution of the inorganic precursors (starting materials) in a suitable solvent to get the liquid source; ii) Generation of a mist from this liquid source using an ultrasonic atomizer; iii) Use of a carrier gas to carry the mist into a pre-heated chamber. iv) Vaporisation of the droplets in the chamber and trapping with a filter, promoting their decomposition to give the respective oxide materials; v) Selective reduction of the metal oxides to produce the respective metallic materials.	11
Liquid Infiltration	Pb/Cu, Pb/Fe, W/Cu/ Nb/Cu, Nb/Fe, Al-C_{60}	i) Mixing of fine reinforcement particles with the matrix metal material; ii) Thermal treatment, whereby the matrix melts and surrounds the reinforcements by liquid infiltration; iii) Further thermal treatment below the matrix melting point, to promote consolidation and eliminate internal porosity.	11, 114-117
Rapid Solidification Process(RSP)	Al/Pb, Al/X/Zr (X = Si, Cu, Ni), Fe alloy	i) Melting of the metal components together; ii) Keeping the melt above the critical line of the miscibility gap between the different components to ensure homogeneity; iii) Rapid solidification of the melt by any process, such as melt spinning.	118-122
RSP with ultrasonics	Al/SiC	Use of ultrasonics for mixing and for improving wettability between the matrix and the reinforcements.	123
High Energy Ball Milling	Cu-Al_2O_3	Milling the powders together till the required nanosized alloy is obtained → Nanocomposite.	124
CVD/PVD	Al/Mo, Cu/W, Cu/Pb	PVD: i) Sputtering/evaporation of different components to produce a vapour-phase; ii) Supersaturation of the vapour phase in an inert atmosphere to promote the condensation of metal nanoparticles; iii) Consolidation of the nanocomposite by thermal treatment under inert atmosphere. CVD: Use of chemical reactions to get vapours of materials, followed by consolidation.	125-129
Chemical Processes (Sol-gel, Colloidal)	Ag/Au, Fe/SiO_2, Au/Fe/Au	Colloidal Method: i) Chemical reduction of inorganic salts in solution to synthesize metal particles; ii) Consolidation of the dry material; iii) Drying and thermal treatment of the resulting solid in reducing atmosphere, such as H_2, in order to promote selective oxide reduction and generate the metal component. Sol-gel process: i) Preparation of two micelle solutions using mesoporous silica containing 0.1 M $HAuCl_4$ (aq.) and 0.6 M $NaBH_4$ (aq.); ii) Mixing under ultraviolet light till complete reduction of the gold. For Fe/Au-containing nanocomposites: i) Synthesis of the iron shell; ii) Preparation of the second shell and drying of the powders after second gold coating; iii) Pressing of the mixture to get the final material..	130-134

Table 4b. Advantages and limitations of processing methods for metal-based nanocomposites.

Process	Advantages	Limitations	Ref.
Spray Pyrolysis	Effective preparation of ultra fine, spherical and homogeneous powders in multicomponent systems, reproductive size and quality.	High cost associated with producing large quantities of uniform, nanosized particles.	11
Liquid Infiltration	Short contact times between matrix and reinforcements; moulding into different and near net shapes of different stiffness and enhanced wear resistance; rapid solidification; both lab scale and industrial scale production.	Use of high temperature; segregation of reinforcements; formation of undesired products during processing.	11, 114-117
Rapid Solidification Process (RSP)	Simple; effective.	Only metal-metal nanocomposites; induced agglomeration and non-homogeneous distribution of fine particles.	118-122
RSP with ultrasonics	Good distribution without agglomeration, even with fine particles.		123
High Energy Ball Milling	Homogeneous mixing and uniform distribution.		124
CVD/PVD	Capability to produce highly dense and pure materials; uniform thick films; adhesion at high deposition rates; good reproducibility.	Optimization of many parameters; cost; relative complexity.	125-129
Chemical Processes (Sol-Gel, Colloidal)	Simple; low processing temperature; versatile; high chemical homogeneity; rigorous stoichiometry control; high purity products.	Weak bonding, low wear-resistance, high permeability and difficult control of porosity.	130-134

Table 4c. Processes for preparing metal-CNT nanocomposite systems.

Process	System	Procedure	Ref.
Electroless Coating	Co-CNT	i) Use of electroless plating bath containing the activated CNTs, the cobalt precursor, the reducing agent $CoSO_4.7H_2O$, the complexing agent and a buffer. CNT with deposit of Co coating results; ii) Thermal treatment at 873 K, 200 torr, under a 10% H_2/N_2 flow gas.	135
Electroless Coating	Sn / CNTs, $SnSb_{0.5}$/ CNT and Sn_2Sb/ CNT	Reduction of $SnCl_2$ and $SbCl_3$ precursors by KBH_4 in the presence of CNTs.	136, 137
Hot Pressing	Al/CNT	Mixing of powders through grinding for 30 minutes and hot pressing at 793 K under a pressure of 25 MPa.	138
Nanoscale Dispersion	Al/CNT	Preparation of the precursor of MWCNT (13 nm dia and 10-50 μm long) with natural rubber and ethyl propylene; mixing with Al powder; rolling into sheets by compression moulding at 353 K; placing of this precursor on an Al (99.85%) plate of 28 μm grain size; heating to 1073 K in N_2 atmosphere for one hour; final cooling.	139
PM/Infiltration	Mg-Al_2O_{3f}-CNT	a) Mechanical mixing of Mg powders with MWCNT (1 vol. %) using alcohol and acid; sinterisation at 550 °C under 25 MPa pressure; b) Infiltration of molten Mg through performs of Al_2O_3 fibers (25 vol. %; 40-100 μm long) covered with MWCNTs under gas pressure.	141

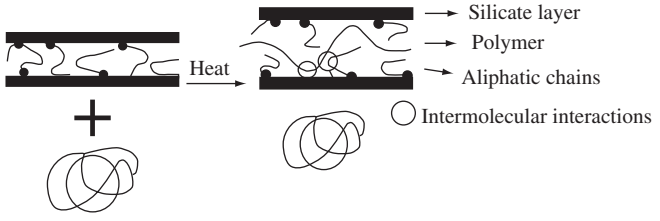

Figure 1. Melt intercalation synthesis of polymer/clay nanocomposites [reproduced from ref. 165 with the kind permission of the authors, the American Chemical Society, USA].

Similarly, different processing techniques, mostly chemical and electrochemical methods, have been employed for the preparation of conducting polymer nanocomposites[19]. Table 6a summarizes these methods, while a relevant categorization of these nanocomposites is presented in Table 6b.

In the case of nanocomposites containing layered reinforcements, depending on the nature of the components (layered silicate, organic cation and polymer matrix), the method of preparation and the strength of interfacial interactions between the polymer matrix and the layered silicate (modified or not), three different types of PLS nanocomposites may be obtained, as illustrated in Figure 2[18].

When the polymer is unable to intercalate between the silicate sheets, a phase-separated composite (Figure 2) is obtained, whose properties stay in the same range as that of traditional microcomposites. On the other hand, in intercalated nanocomposites, the insertion of a polymer matrix into the layered silicate structure occurs in a crystallographically regular fashion, regardless of the clay to polymer ratio. A well ordered multilayer morphology built up with alternating polymeric and inorganic layers is generated. Normally, only a few molecular layers of polymer can be intercalated in these materials.

The in-situ method can be used with mineral/vegetal fibres, with the possibility to attach the polymer to the grafted surface through linking

Table 5a. Processing methods for polymer-based nanocomposite systems.

Process	System	Procedure	Ref.
Intercalation / Prepolymer from Solution	Clay with PCL, PLA, HDPE, PEO, PVA, PVP, PVA, etc.	Employed for layered reinforcing material in which the polymer may intercalate. Mostly for layered silicates, with intercalation of the polymer or pre-polymer from solution. Use of a solvent in which the polymer or pre-polymer is soluble and the silicate layers are swellable.	5, 18, 151-157
In-situ Intercalative Polymerization	Montmorillonate with N6/PCL/ PMMA /PU/Epoxy	Encasing of the layered silicate within the liquid monomer or a monomer solution → formation of polymer between the intercalated sheets. Polymerization by heat or radiation, by diffusion of a suitable initiator or by a catalyst fixed through cation exchange inside the interlayer, before the swelling step.	158-164
Melt Intercalation	Montmorillonate with PS/PEO/PP/ PVP, Clay-PVPH	Annealing of a mixture of the polymer and the layered host above the softening point of the polymer, statically or under shear. Diffusion of polymer chains from the bulk polymer melt into the galleries between the host layers during annealing (Figure 1).	165-169
Template Synthesis	Hectorite with PVPR, HPMC, PAN, PDDA, PANI	In situ formation of the layered structure of the inorganic material in an aqueous solution containing the polymer. The water soluble polymer acts as a template for the formation of layers. Widely used for the synthesis of LDH nanocomposites, but less developed for layered silicates.	170-175
(a) Mixing (b) In situ polymerization	PVA)/Ag; PMMA/Pd Polyester/ TiO_2 PET/$CaCO_3$, Epoxy vinyl ester/ Fe_3O_4 ; Epoxy vinyl ester/γ-Fe_2O_3; Poly (acrylic acid)(PAA)/Ag, PAA/ Ni and PAA/Cu $AgNO_3$, $NiSO_4$ and $CuSO_4$;	(a) Mixing of either polymer or monomer with reinforcing materials; (b1) Dispersion of inorganic particles into a precursor of the polymeric matrix (monomer); (b2) Polymerization of the mixture by addition of an appropriate catalyst; (b3) Processing of this material by conventional moulding technologies. Use of ultrasonics for dispersion in epoxy systems. Exposition of AG systems to 60 Co γ-ray to promote simultaneous polymerization and metal nanoparticle formation.	178-183
Sol-Gel Process	Polyimide/SiO_2; 2-hydroxyethyl acrylate (HEA)/SiO_2, polyimide/ silica. PMMA/ SiO_2, polyethylacrylate/ SiO_2, polycarbonate / SiO_2 and poly (amide-imide)/TiO_2	Embedding of organic molecules and monomers on sol-gel matrices; introduction of organic groups by formation of chemical bonds → In-situ formation of sol-gel matrix within the polymer and/or simultaneous generation of inorganic /organic networks.	24, 184-186

Table 5b. Advantages and limitations of polymer-based nanocomposite processing methods.

Process	Advantages	Limitations	Ref.
Intercalation / Prepolymer from Solution	Synthesis of intercalated nanocomposites based on polymers with low or even no polarity. Preparation of homogeneous dispersions of the filler.	Industrial use of large amounts of solvents.	5, 18, 151-157
In-situ Intercalative Polymerization	Easy procedure, based on the dispersion of the filler in the polymer precursors.	Difficult control of intragallery polymerization. Limited applications.	158-164
Melt Intercalation	Environmentally benign; use of polymers not suited for other processes; compatible with industrial polymer processes.	Limited applications to polyolefins, who represent the majority of used polymers.	165-169
Template Synthesis	Large scale production; easy procedure.	Limited applications; based mainly in water soluble polymers, contaminated by side products.	170-175
Sol-Gel Process	See Table 3b.	See Table 3b.	

Table 5c. Processing methods for polymer-CNT nanocomposite systems.

Process	System	Procedure	Remarks	Ref.
Direct Mixing	Thermoset Resins	Dispersion of CNTs; Cure.		187
Solution Mixing	Thermoplastic Resins (PS/Epoxy)	Dispersion of 0.2-1% CNTs, (100 nm dia, 10 μm long); Removal of solvent or precipitation of polymer; Cure.	Modification of polymer behaviour; synergistic effect; shape memory nanocomposites.	188-193
Melt Mixing	Polymers, N6	Mechanical mixing of CNTs with prepolymer melt followed by extrusion, injection or compression moulding.	Use of 0.2-2.0% MWCNT, twin screw mixer.	49, 194, 195
In-situ Polymerization	Polyaniline-CNT, MMA-CNT, Epoxy-CNT, Poly(ether-ester)	Use of ultrasonics for dispersion in monomer/matrix; Cure.	Preparation of the polymer with CNT, good chemical bonding.	196-202
Others	PP-CNT, PVK-SWCNT, iPP-SWCNT, PANi-SWCNT	Solid-state mechanochemical pulverization; blending + sonication; melt blending; VDP.	0-10 wt. (%) CNTs	203-206

Table 6a. Summary of processing methods for conducting polymer nanocomposites [reproduced from ref. 19 with the permission of the authors and the American Chemical Society, USA]

Polymer of interest (Shell)	Inorganic particle (core)	Significant characterization / Applications
PPy and PAn	SiO_2 (1 μm, 35 nm, 20 nm), SnO_2-Sb(10 nm), Stringy SiO_2 (40-300 nm long)	Stable colloidal form, 'raspberry morphology' and inorganic stable rich surface.
PPy and PAn	CeO_2 (0.52 μm), CuO (1.6 μm), α-Fe_2O_3 (Sph, Polyhedral and spindle shaped), NiO (3.8 μm), SiO_2 (0.46 μm)	Colloidally stable nanocomposite with low dc conductivity and formed without a polymerisation initiator.
PPy and PAn	$BaSO_4$(20 nm), Colloidal gold (7-9 nm), Al_2O_3 membrane	In situ formation of colloidal nanocomposite within the microemulsion or inside the Al_2O_3 membrane.
Ppy, Pan, NVC and PPV	ZrO_2 (20-30 nm), Fe_2O_3 (25-50 nm), SiO_2, n-TiO_2 (~10 nm), Al_2O_3 (35-40 nm), MgO (2-4 μm), CB	Nanocomposites in macroscopic precipitate form or with limited colloidal stability but improved thermal and electrical properties and novel transport properties.
PPy and PAOABSA	MS (15-30 nm), Fe_xO_y (14 nm), Fe_2O_3 (~15-50 nm), γ-Fe_2O_3 (85 nm),	Nanocomposites with significant magnetic susceptibility.
PPy and PAn	BT (~1 μm), $LiMnO_2$, $LiMnO_4$, V_2O_5, β-MnO_2, PMo_{12}, $H_3PMo_{12}O_{40}$, CB, Fe_2O_3 (4 nm, 40 nm)	Nanocomposites with important charge storage and dielectric properties, suitable for cathode applications.
Ppy, Pan, PTh and PEDOT	Pt (~4 nm), PtO_2, Pt, Cu, Pd, SiO_2 (20 nm), & bimetallic couples	Nanocomposites with catalytically important metals; catalytic applications.
PPy and PAn	SiO_2 (20 nm)	Grafted surface nanocomposites - important for immunodiagnostic assays.
PPy	SiO_2, PB, MnO_2, Ta_2O_5, TiO_2	Electrochemically synthesised composite films with improved charge storage properties.
PPy and PAn	WO_3	Nanocomposite films with important ECD application and optical activity.

Table 6b. Categorization of processing methods for conducting polymer nanocomposites [reproduced from reference 19 with the permission of the authors and the American Chemical Society, USA].

Conducting polymer nanocomposites

Inorganic-in-organic | Organic-in-inorganic

Chemical preparation	Electrochemical preparation
Nanocomposites with colloidal stability (SiO_2, SnO_2, $BaSO_4$, etc., as core)	Nanocomposites with charge storage, optical and electrochromic activities (incorporation of MnO_2, SnO_2, CB, PB, WO_3, SiO_2, etc.)
Nanocomposites with improved physical and mechanical properties (Fe_2O_3, ZrO_2, TiO_2, etc., as incorporated materials)	Nanocomposites with catalytic activities (incorporation of catalytically active Pt, Pd, Cu, etc. microparticles and some bimetallic couples like Pd/Cu, etc.)
Nanocomposites with magnetic susceptibility (using Fe_2O_3, γ-Fe_2O_3, etc., magnetic particles)	Nanocomposites with magnetic susceptibility (γ-Fe_2O_3 magnetic macroanion)
Nanocomposites with dielectric, energy storage, piezoresistive and catalytic activities (with BT, POM, PtO_2, TiO_2, Pd, Pt, etc., incorporation)	-
Nanocomposites with grafted surface (NH_2/COOH functional groups on surface and colloidal silica as core)	-

groups (coupling agents), which optimize the interface bonding and, consequently, the mechanical properties[176].

Despite the successful use of these different methods for the preparation of polymer-based nanocomposites, information on various factors is still lacking, such as i) the use of an appropriate method for a specific matrix-reinforcement combination or ii) the maximum amount of reinforcements to give optimum property combinations and lower the cost of the processes, etc. Therefore, it is still necessary

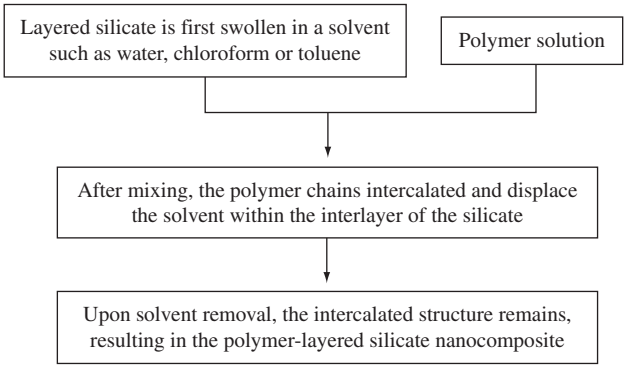

Scheme 2. Intercalation of polymer or pre-polymer from solution.

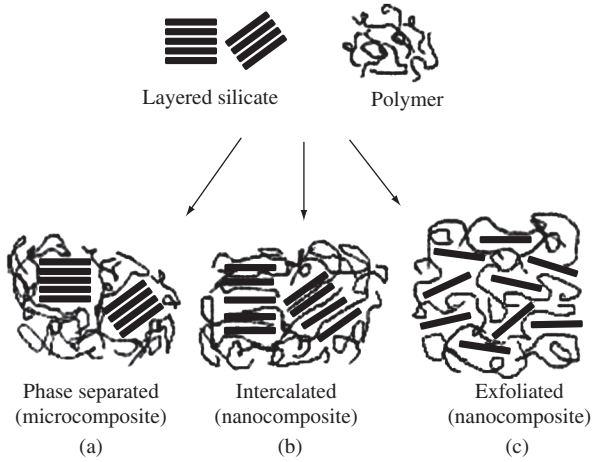

Figure 2. Different types of composites arising from the interaction of layered silicates, polymers: a) Phase-separated microcomposite; b) Intercalated nanocomposite, and c) Exfoliated nanocomposite [reproduced from reference 18 with the kind permission of the authors, Elsevier].

to look into these aspects including use of simulation and modelling techniques.

3. Structure and Properties

The structure of nanocomposites usually consists of the matrix material containing the nanosized reinforcement components in the form of particles, whiskers, fibres, nanotubes, etc.[93]. Different investigators have employed various equipments and techniques for the characterization of nanocomposites, including atomic force microscopy (AFM), scanning tunnelling microscopy (STM), Fourier transformed infrared spectroscopy (FTIR), X ray photoelectron spectroscopy (XPS), nuclear magnetic resonance (NMR), differential scanning calorimetry (DSC), scanning and transmission electron microscopy (SEM/TEM), etc. For example, AFM is a powerful tool to study the surface even down to the nanometre scale, as evident from the work of Veith et al.[303,304]. Simultaneous small angle X ray scattering (SAXS) and X ray diffractometry (XRD) studies have been recently used for quantitative characterization of nanostructures and crystallite structures in some nanocomposites[34,307,308]. In addition, theoretical calculations/simulations have been worked out to predict strength properties, including stress/strain curves[41,52,166,169,207-212,290,291].

Before discussing structure and properties of nanocomposites, including those containing CNTs, a brief description of CNTs will be made here[313-334], because of their unique properties compared to other reinforcements. Briefly, the density of SWCNTs is less than one sixth of that of steel[335] while the density of MWCNT is one half of that of Al[30]. Tensile strengths of SWCNT and MWCNTs are reported[313-316,335] to be in a range much higher than of high strength steel, while Young's modulus values are comparable to those of diamond. They exhibit tremendous resilience, in that they can sustain bending to large angles and restraightening without damage, in which they differ from the plastic deformation of metals and the brittle fracture of carbon fibres. Similarly, theoretical thermal and electrical conductivities are comparable with that of diamond, with an almost negligible thermal expansion coefficient[30]. They also exhibit high thermal stability both in air and in vacuum, compared to the lower values obtained for metal wires in microchips, and high parallel and perpendicular magnetic susceptibilities. Theoretical surface area values of these materials are ca. 3,000 m^2/g [318-321], while the experimentally reported values vary depending on the gas used during the measurements. This information is summarized in Table 7.

Table 7. Properties of Carbon Nanotubes[30,313-318,335].

Properties	SWNT	MWNT	Corresponding values in other known materials
Density (Mgm^{-3})	0.8	1.33-1.40 (Expt.) 1.8 (Theor.)	One sixth of steel and one-half of the density of aluminium.
Surface Area ($m^2.g^{-1}$)	150-1587 (Expt.) 3000 (Theor.)	-	Much higher than known materials.
Elastic modulus (TPa)	1.2	0.4-3.7	Comparable to diamond / 1.4 times of graphite.
Tensile Strength (GPa)	50-500	10-60	Much higher than high-strength steels.
Resilience	Can sustain bending to large angles and restraightening without damage.	-	Different from the plastic deformation of metals and brittle fracture of carbon fibres.
Current carrying capability (Amp/cm^2)	$1 \cdot 10^9$	-	Copper wires burn out at about $1 \cdot 10^6$.
Electrical Conductivity (μΩ)	50-500	-	-
Thermal Conductivity (W/mK)	6000 at 273 K	-	Comparable with that of diamond (3320).
Thermal Stability (K)	3073 in vacuum and 823 in air	-	Metal wires in microchips melt at 873-1273.
Magnetic Susceptibility (emu/kg)	500 (Parallel) 22×10^3 (Perpendicular with plane)	-	-

3.1. Ceramic matrix nanocomposites

Ceramics are usually brittle and easily fractured as consequence of crack propagation. There have been attempts to make ceramics suitable for engineering applications through the incorporation of a ductile metal phase or another ceramic into the matrix. This leads to improved mechanical properties such as hardness and fracture toughness, which occur as a result of the relationship between the different phases, matrix and reinforcements, at the phase boundaries throughout the material. The surface area/volume ratio of the reinforcement materials is of fundamental importance in the understanding of the structure–property relationship in CMNCs. We shall therefore first discuss these improvements in some ceramic-based nanocomposites and relate them with the observed morphologies.

3.1.1. Ceramic matrix-discontinuous reinforcement nanocomposite systems

Table 8 shows examples of ceramic nanocomposites and of the observed improvements in their properties compared to the respective monolithic materials. Table 9 compares the mechanical properties of the Al_2O_3/SiC system and its microcomposite counterpart[39,103-105].

It can be seen from these tables that there is a significant improvement in the strength of the nanocomposite compared with its micro counterpart. The fracture strength, as an example, is noticeably higher because of the higher interfacial interaction between the particles in nanocomposites. Besides, Al_2O_3-5 to 15% SiC systems exhibited[90] superficial grooves of plastic deformation compared to the intergranular fracture observed in monolithic materials. There was no time-dependant wear transition for these composites even at loads of 20-100 N, but pre-transition wear rates of 1-2 x 10^{-8} mm/Nm were observed for both the monolithic and composite materials. The specific wear rate decreased with sliding distance. This enhancement of properties observed in ceramic nanocomposites can also be illustrated by the Si_3N_4/SiC system (Table 10)[106,107].

It can be seen that the nanocomposite presents significant improvements in fracture strength and toughness, high temperature strength and creep resistance compared with its micro counterpart and to the monolithic matrix component. For example, the Si_3N_4/30% SiC system has strength of 1080 MPa up to 1673 K, whereas the strength of the monolithic sample decreases considerably at high temperatures. Furthermore, at 1673 K and tension of 200 MPa, Si_3N_4 fails after 0.4 hours at 0.3% strain, whereas the Si_3N_4/10% SiC nanocomposite does not fail even after 1,000 hours at 1.5% strain.

Coming to morphological studies, Figure 3a-c shows the microstructures of some ceramic matrix nanocomposites of Al_2O_3 and Fe_2O_3 containing a good distribution of Co and Ni nanoparticles or of CNTs. The presence of metal particles leads to the improvement of electrical and thermal conductivities and of magnetic, electronic and optical properties, as well as to the development of novel and unique features due to the nanosized components.

Figure 4 shows SEM and TEM images of the Al_2O_3-SiC nanocomposites, while Figure 5 shows the high resolution TEM photographs. SEM results (Figure 4a) reveal agglomeration of the matrix particles. The grains are ~2 μm in size. TEM analysis (Figure 4b) shows a characteristic intra/intergranular structure. The intragranular SiC particle is approximately 500 nm in size (Figure 4c). In addition, in the upper part of the HRTEM image (Figure 5), a layer of an amorphous phase is clearly visible in a typically (local) edge-on orientation at the interface of two crystalline phases. However, this layer fades away in the lower section of the image, where the two phases seem to merge with an atomic level lattice match pattern[39,103-105].

Figure 6 shows the microstructure of the Si_3N_4/SiC nanocomposite. One can observe that the nanosized SiC particles are intimately dispersed through out the matrix material. In addition, they are embedded within the matrix of large Si_3N_4 grains and at grain boundaries, having inter- and intragranular environments[106,107]. These morphologies help understanding the observed properties.

Another aspect to be noted is the mechanism of growth of the two phases in nanocomposites, as illustrated by AFM photographs[111]. Figure 7 shows AFM images of two metal oxide-based nanocomposite systems, viz., Fe_2O_3/Co_3O_4 and NiO/Co_3O_4. From Figure 7b-c, one can see the production of big particles in the NiO/Co_3O_4 system with increasing supported oxide concentration. TEM images of these oxide systems support different growth mechanisms. In the case of Fe_2O_3/Co_3O_4, small clusters of Fe_2O_3 got wetted on the surface of Co_3O_4, while NiO grew as isolated particles, showing a larger diameter in the NiO/Co_3O_4 system.

Table 8. Examples of ceramic matrix nanocomposites and their properties.

Matrix/Reinforcements	Properties	Reference
Si_3N_4/SiC	Improved strength and toughness	97
$MoSi_2/ZrO_2$	-	98
B_4C/TiB_2,	-	99
Al_2O_3/SiC	-	38
MgO/SiC	-	37
Mullite/SiC	-	100
Al_2O_3/ZrO_2	-	101
Al_2O_3/Mo, Al_2O_3/W	-	102
$Al_2O_3/NdAlO_3$	Improved photoluminescence	73

Table 9. Properties of Al_2O_3/SiC nano- and microcomposites[39, 103].

Properties/Material	Al_2O_3/SiCp composite	Al_2O_3/SiCp nanocomposite
Vickers Hardness [GPa]	-	22
Young's Modulus [GPa]	-	383
Fracture Strength [MPa]	106-283	549-646
Fracture Toughness [$MPam^{1/2}$]	2.4-6.0	4.6–5.5

Table 10. Fracture strength and fracture toughness for Si_3N_4/SiC nano- and microcomposites[106, 107].

Properties/Material	Si_3N_4/SiC composite	Si_3N_4/SiC nanocomposite
Fracture Strength [MPa]	700	1300
Fracture Toughness [$MPam^{1/2}$]	5.3	7

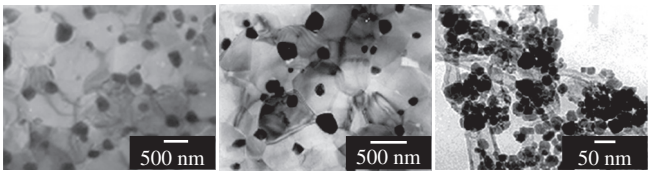

(a) (b) (c)

Figure 3. TEM micrographs of a) Al_2O_3/10 wt. (%) Co b) Al_2O_3/5 vol. % Ni, c) Fe_3O_4/CNTs nanocomposites [reproduced from references 93, 94, 78, respectively, with the kind permission of the authors, Elsevier, the American Chemical Society, USA].

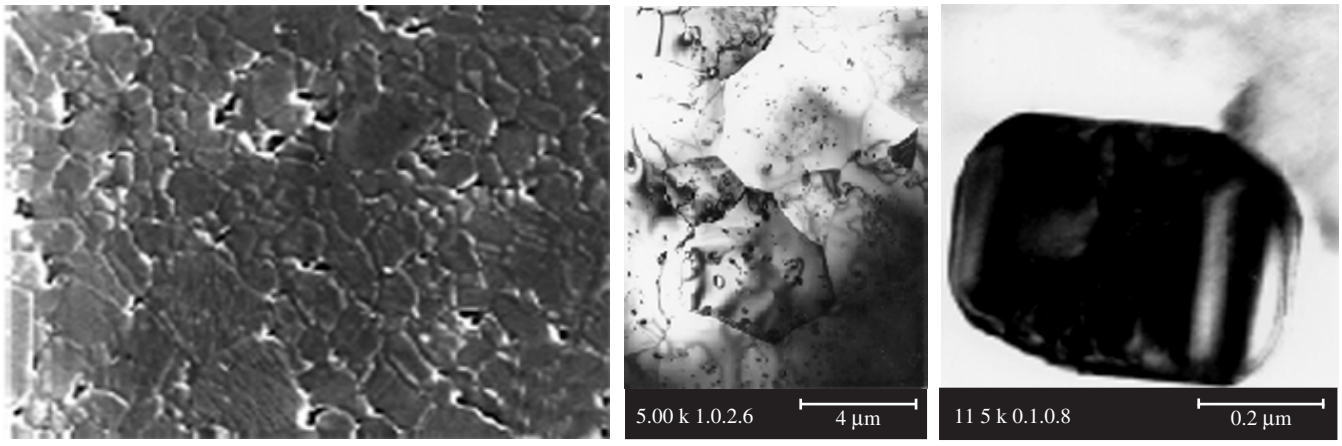

Figure 4. a) SEM, b) TEM images of Al_2O_3/SiC nanocomposites; and c) TEM (high magnification) showing a SiC grain [reproduced from references 103, 104 with the kind permission of the authors, Elsevier].

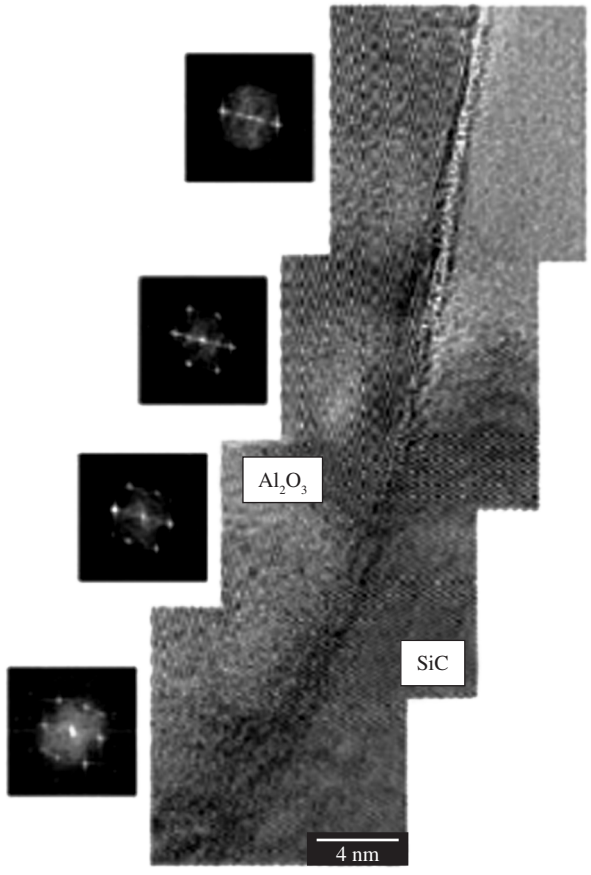

Figure 5. HRTEM image of the interface region between Al_2O_3, SiC particles in the Al_2O_3/SiC nanocomposite [reproduced from reference 39 with the kind permission of the authors, Elsevier].

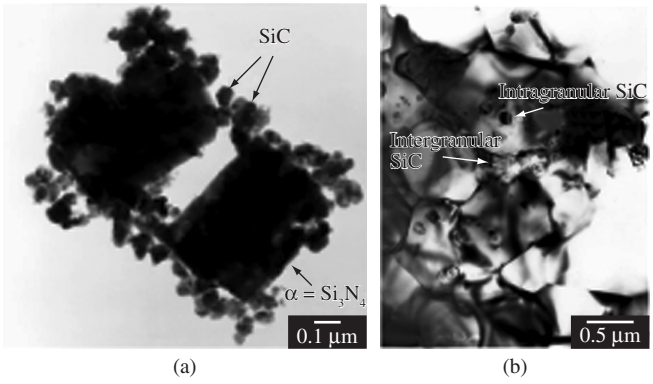

Figure 6. TEM images of Si_3N_4/SiC nanocomposites [reproduced from Reference 107 with the kind permission of the authors, Elsevier, the American Institute of Chemical Engineers @ 1997, AIChME].

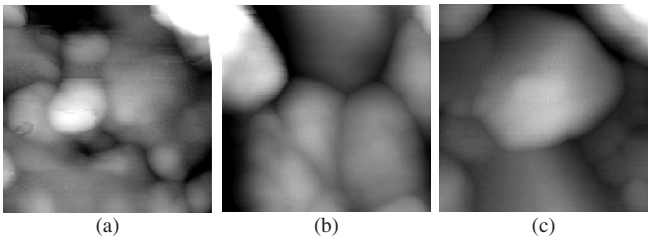

Figure 7. AFM images (0.3 x 0.3 µm^2) of nanocomposite oxides: a) Fe_2O_3/Co_3O_4 (Fe/Co nominal atomic ratio 0.05); b) NiO/Co_3O_4 (Ni/Co nominal atomic ratio 0.05), c) NiO/Co_3O_4 (Ni/Co nominal atomic ratio 0.1) [reproduced from reference 111 with the kind permission of the authors, the American Chemical Society, USA].

3.1.2. Ceramic matrix-CNT Systems

The effect of CNT loading on mechanical properties of the SiO_2/CNT nanocomposites is shown in Figure 8[74]. When the volume content of CNT is lower than 5 vol. %, both bending strength and fracture toughness increase with increasing volume of CNTs. However, loadings higher than 5% cause decrease in these two properties. At 5 vol. %, the increment in strength and fracture toughness, compared with that of monolithic SiO_2, is up to 65 and 100%, respectively. This increase in mechanical properties is due to the large aspect ratio and excellent mechanical properties of CNTs, according to the theory of short fibre-reinforced composites[4]. The decrease in bending strength at high

loading is due to the hindrance caused by CNTs during densification, as they show a higher probability for agglomeration. Consequently, the increased agglomeration leads to the loss of bonding. Also, the higher the loading of CNTs, the higher is their pull out from the matrix during stress transfer[274].

Unusual behaviours such as high contact-damage resistance without a corresponding improvement in toughness have also been reported in Al_2O_3/nanotube composites[91,92]. The microhardness of these systems increases as the CNT content is increased up to 4 wt. (%). This is probably due to grain size effects and the reinforcement role of CNTs, as shown in Figure 9a. However, the effect decreases again above 4 wt. (%), probably due to the difficulty in dispersing CNTs homogeneously in the composite and to the problem of poor cohesion between CNTs and the matrix[107]. This trend is also observed in the wear loss and friction coefficient, as shown in Figure 9b. It can be seen that the wear loss of the 4 wt. (%) composite decreased by nearly 45% as compared to that of the pure matrix. As the CNT content increased above 10 wt. (%), wear losses also notably increased. Friction coefficients decreased gradually as the CNT content increased from 0 to 10 wt. (%), and then dropped sharply at 12.5% CNT content. This trend is attributed to the lubricating properties of the CNTs (graphite)[76].

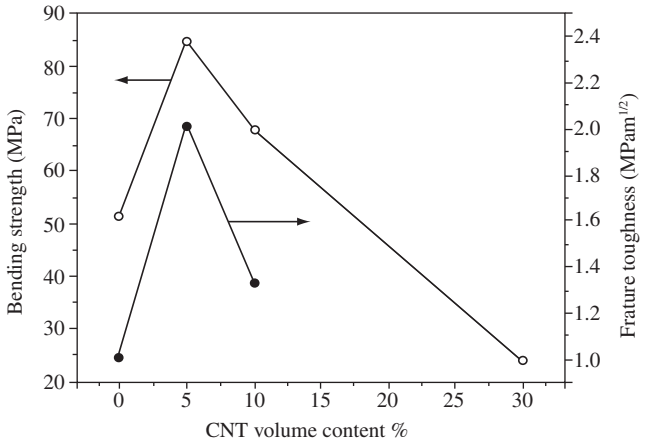

Figure 8. Effect of CNT volume content on the mechanical properties of SiO_2/CNT nanocomposites [reproduced from reference 74 with the kind permission of the authors, Elsevier].

Ma and co-workers prepared SiC/CNTs which showed a 10% improvement in the strength and fracture toughness as compared to the monolithic ceramics[108]. These modest results were attributed to nanotube/matrix debonding and crack deflection[20]. As a consequence, many attempts have been made to develop improved mechanical properties through the incorporation of CNTs in ceramic matrices. However, the observed improvements were not as dramatic as expected. In this context, recently, Zhan et al.[109] successfully applied SWCNTs in the reinforcement of ceramic composites through spark-plasma sintering (SPS), which resulted in a 194% increase in fracture toughness over pure alumina [~9.7 MPam$^{1/2}$ in the 10 vol. % SWCNT/Al_2O_3 nanocomposite]. Also, the electrical properties of ceramic / CNTs nanocomposites have been sharply enhanced, as illustrated in Table 11, due to the outstanding electrical properties of CNTs[110].

Using Griffith's theory and residual stress around nanoparticles in the matrix, Awaji et al.[36] have proposed a mechanism for toughening and strengthening in ceramic-based nanocomposites. They observed that the coefficient of thermal expansion of both matrix and nanoparticles had an effect on residual stresses which was sufficient to cause lattice defects such as dislocations around particles in ceramics. Dislocations were also generated around the particle by the nanoparticles in the matrix.

A 24% increase in fracture toughness (3.4-4.2 MPam$^{1/2}$) over the matrix was observed in nanograined Al_2O_3 composite (average diameter 39 nm) containing 10 vol. % MWCNT[85], which was attributed to the oxidation of CNTs before dispersion. In this case the material was produced in three conditions, viz., mixed, hot pressed (1573 K) and

Table 11. Electrical conductivity of CNT ceramic nanocomposites [reproduced from reference 110 with permission of the authors and the American Institute of Physics, USA].

Materials	Electrical conductivity (S/m)
Pure Al_2O_3	10^{-12}
Al_2O_3/CNT 5.7-vol. %/Carbon Black	15
Al_2O_3/SWCNT 5.7-vol. %	1050
Al_2O_3/SWCNT 10-vol. %	1510
Al_2O_3/SWCNT 15-vol. %	3345
Al_2O_3/Fe 4.3-vol. %/ CNT 8.5-vol. %	40-80
Al_2O_3/Fe 4.3-vol. %/ CNT 10-vol. %	280-400

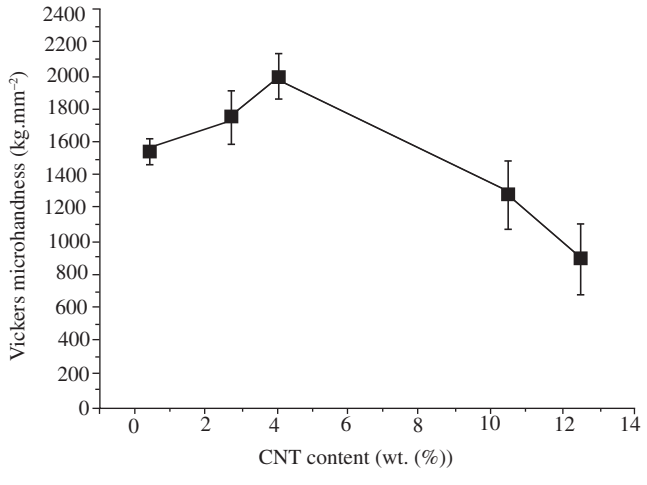

(a)

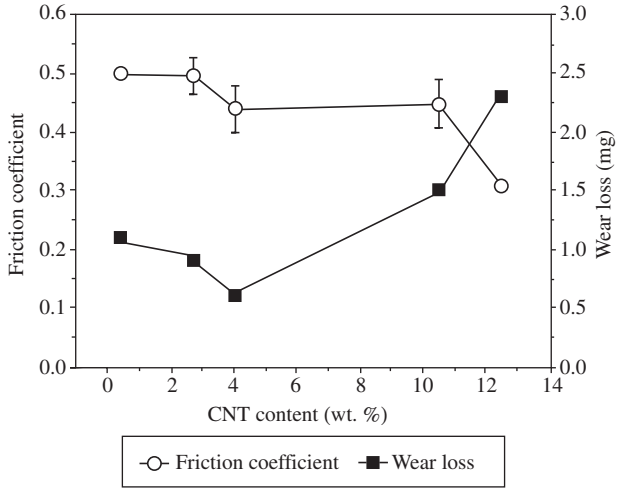

(b)

Figure 9. Variations of a) microhardness, and b) friction coefficient, wear loss as a function of CNT content in Al_2O_3/CNT materials [reproduced from reference 76 with the kind permission of the authors, Elsevier].

sintered to near theoretical density. Figures 10 and 11 show TEM and SEM images of the SiO_2/CNT and Al_2O_3/CNT systems respectively[74,76], where it can be seen that CNTs are homogeneously dispersed in both matrices. This could explain the observed strength properties.

It can be seen that each processing method has its own advantages in yielding appropriate structures and properties for each system, and hence there is need to find out proper combinations of processing, together with the suitable systems, to arrive at optimum properties.

3.2. Metal matrix nanocomposites

3.2.1. Metal – discontinuous reinforcement systems

Table 12 illustrates examples of some metal matrix nanocomposites and their respective properties.

The α-Fe/$Fe_{23}C_6$/Fe_3B system provides a good example of how unique properties may arise from metal nanocomposites. Table 13 shows the measured hardness values (GPa) of the ingot and ribbon samples prepared from this system[122]. Vickers hardness values of these two forms of the alloy produced by Branagan and Tang[122] were found to be 10.3 and 11 GPa in the as-solidified condition. The ribbon variety showed increased hardness with increasing heat treatment temperature, showing a maximum of 16.2 GPa at 973 K [higher than any existing commercial steel and hard alloys] and there after decreasing to 10.5 GPa at 1123 K. This can be compared to the decreasing trend of the ingot type (8 and 6.6 GPa at 873 and 973 K respectively).

The Al/SiC system also illustrates the advantages of metal nanocomposites compared to their micro counterparts[145-147]. Figure 12a shows plots of Vickers hardness vs. SiC content, while Figure 12b presents plots of Young's and shear modulus as a function of SiC content. There is a linear increase in hardness with increasing volume fraction of the harder phase (SiC) until the maximum value of 2.6 GPa for the sample that contains 10 vol. % of SiC. The values of Young's and shear modulus increase significantly with increasing SiC content, suggesting the formation of a nanocomposite material containing a brittle phase (SiC) embedded in the ductile Al matrix. Table 14 shows some mechanical properties of both nano- and microcomposites of Al/SiC.

It can be clearly seen that the Al/SiC nanocomposite exhibits notably higher Young's modulus and hardness than its micro counterpart. For example, the nanocomposite shows 12.6% increase in hardness and 105.1% in Young's modulus[145-147]. Also, Al/Pb nanocomposites exhibited improved frictional features[119-121]. The nanosized dispersoids lowered the coefficient of friction [0.3 for nanocomposite compared to 0.42 for the microcomposite] due to the formation of a uniform lead-rich tribo layer, with material transfer being an order of magnitude lower than in the micro-sized counterpart. The comparative wear loss of nano and microsized Al/Pb composites is shown in Figure 13[119].

Coming to the morphological studies of metal matrix-based nanocomposites, analysis of the structure and identification of the nanophases in α-Fe/$Fe_{23}C_6$/Fe_3B alloys using X ray diffraction and TEM with EDAX revealed the existence of two cubic and one tetragonal phase. The three phases exhibited the size of 4 μm [4,000 nm] in the ingot alloy, while in the heat-treated ribbon alloy the size of the phases was in the range of 100-130 nm. Based on these, the observed hardness was attributed to the nanostructure and to the super saturation of Cr and W above their equilibrium solubility in Fe. These studies also suggested the possible synthesis of very hard and inexpensive materials for three bodies wear applications and to replace expensive hard metals such as in cobalt-based materials. Figure 14 shows TEM/SAED images of this

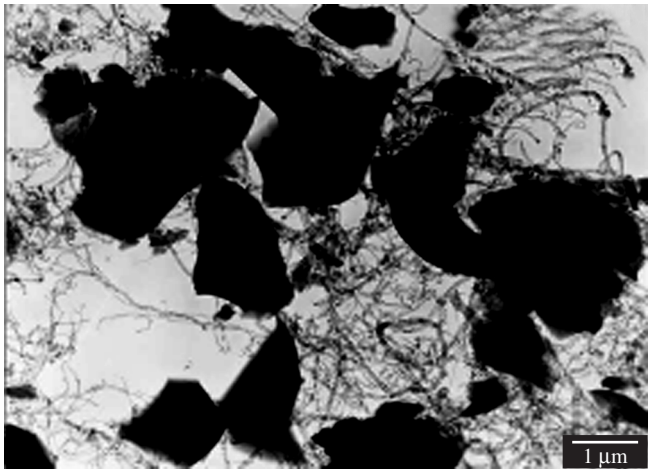

Figure 10. TEM image of CNT, SiO_2 nanocomposite mixture [reproduced from reference 74 with the kind permission of the authors, Elsevier].

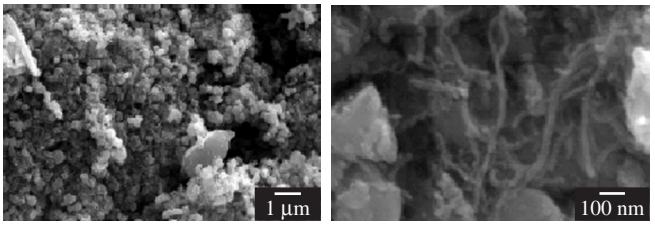

(a) (b)

Figure 11. SEM micrographs of Al_2O_3/CNT materials: a) at low magnification, and b) at high magnification [reproduced from reference 76 with the kind permission of the authors, Elsevier].

Table 12. Examples of metal nanocomposites and their properties.

Matrix/reinforcement	Properties	Reference
Ag/Au	Improvement in catalytic activity	96
Ni/PSZ and Ni/YSZ	Improved hardness and strength	5, 13
Cu/Nb	Improved microhardness	123
Al/AlN	Higher compression resistance and low strain rate	95
Al/SiC	Improved hardness and elastic moduli	143
CNT/Sb and CNT/$SnSb_{0.5}$	Improvements in Li^+ intercalation properties	136, 137
α-Fe/$Fe_{23}C_6$/Fe_3B	Drastic improvement in hardness	122
Cu/Al_2O_3	Improved microhardness	124
CNT/Fe_3O_4	Improved electrical conductivity	78

Table 13. Hardness values (GPa) of the ingot and ribbon samples prepared from the Fe/$Fe_{23}C_6$/Fe_3B nanocomposite [reproduced from reference 122 with the permission of the Authors and Elsevier].

Sample	Ingot	Ribbon
As-solidified	10.3	11.0
600 °C	8.0	11.0
650 °C	-	15.6
700 °C	6.6	16.2
750 °C	-	12.2
800 °C	6.5	12.0
850 °C	-	10.5

nanocomposite. The three iron-containing phases are homogeneously distributed over the entire material[122].

In the case of Al/SiC nanocomposites (Figure 15), only two phases are visible in the TEM images: SiC (granular fine grains) and Al (overall matrix). No more sharp ring-spot patterns have appeared in the electron diffraction pattern (SAED), indicating the formation of fine, nanosized powders[147] containing the brittle SiC phase embedded in the ductile Al matrix.

Other metal-ceramic nanocomposites are shown in the SEM and TEM photographs of Figure 16. Figure 16a is a SEM micrograph of Fe/MgO composite heat treated at 873 K and reduced at 1073 K[11]. Volume changes occurred due to O_2 atoms released from Fe_2O_3 during reduction. Figure 16b, c presents TEM micrographs of uniformly distributed nanosize ceramic particles in Al and Ag metal matrices[95,96] respectively. Nearly spherical particles of Ag isolated from each other can be seen in Figure 16c. This study revealed that Ag particles of size smaller than pore size (10 nm) are size-defined and stabilized. Similar observations have been made with other noble metals such as Au and Pd.

In the case of Al-Pb nanocomposites, micrographs showing the worn surfaces (not shown here) revealed delamination in the early

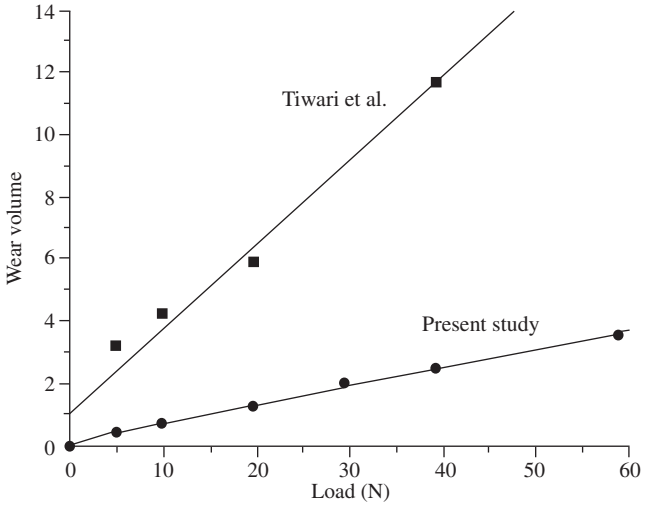

Figure 13. Wear loss of nanosized vs. microsized leaded Al alloys [reproduced from reference 78 with the kind permission of the authors, the American Chemical Society, USA].

Table 14. Properties of Al/SiC nano- and microcomposites[145-147].

Properties / Material	Al/SiC composite	Al/SiC nanocomposite
Young's modulus (GPa)	88.4	100
Hardness (H_v) (Kg/mm^2)	78	160

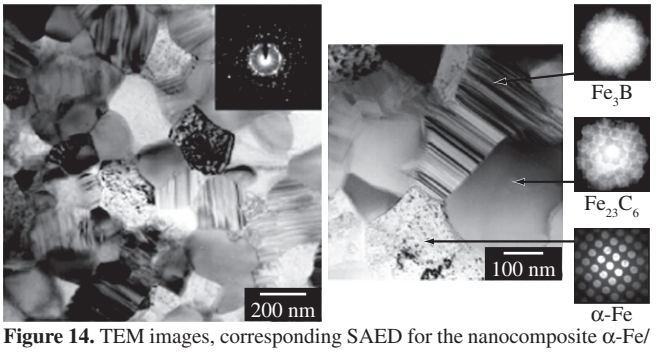

Figure 14. TEM images, corresponding SAED for the nanocomposite α-Fe/$Fe_{23}C_6$/Fe_3B ribbons heat-treated at 850 °C [reproduced from reference 122 with the kind permission of the authors, Elsevier].

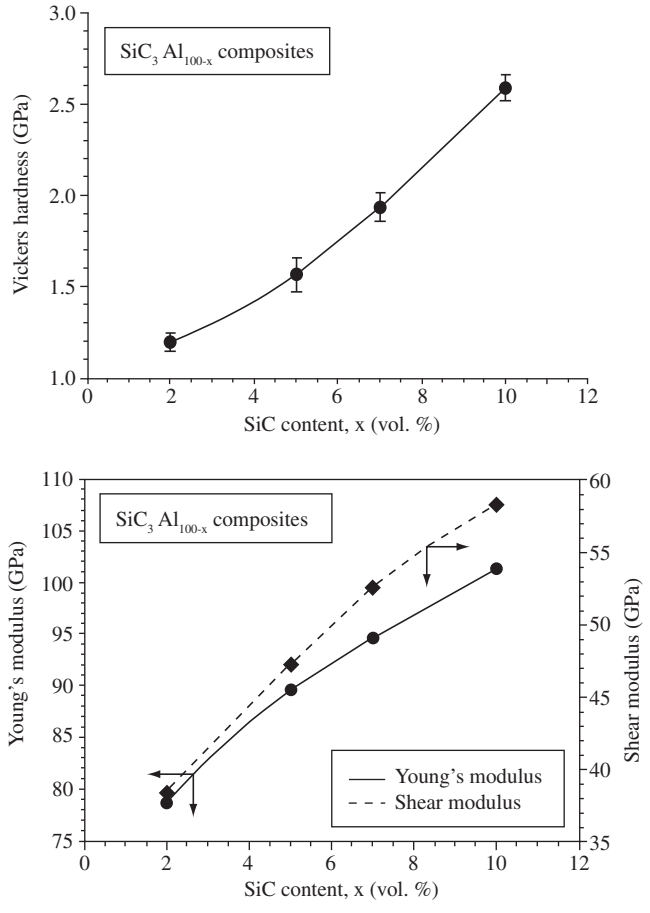

Figure 12. Correlation between SiC content, x, Vicker's hardness, Young's modulus, shear modulus of consolidated Al_{100-x}/SiC_x nanocomposites [reproduced from reference 147 with the kind permission of the author, Elsevier].

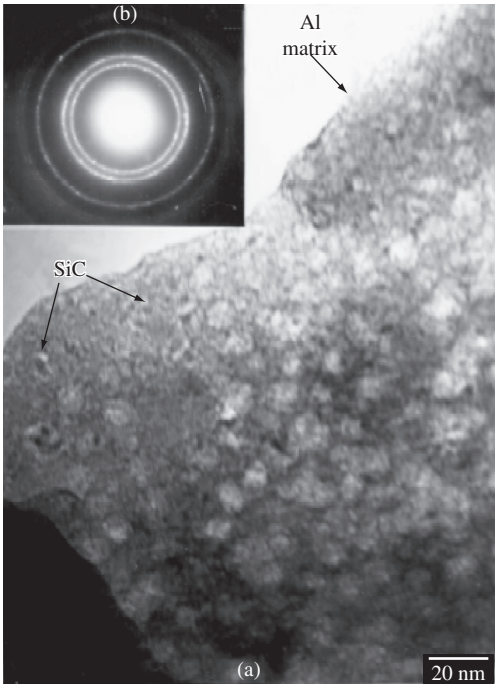

Figure 15. a) TEM image, b) the corresponding SAED of mechanically solid state mixed Al/SiC nanocomposite [reproduced from reference 147 with the kind permission of the author, Elsevier].

stage of wear, while the behaviour at late stages was affected by the processing technique. In addition, some elongation of particles was also observed, along with coarsening of Pb particles during sliding, due to dislocation-aided diffusion.

3.2.2. Metal matrix-CNT composites

Let us now look into the CNT-containing metal matrix nanocomposites. Electrical properties of an Al/CNT system measured between 4.2 K and room temperature revealed an increase from 4.9 to 6.6 μΩ cm at room temperature for 1 and 4 wt. (%) CNTs, but a decrease to 5.5 μΩ cm for 10 wt. (%) CNT (Figure 17), compared to the value of 3.4 μΩ cm for the Al matrix. At lower temperatures [70-80 K], resistivities of all composites decreased linearly, as in the case of metals, with an abrupt drop of about 90%. The mechanism of these changes is yet to be understood.

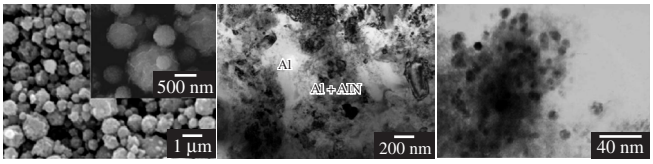

Figure 16. TEM micrographs of a) Fe/MgO; b) Al/AlN and c) Ag/SiO_2 nanocomposites [reproduced from references 11, 95, 96 respectively, with the kind permission of the authors, Elsevier].

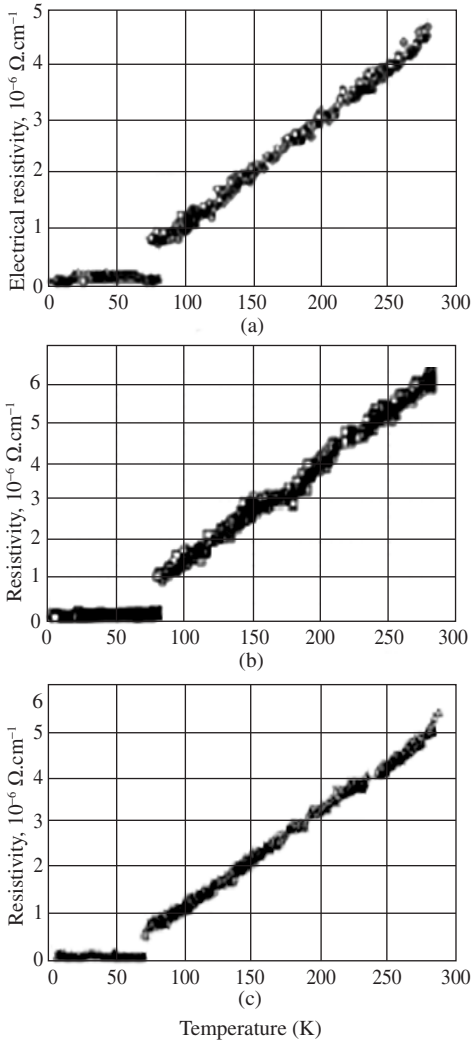

Figure 17. Dependence of electrical resistivity in Al/CNT composites with temperature: a) Al/CNT 1 wt. (%), b) Al/CNT 4 wt. (%), and c) Al/CNT 10 wt. (%) [reproduced from reference 138 with the kind permission of the authors, Elsevier].

On the other hand, compression testing of these Al-CNT composites[139] showed identical stress strain curves for both the composite without the precursor and pure Al, except for large elastic strain, while those with the precursor, though similar in shape, exhibited increased compression stresses. At a higher MWCNT loading (1.6 vol. %), proof stress increased seven fold, in contrast to a not so remarkable improvement in polymer-CNT composites[196,197]. Fractographs of the composite revealed no MWCNT aggregates, but instead their uniform distribution without any pullouts. The enhanced mechanical property has been attributed to the confinement of the Al matrix by the MWCNTs on nanoscale.

Internal friction measurements on Mg-based nanocomposites as a function of temperature up to 500 K revealed almost identical spectra for both the composites [Al-Saffil covered with CNT and Al-Saffil-CNTs] with thermal hysteresis[141]. A maximum damping was observed at about 300 K for 1 Hz frequency, associated with the maximum shear modulus for both the composites. On the other hand, larger hysteresis and rapid increase of internal friction - reaching a maximum at 350 K - was observed for the third composite [Mg 1 vol. % CNT]. However, shear modulus decreased for all three composites, being about 20% higher for Mg-Saffil-CNT than that for Mg-Saffil. SEM fractographic studies showed an Mg matrix embedded with CNTs and covering of saffil fibres with CNTs.

In the case of Sn_2Sb/CNT nanocomposites, higher specific capacity than that shown by CNTs and improved cyclability relative to unsupported Sn–Sb alloy particles were observed. This behaviour was attributed to the high dispersion of Sn_2Sb in the CNT matrix. SEM and TEM examinations confirmed[136] the presence of nanometric Sn_2Sb particles homogeneously dispersed in the CNTs (Figure 18).

In the case of Al/CNT nanocomposites (Figure 19), a single carbon nanotube is seen to be embedded in the Al matrix (Figure 19b)[138].

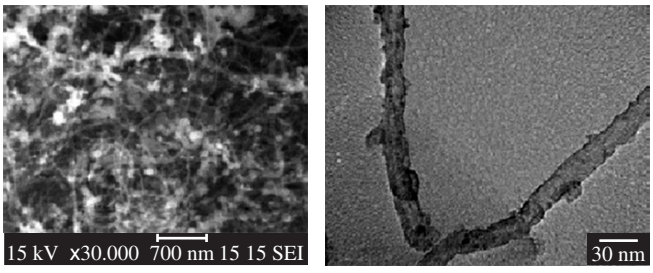

Figure 18. a) SEM, and b) TEM images of Sn_2Sb/CNTs nanocomposites [reproduced from reference 136 with the kind permission of the authors, Elsevier].

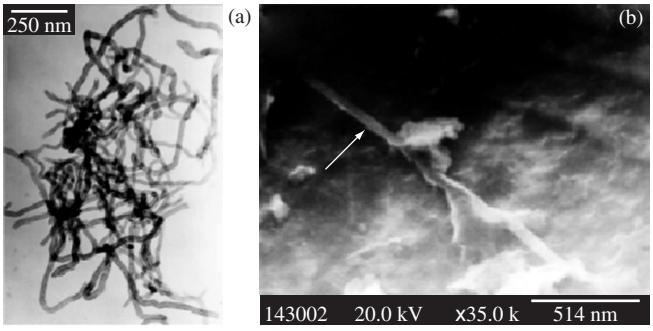

Figure 19. a) TEM images of CNTs, and b) SEM image of Al/CNT 1 wt. (%) [reproduced from reference 138 with the kind permission of the authors, Elsevier].

Furthermore, agglomerates of carbon nanotubes can be found at the grain boundaries of the aluminium matrix.

3.3. Polymer matrix nanocomposites

Structure-property correlations in polymer nanocomposites have been extensively dealt with in a recent book[292], which describes the mechanical properties of polymers based on nanostructure and morphology. Table 15 presents examples of these properties.

3.3.1. Polymer matrix - discontinuous reinforcement (non-layered) nanocomposites

The reinforcing materials employed in the production of polymer nanocomposites can be classified according to their dimensions* [18]. For example, when the three dimensions are in the nanometre scale, they are called isodimensional nanoparticles. Examples include spherical silica, metal particles and semiconductor nanoclusters[219]. The second kind of reinforcement is formed by nanotubes or whiskers, which contain two dimensions in the nanometre scale and one larger, forming an elongated structure. Carbon nanotubes and cellulose whiskers, extensively studied as reinforcing nanofillers, can be included in this second category. The third type of reinforcement is characterized by only one dimension in the nanometre range[220-222]. In this group, the filler contains sheets one to a few nanometres thick and hundreds to thousands nanometres long. This family is called polymer-layered nanocomposites[2,18,26]. These materials are obtained by intercalation of the polymer (or a monomer subsequently polymerized) inside the galleries of the layered host. Many synthetic and natural crystalline hosts that are able, under specific conditions, to intercalate a polymer have been described. Examples include graphite, metal chalcogenides (MoS_2, for example), clays, layered silicate (montmorillonite, hectorite, saponite, fluoromica, fluorohectorite, vermiculite and kaolinite) and layered double hydroxides. Nanocomposites based on clay and layered silicates have been widely investigated due to the availability of clay starting materials and their well-known intercalation chemistry as mentioned earlier[18,50,51,223].

Figure 20 shows the variation in quasi-static fracture toughness as a function of the volume percentage of TiO_2 in the polyester/TiO_2 nanocomposite. The addition of TiO_2 particles has a great effect on fracture toughness. At loadings of 1, 2 and 3 vol. %, an increase of 57, 42 and 41%, respectively, can be observed, when compared with that of the original polyester. However, at 4 vol. % TiO_2, toughness (0.55 $MPam^{1/2}$) decreased approximately to the value given by the polyester matrix (0.54 $MPam^{1/2}$).This variation can be explained in terms of nanocomposite structure, as illustrated in Figure 21.

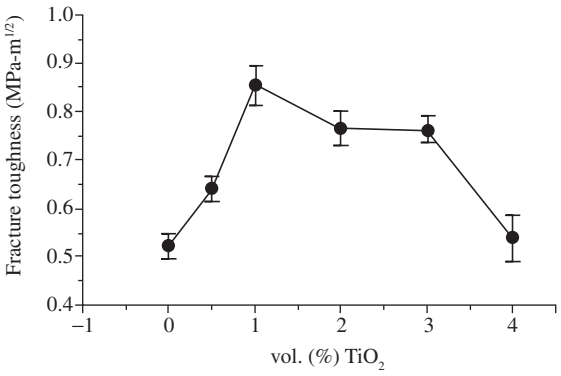

Figure 20. Variation of quasi-static fracture toughness as a function of volume fraction of TiO_2 nanoparticles in the polyester/TiO_2 nanocomposite [reproduced from reference 180 with the kind permission of the authors, Elsevier].

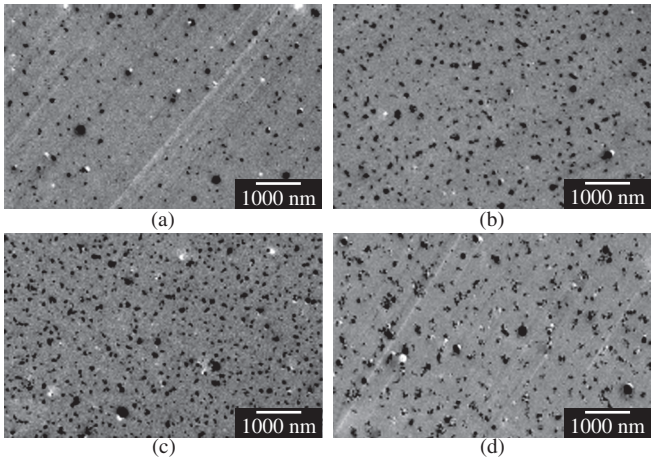

Figure 21. TEM micrographs depicting the level of TiO_2 nanoparticle dispersion within the polyester matrix in the polyester/TiO_2 nanocomposite. Volume fraction of particles: a) 1 vol. %; b) 2 vol. %; c) 3 vol. %; and d) 4 vol. % [reproduced from reference 180 with the kind permission of the authors, Elsevier].

Table 15. Examples of polymer-matrix nanocomposites and their properties[18,25,26,180,184].

Matrix/reinforcement	Properties
Polypropylene/montmorillonite	Improved tensile strength, strain at break, stiffness, Young's modulus and tensile stress
Nylon-6/Layered-silicates	Improved storage modulus, tensile modulus, HDT, tensile stress and reduced flammability.
Polylactide/Layered-silicates	Improved bending modulus, bending strength, distortion at break, storage modulus, gas barrier properties and biodegradability.
Epoxy/Layered-silicates	Improved tensile strength and modulus.
Polyimide/montmorillonite	Improved tensile strength, elongation at break and gas barrier properties.
Polystyrene/Layered-silicates	Improved tensile stress and reduced flammability.
Polyethylene oxide/Layered-silicates	Improved ionic conductivity.
Poly(methyl methacrylate)/Pd	Improved thermal stability.
Polyester/TiO_2	Improved fracture toughness and tensile strength.
Epoxy/SiC	Improved microhardness, storage modulus and elastic modulii.

*In the majority of publications on clay and layered compounds [e.g. R. Schöllhorn, Angew. Chem. Int. Ed. Engl., 19 (1980) 983], layered structures are classified as two-dimensional (grown preferentially in two dimensions). This is opposite to the usual interpretation given by polymer nanocomposite scientists, who consider the number of nanodimensions of the reinforcing agents to classify them. In the case of layered structures, they are in the nanorange in only one dimension, though they may possess three dimensions and hence the material is termed as 'one-dimensional'. On the same line, nanoparticles and nanotubes, which have three and two nanorange dimensions respectively, are classified as isodimensional and two-dimensional respectively. Following the majority of the papers dealing with polymer nanocomposites, which use the nomenclature adopting the number of nanorange dimensions, the same terminology will be followed throughout this paper.

It can be observed that the specimens containing 1, 2 and 3 vol. % TiO_2 show excellent particle dispersion. Conversely, considerable agglomeration was present in the specimens containing 4 vol. % TiO_2. Authors have assigned the initial increase in fracture toughness, followed by the precipitous decline observed at 4 vol. %, to the level of dispersion of nanoparticles within the matrix and to the weak bonding between the titania particles and the polyester[180].

The structure of polymer nanocomposites reinforced with isodimensional particles is similar to that of ceramic and metal nanocomposites. In this type, the reinforcement material is distributed all over the polymer matrix, as illustrated in Figure 22. The microstructure of some particle-reinforced polymer nanocomposites is shown in Figure 23. Figure 23a shows the TEM micrograph of polyacrylic acid/silver nanocomposite, showing spherical Ag particles of 10-80 nm size[183]. Secondary aggregates are formed due to the low viscosity nature of the composite solution. Figure 23b shows the TEM micrograph of an oxidised poly (4-vinylpyridine) homopolymer-Fe_2O_3 nanocomposite showing ultrafine and crystalline spherical particles of the dispersoids in the 20-200 nm range[223]. In this case, the particles retain the nanosize dimension due to the protective action of the polymer layer.

SEM analyses of PET-uncoated $CaCO_3$ nanocomposites (Figure 23c) show large particles which seem to be quite welded to PET[181]. On coating, these particles get even larger, but again are well welded. Figure 23d, on its turn, is a field emission SEM of transparent polymaleimide-27.4 wt. (%) silica nanocomposite without any addition of colloidal silica, synthesised by the sol-gel process and showing discrete domains of an inorganic phase with narrow particle size distribution (10-20 nm)[224]. This composite showed better thermal stability with higher Tg (527 K-254 °C) compared to 458 K (185 °C) for the *N*-butyl-substituted polymaleimides, and a higher decomposition temperature of 834 K (561 °C) compared to *N*-alkyl-substituted polymaleimides.

Most of the properties observed in polymers-discontinuous reinforcement systems are directly related to their structure. For example, PSM/CdSe nanocomposite (PSM = poly (styrene-alt-maleic anhydride) showed an emission peak at 540 nm in its photoluminescence spectrum, which was close to the absorption edge of the obtained CdSe particles[225]. According to the authors, this type of near band edge emission is typical of surface-passivated nanocrystalline CdSe. For nanoparticles, a large percentage of defects are located at the surface. If these defects are not passivated, non-radiative recombination will occur, as they act as traps for electron and hole annihilation. Therefore, it is conceivable that PSM modified the surface structure and enhanced the luminescence properties of CdSe nanoparticles[225]. As can be seen from TEM images of this material (Figure 24), CdSe nanoparticles are uniform and monodisperse, with an average size of about 17 nm. In this case, it is feasible that PSM played an important role in controlling the size and the monodispersion of the nanoparticles[225]. Interactions between PSM and CdSe particles were also investigated and are supported by IR and UV-visible spectroscopy.

In the PVA/Ag nanocomposite system, a strong influence of the Ag nanofiller (~20 nm) was observed on the material strength and thermal properties, even at low concentration (<1 wt. (%))[178]. For example, the glass transition was shifted towards higher temperatures by 20 K and the thermal stability was improved by about 40 K in the case of the nanocomposite containing 0.73 wt. (%) Ag. Also, nanocomposite films showed deformation behaviour characteristic of semicrystalline materials, with a clearly distinguished yield point, while no yield point was observed in the deformation of the pure PVA matrix. These changes in the thermal and mechanical behaviour of PVA in the presence of the Ag nanofiller were discussed in terms of polymer chains attached to the surface of Ag nanoparticles. The improved thermal stability was explained on the basis of the reduced mobility of the PVA chains in the nanocomposite. In this system, a strong influence of nanoparticles on the material strength was also observed. The stress at break of the nanocomposite film with 0.33 wt. (%) of silver was almost 100% higher than the corresponding value for the pure matrix. Finally, the strain at break slightly decreased with increasing nanoparticle content[178].

From the phase contrast AFM of poly-para-xylylene composites containing Pd or Sn nanoparticles (Figure 25a-c), prepared by vacuum co-condensation of both the metal and the polymer[47], one can identify surface imperfections as well as metal particle sizes (7-10 nm). Surface morphology seemed to depend on the type of metal, with good surface uniformity for Pd. In the Pd case, particles were identified as an inor-

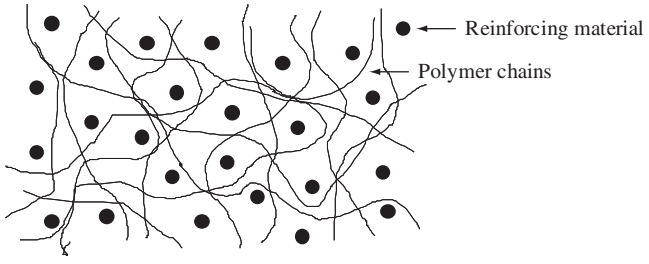

Figure 22. Typical structure of particle-reinforced polymer nanocomposites.

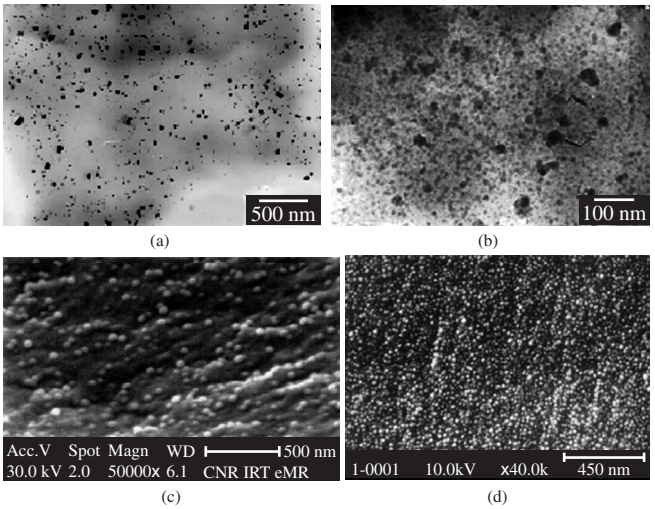

Figure 23. TEM photograph of a) PAA/Ag; b) PVP/Fe_2O_3; c) PET/$CaCO_3$, and d) PMI/SiO_2 nanocomposites. PAA = polyacrylic acid, PVP = 4-polyvinylpyridine, PET = poly(ethylene terephthalate), PMI = polymaleimide [reproduced from references 183, 223, 181, 224 respectively, with the kind permission of the authors, Elsevier, Springer Science, Business Media].

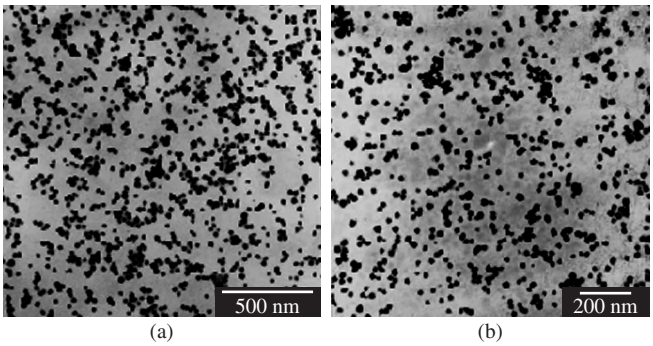

Figure 24. TEM images of the PSM/CdSe nanocomposite (PSM = poly(styrene-alt-maleic anhydride) [reproduced from reference 225 with the kind permission of the authors, Elsevier].

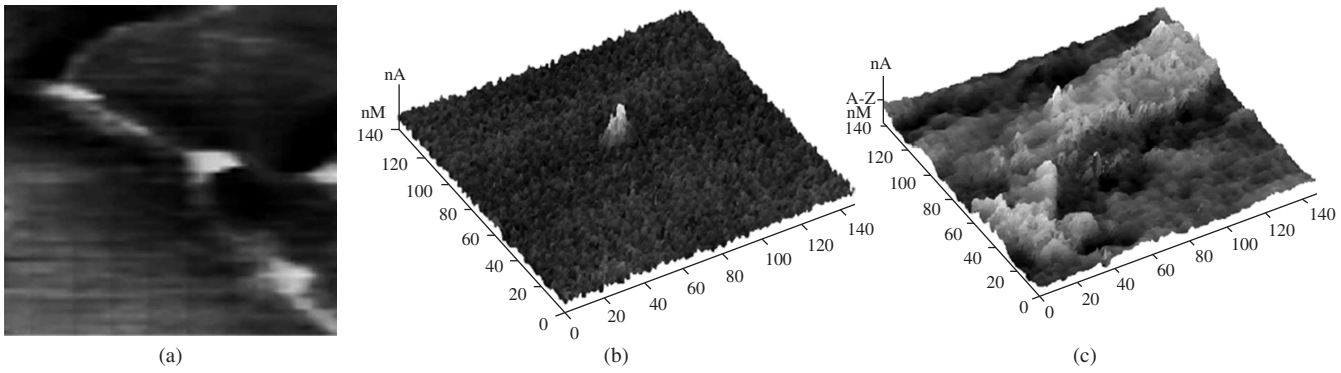

Figure 25. a) Phase-contrast AFM image of poly-para-xylylene/Pd nanocomposite. Dark regions are polymer spherulites; light spots are Pd nanoparticles situated at the boundary between polymer spherulites; b) AFM phase contrast image of poly-para-xylylene/Sn 8 vol. % nanocomposite; and c) AFM phase contrast image of the poly-para-xylylene/Sn 16 vol. % nanocomposite [reproduced from reference 47 with the kind permission of the authors, Elsevier].

ganic phase with spherical globules of ~200 nm size. In the case of tin, separated Sn particles localized on polymer spherulites (Figure 25b) and aggregates of Sn nanoparticles connected in continuous chains are evident. The ionic conductivity of these nanocomposites is reported to have improved when compared with that of the pure polymer.

3.3.2. Polymer nanocomposites with layered reinforcements

Polymer layered silicate (PLS) nanocomposites have attracted great interest due to their improved properties compared with the pure polymer and conventional micro and macrocomposites. Some of these improvements include high moduli, increased strength and heat resistance, decreased flammability and gas permeability and increased biode gradability[1,158,166,207,210,211,235-243]. Two particular characteristics of layered silicates are generally considered for PLS nanocomposites. The first is the ability of the silicate particles to disperse into individual layers (totally delaminated or exfoliated). The second is the ability to fine-tune their surface chemistry through ion exchange reactions with organic and inorganic cations. These two are, of course, interrelated, since the degree of dispersion of a layered silicate in a particular polymer matrix depends on the interlayer ionic species.

Although the intercalation chemistry of polymers towards layered silicates has long been known[245,246], the field of PLS nanocomposites has recently gained impressive attention, due to two important findings. Firstly, the results obtained on Nylon-6 (N6)/montmorillonite (MMT) nanocomposites, which showed that a small concentration of layered silicate lead to remarkable changes in thermal and mechanical properties[26]. Secondly, the observation by Vaia et al.[247] that it is possible to melt-mix polymers with layered silicates, without the use of organic solvents.

The structural family called the 2:1 phyllosilicates is the most commonly used layered silicate in polymer nanocomposites. Their two-dimensional layers are made up of two tetrahedrally coordinated silicon atoms fused to an edge-shared octahedral sheet of either aluminium or magnesium hydroxide. The layer thickness is around 1 nm and its lateral dimensions may vary from 300 Å to several micra or larger, depending on the nature of the silicate[26]. Stacking of these layers generates a regular van der Waals gap, which is called the 'interlayer' space or the 'gallery'. Isomorphic substitution within the layers produces negative charges that are counterbalanced by alkaline or alkaline earth cations located in the interlayer. This occurs, for example, when Mg^{2+} or Fe^{2+} replaces Al^{3+} or when Li^{+} replaces Mg^{2+}. Because the forces that hold the stacks together are relatively weak van der Waals interactions, the intercalation of small molecules between the layers is simple[143]. In some cases, the hydrated interlayer cations can be exchanged by ion-exchange reactions with cationic surfactants including primary, secondary, tertiary and quaternary alkylammonium or alkylphosphonium. In organosilicates, these alkylammonium or alkylphosphonium cations lower the surface energy of the inorganic host and improve the wetting characteristics of the polymer matrix, resulting in a larger interlayer spacing. Moreover, these cations provide functional groups that can react with the polymer matrix or initiate the polymerization of monomers to improve the strength of the interface between the inorganic component and the polymer matrix[50,245,248,249].

Montmorillonite, hectorite and saponite are the most commonly used layered silicates. Their structure is presented in Figure 26 and their formulae in Table 16[235]. When the hydrated cations are ion-exchanged with bulkier organic cations, a larger interlayer spacing is usually obtained (Figure 26).

The main reason for the remarkable improvements observed in polymer/layered-silicate nanocomposites is the stronger interfacial interaction between the matrix and the silicate, compared to conventional filler-reinforced systems. Some examples will be given below in order to illustrate this statement.

The incorporation of MMT (montmorillonite) into a Nylon-6 matrix has led to a significant improvement in its mechanical properties. The Young's modulus (or tensile modulus), for example, of pure Nylon-6 (1.11 GPa) was strongly improved when the nanocomposite was formed. The Nylon-6/MMT with a filler content of 4.1 wt. (%) gave a value of 2.25 GPa, which corresponds to an increase of 102.7%[208,209]. Figure 27 represents the dependence of tensile modulus E, at 393 K (120 °C), on clay content for organo-modified montmorillonite- and saponite-based nanocomposites[208]. Results clearly show that the increase in Young's modulus in these systems is related to the average length of the layers and, consequently, to the aspect ratio of the dispersed nanoparticles as well as the extent of their exfoliation. Also, regarding Nylon-6 nanocomposites, a strong interaction between matrix and silicate layers occurs via formation of hydrogen bonds.

This behaviour can also be supported by maleic anhydride modified by propylene (PP-MA)/LS anocomposites. Table 17 represents the variation of the Young's modulus as a function of filler and maleic anhydride contents for both the nano and the microcomposite. These results indicate that the nanocomposite shows higher Young's modulus than the pure PP matrix. Also, a significant increase, as compared to the PP microcomposite, was observed as the amount of MA added to the polymer matrix was increased[250].

Important improvements on the stress at break were also observed in Polymer/LS systems. In thermoplastic-based nanocomposites, the stress at break, which expresses the ultimate strength that the material can bear before breaking, varies depending on the nature of the interactions between the matrix and the filler. Table 18 shows some

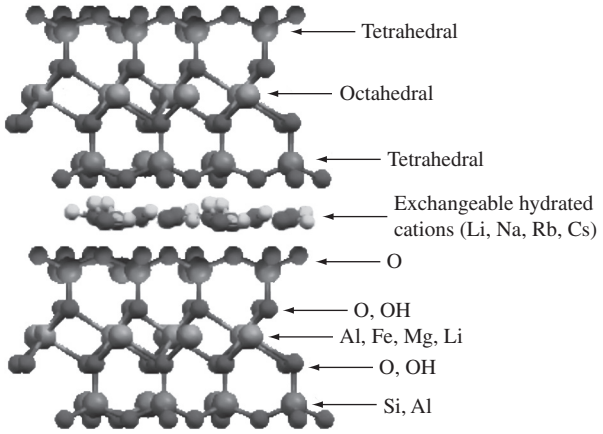

Figure 26. Schematic representation of the structure of 2:1 phyllosilicates.

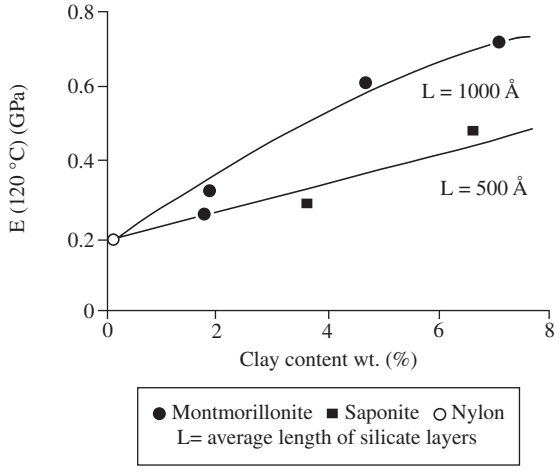

Figure 27. Dependence of tensile modulus (E) at 120 °C on clay content for organomodified montmorillonite-, saponite-based nanocomposites [reproduced from reference 208 with the kind permission of the authors, the Materials Research Society].

examples of tensile stress in different nanocomposite systems. According to these results, some important conclusions can be drawn, as discussed below.

Exfoliated Nylon-6 and intercalated PMMA nanocomposites exhibited a great increase in the stress at break[251]. This can be due to the polar (PMMA) and ionic interactions (Nylon-6 grafted onto the layers) between the matrix and the silicate layers. This increase is larger in Nylon-6 nanocomposites[250-252]. On the other hand, propylene-based nanocomposites showed only a slight enhancement in tensile stress, which can be explained by the lack of interfacial adhesion between non-polar PP and polar-layered silicates. However, addition of maleic anhydride-modified polypropylene to the polypropylene matrix has confirmed to be effective in the intercalation of the PP chains and the maintenance of the ultimate stress at an acceptable level[18]. Finally, regarding PS-intercalated nanocomposites, the ultimate tensile stress is significantly decreased compared to that given by the PP matrix and drops down at higher filler contents[252]. The authors have attributed this finding to the weak interactions at the polystyrene-clay interface. It is important to note that in previous compositions in which polar interactions were developed, strengthening at the filler matrix interface was observed[18].

Table 16. Chemical formulae of 2:1 phyllosilicates [reproduced from reference 26 with permission of the authors and Elsevier].

2:1 Phyllosilicate	Chemical formula
Montmorillonite	$M_x(Al_{4-x}Mg_x)Si_8O_{20}(OH)_4$
Hectorite	$M_x(Mg_{6-x}Li_x)Si_8O_{20}(OH)_4$
Saponite	$M_xMg_6(Si_{8-x}Al_x)O_{20}(OH)_4$

"M" Represents exchangeable cations and "x" the degree of isomorphous substitution.

Table 17. Young's modulus for PP-MA based micro- and nanocomposites as a function of filler and maleic anhydride contents [reproduced from reference 250 with permission of the authors and the American Institute of Physics, USA].

Sample	Filler content (wt. (%))	MA content (wt. (%))	Young's modulus (Mpa)
PP	0	0	780
microcomposite	6.9	0	830
nanocomposite	7.2	7.2	838
nanocomposite	7.2	14.4	964
nanocomposite	7.2	21.6	1010

Table 18. Tensile stress evolution for nanocomposites based on various thermoplastic matrices [reproduced from ref. 18 with permission of the authors and Elsevier].

Matrix	Tensile stress (MPa)	Nanofiller content (wt. (%))	Structure	Tensile stress (MPa)
Nylon-6	68.6	4.7	Exfoliated	97.2
Nylon-6	68.6	5.3	Exfoliated	97.3
Nylon-6	68.6	4.1	Exfoliated	102
PMMA	53.9	12.6	Intercalated	62.0
PMMA	53.9	20.7	Intercalated	62.0
PP-MA 7.2 wt. (%)	31.4	5.0	Intercalated	29.5
PP-MA 21.6 wt. (%)	32.6	4.8	Intercalated	31.7
PS	28.7	11.3	Intercalated	21.7
PS	28.7	17.2	Intercalated	23.4
PS	28.7	24.6	Intercalated	16.6
PS	28.7	34.1	Intercalated	16.0

Usually, when LS are dispersed in thermoplastics such as PMMA, PS or PP, the elongation at break is reduced [251,252]. The reported decrease in elongation is from 150% in pure PP matrix, to 105% for a 6.9 wt. (%) non-intercalated clay microcomposite. On the other hand, in a nanocomposite filled with 5 wt. (%) silicate layers, the more pronounced drop was 7.5%. Conversely, this loss in ultimate elongation did not occur in elastomeric epoxy or polyol polyurethane matrices[253,254]. In these cases, introduction of the nanoclay in cross-linked matrices causes an increase of the elongation at break. This is shown in Figure 28 for epoxy nanocomposites, which are prepared from magadiite modified with methyl-octadecylammonium or trimethyloctadecylammonium ions and a conventional composite prepared from magadiite modified with octadecylammonium[254]. While a drop in the elongation at break can be observed for the conventional composite, a slight improvement in this property can be observed for the intercalated nanocomposite.

Finally, exfoliated nanocomposites display a large increase in the elongation at break. This is probably due to the plasticizing effect of the galleries, their contribution to the formation of dangling chains and conformational effects at the clay-matrix interface. The combination of improved stiffness (Young's modulus), toughness (stress at break) and elasticity (strain at break) makes elastomeric nanocomposites suitable candidates for the generation of a new family of high performance materials.

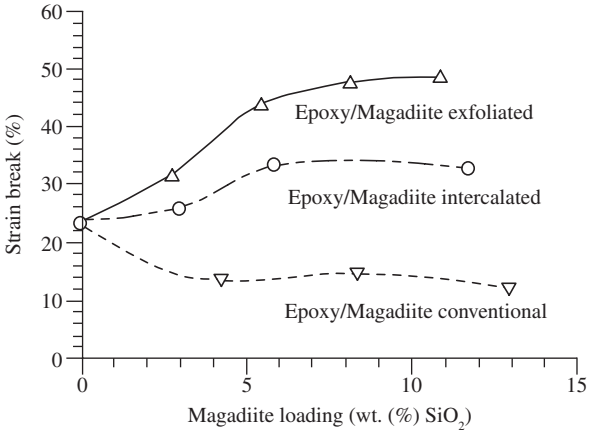

Figure 28. Strain at break values for exfoliated, intercalated epoxy/magadiite nanocomposites [reproduced from reference 254 with the kind permission of the authors, the American Chemical Society, USA].

Polyimide is another example of a polymer matrix material showing an increase in both stress and elongation at break [255]. For example, when filled with montmorillonite exchanged with hexadecylammonium, these properties increase with the filler loading at least up to 5 wt. (%). At higher filler contents, both properties drop towards values lower than those described for the filler-free matrix due to the formation of non-exfoliated aggregates which make these composites more brittle.

Another nanocomposite system studied in great detail is Nylon-6/protonated aminododecanoic acid, which has been studied for its impact resistance properties. The nanocomposite synthesized by in situ intercalative polymerization had its Izod impact strength reduced from 20.6 to 18.1 J/m compared with the pure matrix when 4.7 wt. (%) of nanoclay was incorporated. Charpy impact testing showed a similar reduction from 6.21 kJ/m^2 to 6.06 kJ/m^2 for the 4.7 wt. (%) nanocomposite[52,256]. Table 21 presents the effect of MMT content and Nylon-6 molecular weight on the tensile modulus of MMT modified with $(HE)_2M_1R_1$[†] [257]. A substantial improvement in stiffness can be seen, which increases with increasing matrix molecular weight (at any given concentration) for all Nylon-6 nanocomposites, i.e., low (LMW), medium (MMW) and high molecular weights (HMW). A slightly larger modulus of 2.82 GPa for LMW may be the result of a higher degree of crystallinity giving faster crystallization kinetics during the cooling of the specimen after injection moulding. Yield strength, on its turn, increases with the content of MMT, but while the HMW- and MMW-based nanocomposites show a steady increase in strength with the increasing content of clay, the LMW-based nanocomposites show a less pronounced effect. Also, increase in strength relative to the virgin matrix for the HMW composite is nearly twice that of the LMW composite at the highest clay content. Regarding the elongation at break for two different rates of extension, results show that the pure matrix is very ductile at a test rate of 0.51 cm/min. Increasing clay content leads to a gradual decrease in ductility. The elongation at break for the LMW-based nanocomposites decreases rapidly at low MMT content (around 1 wt. (%)). This larger reduction in the LMW-based systems may be due to the presence of stacked silicate layers, as seen in Figure 29[257]. The higher testing rate of 5.1 cm/min yields similar trends, but the absolute level of the elongation at break is significantly lower. The strain decreases for all nanocomposites when compared to the pure matrix polymer.

This good resistance to impact, high Young's modulus, good flexural modulus and a notable enhancement in the heat distortion temperature, going from 338 K (65 °C) for pure Nylon-6 to more than

Table 19. Mechanical properties of some N6/$(HE)_2M_1R_1$ nanocomposites [reproduced from ref. 257 with permission of the authors and Elsevier].

N6/$(HE)_2M_1R_1$	Modulus (GPa)	Yield strength (MPa)	Strain (%)	Elongation at break (%) Crosshead speed		Izod impact strength (J/m)
				0.51 cm/min	5.1 cm/min	
LMW						
0.0 wt. (%) MMT	2.82	69.2	4.0	232	28	36.0
3.2 wt. (%) MMT	3.65	78.9	3.5	12	11	32.3
6.4 wt. (%) MMT	4.92	83.6	2.2	2.4	4.8	32.0
MMW						
0.0 wt. (%) MMT	2.71	70.2	4.0	269	101	39.3
3.1 wt. (%) MMT	3.66	86.6	3.5	81	18	38.3
7.1 wt. (%) MMT	5.61	95.2	2.4	2.5	5	39.3
HMW						
0.0 wt. (%) MMT	2.75	69.7	4.0	3.4	129	43.9
3.2 wt. (%) MMT	3.92	84.9	3.3	119	27	44.7
7.2 wt. (%) MMT	5.70	97.6	2.6	4.1	6.1	46.2

[†]The substituents on the quaternary ammonium compound used to form the organoclay are identified in this shorthand notation where R = rapeseed, HE = hydroxyethyl, M = methyl. Rapeseed is a natural product composed predominantly of unsaturated C_{22} alkyl chains (45%)[257].

423 K (150 °C) for the nanocomposite, have allowed this material to replace glass fibre-reinforced nylon or polypropylene in the production of timing belt covers of automotive engines[258].

Coming to dynamic strength properties, it is well known that dynamic mechanical analysis (DMA) measures the response of a given material to a cyclic deformation (usually tension or three-point flexion type deformation) as a function of temperature. Results are expressed by three main parameters, which are the storage modulus (E'), corresponding to elastic response to deformation; the loss modulus (E''), corresponding to plastic response to deformation and tan δ, that is the (E'/E'') ratio, useful for determining the glass transition temperature, for example. PS nanocomposites have been characterized by DMA analysis[252]. No significant difference in E' was observed between the pure PS and a nanocomposite intercalated with 17.2 wt. (%) of Na-montmorillonite in the temperature range of 293-413 K (20-140 °C), indicating lack of influence of intercalated nanocomposites on the elastic properties of the matrix. However, shift and broadening of tan δ values towards higher temperatures for the nanocomposite suggests an increase in the glass transition temperature and some broadening of this transition. This can be assigned to restricted segmental motions at the organic-inorganic interface of the intercalated systems.

However, a different behaviour on DMA properties is observed when blending copolymers, such as the symmetric styrene-butadiene-styrene [SBS] block copolymers, are previously used to modify the matrix[259]. For example, when SBS is melt-blended with a montmorillonite modified by dimethyldioctadecylammonium, a nanocomposite in which only the PS blocks can intercalate within the layered silicates is produced. In this material, a large improvement of the storage modulus at 25 °C was observed. Figure 30 shows these results for this nano- and its microcomposite counterpart[259].

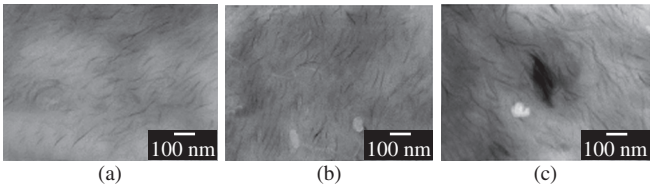

Figure 29. Bright field TEM images of melt compounded nanocomposites containing 3 wt. (%) MMT based on a) HMW, b) MMW, and c) LMW Nylon-6 [reproduced from reference 257 with the kind permission of the authors, Elsevier].

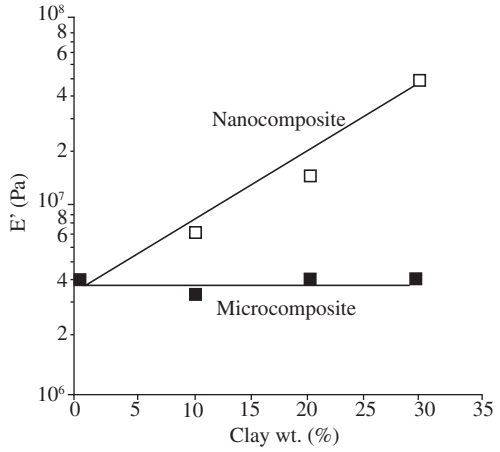

Figure 30. Trend of the Storage Modulus (E`) at 531 K for SBS-based nanocomposites, microcomposites as a function of the filler level [reproduced from reference 259 with the kind permission of the authors, the Materials Research Society, USA].

This figure compares the values of the storage moduli for two sets of samples in which the reinforcement content varied from 0 to 30 wt. (%). Values were recorded for nanocomposites filled with organomodified clay and for composites prepared by melt-blending the SBS matrix and Na-montmorillonite under the same conditions. There is a sharp increase in elastic modulus for nanocomposites, while microcomposites do not present any improvement in this property.

DMA properties were also studied for the widely used bifunctional diglycidyl ether of bisphenol-A (DGEBA) containing different amounts (2-10 wt. (%)) of layered silicate, and prepared by a two steps chemical method (173 to 323 K and from 323 to 573 K). Results indicated that, with increasing organic clay content in the composite, the relaxation temperatures of the cured system decreased, while the presence of modified layered silicate improved both toughness and stiffness of the matrix[260]. AFM phase contrast images (Figure 31) show stacked layers of silicates in the product, even though they are not distributed homogeneously throughout the material. The high magnification shown in Figure 31(b) reveals the striated structure in the 5 wt. (%) layered silicate-containing nanocomposite, with increasing phase intervals at the top of the surface. However, no individual layers could be seen by TEM.

The dependence of the storage modulus for polyimide-based nanocomposites filled with 2 wt. (%) of organic clays and for the unfilled matrix is shown in Figure 32. At any temperature, higher storage moduli result from the better nanofiller dispersion. Moreover, the large difference between exfoliated montmorillonite- and exfoliated mica-based nanocomposites can be explained by the respective aspect

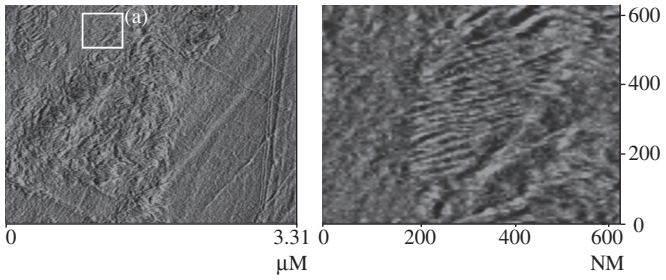

Figure 31. Phase contrast AFM images of DETDA (diethyltoluenediamine)-cured DGEBA (diglycidylether of bisphenol) containing 5 wt. (%) organoclay [reproduced from reference 260 with the kind permission of the authors, Elsevier].

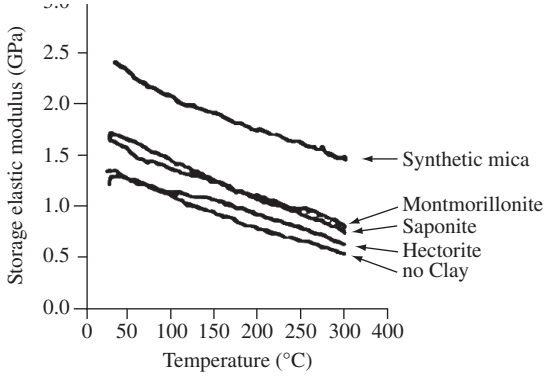

Figure 32. Temperature dependence of storage elastic modulus for polyimide-based nanocomposites filled with 2 wt. (%) of organomodified synthetic mica, montmorillonite, saponite, hectorite [reproduced from reference 255 with the kind permission of the authors, John Wiley & Sons Inc.]

ratio of the dispersed silicate layers, with lengths of 0.218 and 1.23 mm for montmorillonite and synthetic mica respectively, as observed by TEM studies.

From Figure 32, it is also evident that the glass transition temperature decreases (~288 K) with increasing clay content for this nanocomposite. The influence of dispersion and length of the layered particles has thus been demonstrated in the case of these nanocomposites using various organoclays (hectorite, saponite, montmorillonite and synthetic mica)[210,255]. Mica and montmorillonite clays lead to exfoliated-structures, while a partially exfoliated-intercalated structure was obtained for saponite and a mainly intercalated morphology was attributed to the hectorite-based nanocomposite.

Furthermore, DMA studies carried out on organoclays exfoliated within cross-linked matrices revealed a very noticeable improvement in storage modulus, especially above T_g. For example, the epoxy/montmorillonite 4 vol. % nanocomposite below T_g showed a 58% increase[164]. In this case, a well-ordered exfoliated nanocomposite (silicate layers separated by approximately 100 Å) was formed. At 331 K, E' equals 2.44 and 1.55 GPa for the nanocomposite and the unfilled cross-linked matrix, respectively. At 423 K, which is above T_g, the reported E' values are 11 and 50 MPa for the unfilled and filled epoxy, respectively. This enhancement corresponds to a storage modulus improvement by a factor of 4.5. Also, an interesting result could be observed in nitrile rubber/organoclay nanocomposites[258]. A three-fold increase in the storage modulus was described through the simple dispersion/exfoliation of 10 parts of organoclay per 100 parts of rubber, with a modulus as high as 8.8 MPa. This value is similar to what can be obtained with the same matrix filled with 40 parts of carbon black per 100 parts of rubber. As a result, the amount of filler can be reduced by a factor of four. Overall, the storage elastic modulus appears to be substantially enhanced at temperatures above T_g for exfoliated nanocomposites filled with layered silicates. A possible explanation for such an improvement could be the creation of a three-dimensional network of interconnected long silicate layers, strengthening the material through mechanical percolation.

Mechanical properties of layered nanocomposites typically resemble those of ceramic materials. Flocculated nanocomposites are, conceptually, the same as intercalated nanocomposites. Silicate layers are sometimes flocculated due to hydroxylated edge–edge interaction of the silicate layers, and when they are completely and uniformly dispersed in a continuous polymer matrix, an exfoliated or delaminated structure is obtained. The individual clay layers are separated in a continuous polymer matrix by an average distance that depends on clay loading. Usually, the clay content of an exfoliated nanocomposite is much lower (4-5 wt. (%)) than that of an intercalated (11-34 wt. (%)) nanocomposite. Figure 33 shows TEM images of intercalated and exfoliated polymer-layered silicates nanocomposites[26].

Let us now look at other physical properties such as thermal stability, ionic conductivity gas barrier, flame retardancy, etc., of layered nanocomposites. Polymer/LS nanocomposites show improvements in their thermal stability. The PMMA/montmorillonite 10 wt. (%) nanocomposite, for example, degraded at temperatures 40 ± 5 °C is superior to pure PMMA[246]. In the poly (dimethylsiloxane) (PDMS)/10 wt. (%) organomontorillonite nanocomposite, a dramatic shift in the weight loss towards higher temperatures was recorded[261]. These improvements were due to the decrease in permeability, usually observed in exfoliated nanocomposites, which hinders the diffusion of volatile decomposition products. In this context, the silicate layers act as a superior insulator and mass transport barrier to the volatile products generated during decomposition.

Fire relevant properties, such as heat release rate (HRR), peak heat release rate (PHRR), smoke production and CO_2 yield are vital to the evaluation of the fire safety of the material. As a result, the decreased flammability of nanocomposites is one of their most important features. Table 20 shows cone calorimeter data for three different kinds of polymers and their respective nanocomposites with MMT. It can be seen that all MMT-based nanocomposites exhibited reduced flammability. The peak HRR is reduced by 50-75% for N6, PS, and PP-g-MA nanocomposites[243]. In general, the flame retardant mechanism of nanocomposites involves a high-performance carbonaceous-silicate char, which builds up on the surface during burning and serves as a barrier to both mass and energy transport. This mechanism has also been supported by recent studies concerning PS/MMT nanocomposites[262]. Studies of the

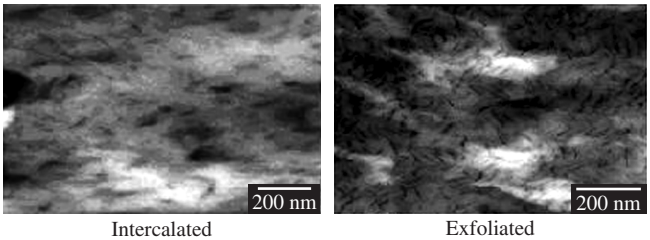

Intercalated (a) Exfoliated (b)

Figure 33. TEM images showing a) intercalated, and b) exfoliated polymer-clay nanocomposites [reproduced from 26 with the kind permission of the authors, Elsevier].

Table 20. Cone calorimeter data for various polymers and their nanocomposites with organically modified layered-silicates (OMLS) [reproduced from references 243 with permission of the authors and the American Chemical Society, USA].

Sample (structure)	% residue yield (±0.5)	Peak HRR ($kW.m^{-2}$) (D%)	Mean HRR ($kW.m^{-2}$) (D%)	Mean Hc ($MJ.kg^{-1}$)	Mean SEA ($m^2.kg^{-1}$)	Mean CO yield ($kg.kg^{-1}$)
N6	1	1010	603	27	197	0.01
N6/MMT 2% (delaminated)	3	686 (32)	390 (35)	27	271	0.01
N6/MMT 5% (delaminated)	6	378 (63)	304 (50)	27	296	0.02
PS	0	1120	703	29	1460	0.09
PS/silicate mix 3% (immiscible)	3	1080	715	29	1840	0.09
PS/MMT 3% (intercalated/delaminated)	4	567 (48)	444 (38)	27	1730	0.08
PP-g-MA	5	1525	536	39	704	0.02
PP-g-MA/MMT - 2% (intercalated/delaminated)	6	450 (70)	322 (40)	44	1028	0.02
PP-g-MA/MMT 4% (intercalated/delaminated)	12	381 (75)	275 (49)	44	968	0.02

fire retardant properties of exfoliated Nylon-12 (2 wt. (%) / 3 wt. (%)) or intercalated PP/montmorillonite 2 wt. (%) nanocomposites have revealed 63% reduction in the HRR peak.

Another important feature of polymer/layered silicate nanocomposites is their gas-barrier properties. Clays are believed to increase the barrier properties by creating a maze or 'tortuous path' (Figure 34) that retards the progress of the gas molecules through the matrix[26]. This can be illustrated by the polyimide/clay nanocomposite, which showed significantly improved barrier properties[210, 255]. This system, containing only a small fraction of OMLS (organically modified layered silicates), exhibited reduction in the permeability of small molecule gases, e.g. O_2, H_2O, He, CO_2 and ethylacetate vapours[210]. For example, at 2 wt. (%) clay loading, the permeability coefficient of water vapour was decreased ten-fold with synthetic mica relative to pristine polyimide. Figure 35 shows the oxygen gas permeability measurements for PLA/OMLS nanocomposites (PLA = polylactide)[263]. The relative permeability coefficient value, i.e. $P_{PLACN} = P_{PLA}$, where P_{PLACN} and P_{PLA} are permeability coefficients of nanocomposite and pure PLA respectively, is plotted as a function of the wt. (%) of OMLS. Data were fitted with the Nielsen theoretical expression[263]. There is a significant decrease in the O_2 permeability for the nanocomposites, which is more pronounced at higher clay contents. Polyurethane urea (PUU)/OMLS nanocomposites also reported reduced H_2O vapour permeability.

The effect of different types/shapes of fillers (2 wt. (%)) such as organoclay, either exfoliated montmorillonite, synthetic mica or intercalated clay tactoids (hectorite and saponite), on water permeability of both partially and totally exfoliated polyimide-based nanocomposites has been reported by Yano et al.[255]. Results of this study are given in Figure 36, where one can observe a drastic decrease in relative permeability with the increasing length of the clay. In other words, the best gas barrier properties will be obtained by fully exfoliated rather than long layered silicates. Consequently, the presence of spherical, plate, cylindrical, etc., fillers introduces a tortuous path for a diffusing penetrant. The reduction of permeability arises from the longer diffusive path that the penetrants have to travel in the presence of reinforcements.

Nanocomposites systems have also shown to be able to increase the ionic conductivity of polyethylene oxide (PEO)[167]. The PEO/Li-montmorillonite 60 wt. (%) intercalated nanocomposite showed a significant improvement regarding the stability of ionic conductivity at lower temperature compared to a conventional PEO/$LiBF_4$ mixture (Figure 37)[167].

This improvement is due to the fact that PEO is not able to crystallize when intercalated. This eliminates the presence of crystallites, which are non-conductive in nature. The conductivity of PEO/

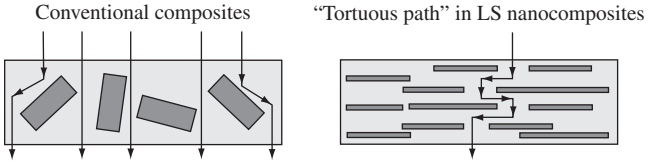

Figure 34. "Maze or tortuous path" in polymer/layered silicate nanocomposites [reproduced from reference 26 with the kind permission of the authors, Elsevier].

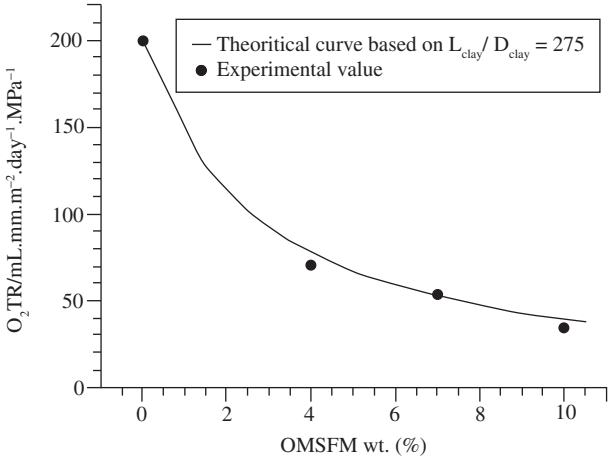

Figure 35. Oxygen gas permeability of neat PLA, various PLACNs as a function of OMLS content, measured at 20 °C, 90% relative humidity [reproduced from reference 263 with the kind permission of the authors, the American Chemical Society, USA].

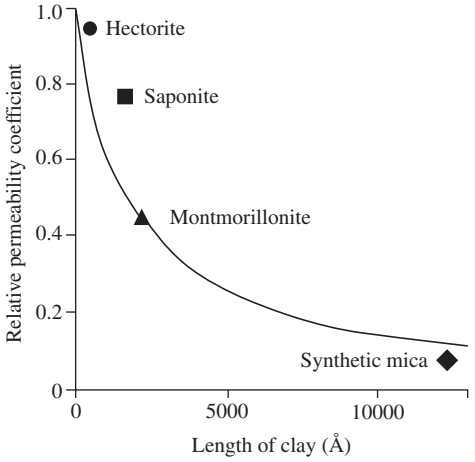

Figure 36. Clay length dependence on the relative permeability coefficient for poly(imide)/clay nanocomposites [reproduced from reference 255 with the kind permission of the authors, John Wiley & Sons Inc.].

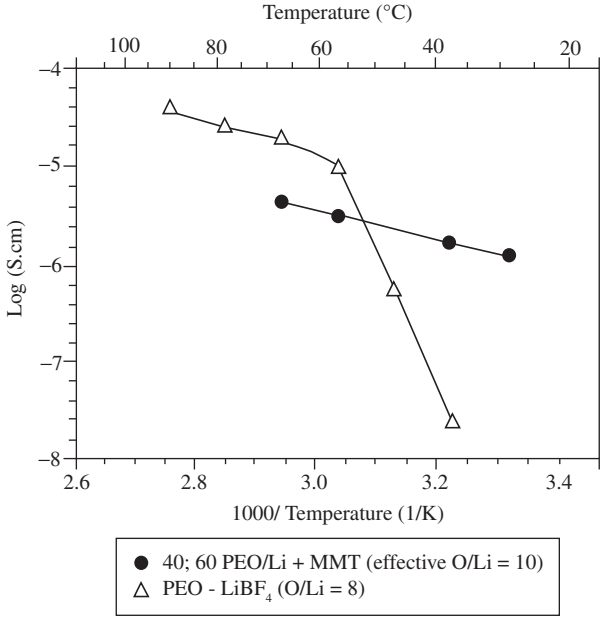

Figure 37. Arrhenius plots of ionic conductivity for $LiBF_4$/PEO, PEO Li^+ montmorillonite intercalated nanocomposite [reproduced from reference 167 with the kind permission of the authors, Wiley-VCH Verlag GmbH & Co.]

Li-montmorillonite nanocomposite is 1.6 x 10^{-6} Ω.cm^{-1} at 333 K and exhibits weak temperature dependence, with an activation energy of 2.8 kcal/mol. Therefore, the higher ionic conductivity at ambient temperature compared to conventional $LiBF_4$/PEO electrolytes and the single ionic conductor behaviour makes PEO/Li-montmorillonite nanocomposite a new promising electrolyte material.

Another outstanding feature of polymer nanocomposites prepared with OMLS as reinforcements is their noticeably improved biodegradability properties. Figure 38 shows real pictures of PLA/MMT 4 wt. (%) nanocomposites and their biodegradability process. Figure 39 shows the time dependence of the residual weight of the reinforcement (R_w) and the matrix molecular weight (M_w) for PLA and PLA/4 wt. % MMT under compost at 58 ± 2 °C [263,265].

It is very clear that the biodegradability of PLA is significantly enhanced after the incorporation of MMT. Within one month, both the M_w and the percentage of weight loss are at the same level for neat PLA and PLA/MMT 4 wt. (%). A sharp change then occurs in the weight loss of PLA/MMT 4 wt. (%) after one month. Finally, the nanocomposite is completely degraded after 2 months. This behaviour is accounted for the presence of terminal hydroxylated edge groups in the silicate layers, which start heterogeneous hydrolysis of the PLA matrix after absorbing water. Since this process takes time to start, the weight loss and degree of hydrolysis for PLA and PLA/4 wt. (%) MMT are almost the same up to 1 month. Other systems which showed large improvements in their biodegradability are PCL/OMLS and aliphatic polyester-based nanocomposites[18,26,266].

Another way of increasing the biodegradability of resulting materials is by addition of natural fibres. The use of renewable resources for making biodegradable polymers and reinforcements for nanocomposites may lead not only to the achievement of desirable properties, but also to the replacement, in the near future, of polymers obtained from non-renewable sources. This may help minimizing environmental degradation and waste disposal problems associated with the extensive use of the synthetic polymers in the world.

It is to be noted that a persistent stress on use of high technology reinforcements, such as CNTs, in the development of polymer nanocomposites may be a limiting factor in view of their high cost. In this scenario, the possibility of using large quantities of inexpensive natural nanofibrous materials may be explored. Such materials include the natural clay-serpentine group (chrysotile, antigorite, lizardite, amesite), nanolayers of the kaolin group (kaolinite, dickite, nacrite), ribbons of the sepiolite-paligorskite group (sepiolite, paligorskite), imogolite of volcanic origin and other minerals with graftable surfaces[176]. Further, synthetic materials made from the double hydroxide or hydroxyl salt groups with layered or fibrous structures, and even graftable single hydroxides having low cost and involving very common elements, will also play an important role in the future. In addition, vegetable fibres disposed of as agricultural production waste can be also reduced to nanosize range materials and used as reinforcement agents[336]. Even in such non-graftable reinforcement surfaces, one can choose an appropriate chemical treatment and moulding temperature and carefully select the polymer to arrive at the best chemical compatibilization, leading to the optimized properties of the resulting materials. It is observed that these treatments usually improve the surface adhesive characteristics of the vegetable fibres through the removal of non-crystalline components such as lignin and hemicelluloses.

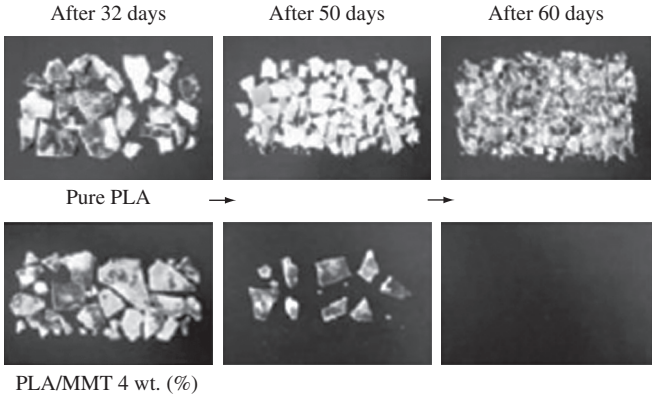

Figure 38. Biodegradability studies for neat PLA, PLA/MMT 4 wt. (%). The initial dimensions of the crystallized samples were 3 x 10 x 0.1 cm^3 [reproduced from reference 263 with the kind permission of the authors, Elsevier, the American Chemical Society, USA].

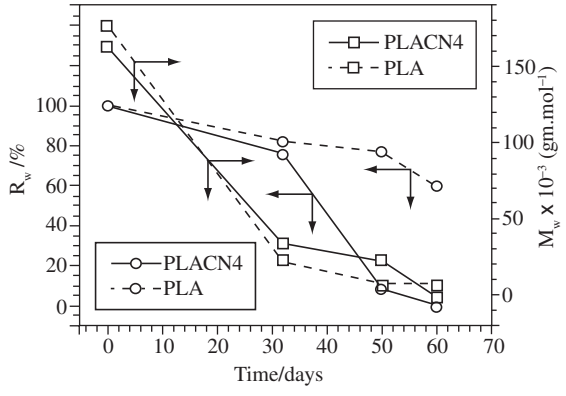

Figure 39. Time dependence of the residual weight, R_w, of the matrix molecular weight, M_w, for PLA, PLA/MMT 4 wt. (%) under compost at 58 ± 2 °C [reproduced from reference 265 with the kind permission of the authors, Elsevier].

3.3.3. Polymer-nanofibre / CNT nanocomposites

Carbon nanofibres, which are known to range from disordered "bamboo-like" to highly ordered "cup stacked" graphite structures, and have diameters in the range of 50-200 nm, have been employed as reinforcing materials in a variety of polymer matrix compounds, including both thermoset polymers such as epoxy, polyimide and phenolic, and thermoplastic polymers, as polypropylene, polystyrene, PMMA, Nylon 12, and PEEK[293,299]. Properties of nanotubes have already been given in Table 12. Young's modulus and tensile strength of the PP nanocomposites were found to increase due to the good adhesion of oxidised carbon fibres, but stiffness showed a reverse trend with the increasing volume fraction of the fibres. Even compressive strength and torsional moduli of the nanocomposites were found to be higher than that from the PEEK matrix. These scanty results on nanofibre-containing polymer composites reveal a need for more detailed and systematic studies on the dispersion and adhesion aspects, considering the varying morphologies of the fibres.

Thostenson and Chou[230,231] have described the elastic properties of aligned MWCNTs in a polystyrene matrix nanocomposite system. Adopting 'micromechanics' approach, they have derived the axial elastic properties of CNTs considering equivalent effective fibre properties, viz., tube diameter, distribution and volume distribution as a function of tube diameter. This gives a relationship between Young's modulus and various dimensions of fibres, including their volume. Similar relationships of physical and mechanical properties would probably help in producing materials for specific applications.

Significant toughening of polymer matrices after CNT incorporation has been reported. A phenol-based nanocomposite using CNTs with tube diameter <50 nm and length >0 μm showed an enhancement in Young's modulus and strength. SEM images of brittle tensile fracture

surfaces showed fairly uniform nanotube distribution and nanotube pullout[232]. Epoxy/DWCNT (double-wall carbon nanotubes) nanocomposites showed increased strength, Young's modulus, fracture toughness and strain to failure at a nanotube content of only 0.1 wt. (%)[233]. In this system, the nanotubes were highly dispersed in the polymer matrix. Also, phenylethyl terminated polyimide/MWCNT nanocomposites exhibited increased tensile Young's modulus and reduced tensile strength and ultimate strain. In this system, the nanotubes were a few hundred μm in length and 20-100 nm in diameter[234]. The polyethylene/MWCNT nanocomposite showed an increase in strain energy density by 150% and in ductility by 140%. Polyacrylonitrile/MWNTs systems showed 80% increase in energy to yield and energy to break[27]. Finally, silicone elastomer-SWCNT reinforced composites have shown dramatic increases in both stiffness and strength[30].

Coming to the morphological studies of CNT-containing polymer nanocomposites, Figure 40 represents a TEM image of polystyerene containing 5 wt. (%) nanocomposite film processed by Thostenson and Chou[230,231]. Large-scale dispersion and alignment of carbon nanotubes in the polymer matrix can be observed from this image, which could explain the observed properties.

Similarly, nanotubes are separated into individual tubes in the microstructure of epoxy/CNTs as shown in Figure 41, indicating their good dispersion. Also, they remain curved in the nanocomposite as a result of their sharp flexibility[150].

To conclude, CNT-polymer composites, though may pose greater challenges for the Materials Scientists, will exhibit unique properties as mentioned above and hence offer greater potentials in terms of applications. This is presented in the next Section.

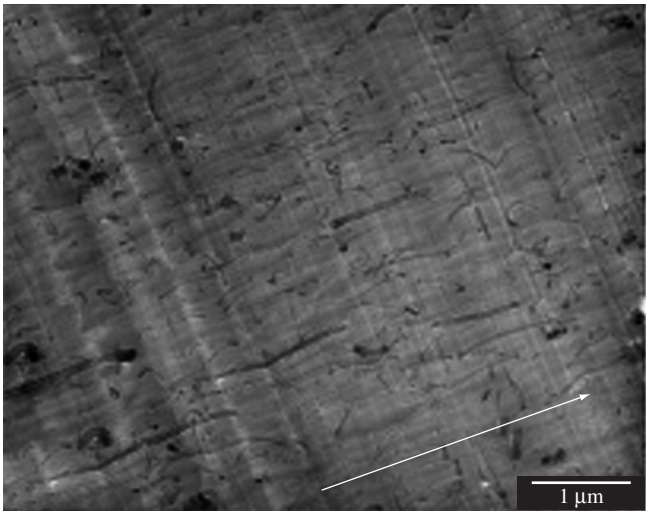

Figure 40. TEM micrograph of process-induced orientation in nanocomposite ribbons. The arrow indicates the direction of alignment taken as the principal direction with a nanotube orientation of 0° [reproduced from reference 230 with the kind permission of the authors, the Institute of Physics Publishing, USA].

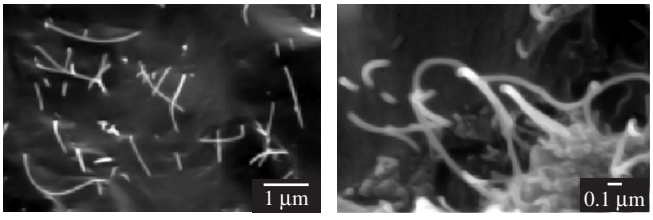

Figure 41. SEM micrographs showing the distribution of CNTs through epoxy resin [reproduced from reference150 with the kind permission of the authors, the American Institute of Physics, USA].

4. Applications of Nanocomposites[2,16-35,258,305,310,337-378]

From the foregoing, it becomes evident that nanocomposites may provide many benefits such as enhanced properties, reduction of solid wastes [lower gauge thickness films and lower reinforcement usage] and improved manufacturing capability, particularly for packaging applications. Tables 21 to 23 present potential applications of ceramic-, metal- and polymer-based nanocomposites, respectively. As it can be observed, the promising applications of nanocomposite systems are numerous, comprising both the generation of new materials and the performance enhancement of known devices such as fuel cells, sensors and coatings. Although the use of nanocomposites in industry is not yet large, their massive switching from research to industry has already started and is expected to be extensive in the next few years.

For instance, the $(Al_{1-x}Ti_xN)/\alpha$-Si_3N_4 super hard nanocomposite, which has been developed by the Czech company SHM Ltd. as a

Table 21. Potential applications of ceramic nanocomposite systems.

Nanocomposites	Applications
SiO_2/Fe	High performance catalysts, data storage technology.
ZnO/Co	Field effect transistor for the optical femtosecond study of interparticle interactions.
Metal oxides/Metal	Catalysts, sensors, opto-electronic devices.
$BaTiO_3$/SiC, PZT/Ag	Electronic industry, high performance ferroelectric devices.
SiO_2/Co	Optical fibres.
SiO_2/Ni	Chemical sensors.
Al_2O_3/SiC	Structural materials.
Si_3N_4/SiC	Structural materials.
$Al_2O_3/NdAlO_3$ & $Al_2O_3/LnAlO_3$	Solid-state laser media, phosphors and optical amplifiers.
TiO_2/Fe_2O_3	High-density magnetic recording media, ferrofluids and catalysts.
Al_2O_3/Ni	Engineering parts.
$PbTiO_3/PbZrO_3$	Microelectronic and micro-electromechanical systems.

Table 22. Potential applications of metal nanocomposite systems.

Nanocomposites	Applications
Fe/MgO	Catalysts, magnetic devices.
Ni/PZT	Wear resistant coatings and thermally graded coatings.
Ni/TiO_2	Photo-electrochemical applications.
Al/SiC	Aerospace, naval and automotive structures.
Cu/Al_2O_3	Electronic packaging.
Al/AlN	Microelectronic industry.
Ni/TiN, Ni/ZrN, Cu/ZrN	High speed machinery, tooling, optical and magnetic storage materials.
Nb/Cu	Structural materials for high temperature applications.
$Fe/Fe_{23}C6/Fe_3B$	Structural materials.
Fe/TiN	Catalysts.
Al/Al_2O_3	Microelectronic industry.
Au/Ag	Microelectronics, optical devices, light energy conversion.

Table 23. Potential applications of polymer nanocomposite systems.

Nanocomposites	Applications
Polycaprolactone/SiO_2	Bone-bioerodible for skeletal tissue repair.
Polyimide/SiO_2	Microelectronics.
PMMA/SiO_2	Dental application, optical devices.
Polyethylacrylate/SiO_2	Catalysis support, stationary phase for chromatography.
Poly(p-phenylene vinylene)/SiO_2	Non-liner optical material for optical waveguides.
Poly(amide-imide) / TiO_2	Composite membranes for gas separation applications.
poly(3,4-ethylene-dioxythiophene)/V_2O_5	Cathode materials for rechargeable lithium batteries.
Polycarbonate/SiO_2	Abrasion resistant coating.
Shape memory polymers/SiC	Medical devices for gripping or releasing therapeutics within blood vessels.
Nylon-6/LS	Automotive timing-belt – TOYOTA.
PEO/LS	Airplane interiors, fuel tanks, components in electrical and electronic parts, brakes and tires.
PLA/LS	Lithium battery development.
PET/clay	Food packaging applications. Specific examples include packaging for processed meats, cheese, confectionery, cereals and boil-in-the-bag foods, fruit juice and dairy products, beer and carbonated drinks bottles.
Thermoplastic olefin/clay	Beverage container applications.
Polyimide/clay	Automotive step assists - GM Safari and Astra Vans.
Epoxy/MMT	Materials for electronics.
SPEEK/laponite	Direct methanol fuel cells.

tribological coating for tools, is suitable for hard and dry cutting operations such as drilling, turning and milling, and is reported to be now industrialized[337,339]. In this case, a novel method, which employs vacuum arc coating with a rotating cathode, is used for commercial production. This super hard $(Al_{1-x}Ti_x)N/\alpha\text{-}Si_3N_4$ possess high tensile strength, in the range of 10-110 GPa, and a lifetime 2-4 times higher than that of the materials currently employed as wear resistant coatings.

Similarly, one of the leading application areas is the automotive sector, with striking impact due to improved functionalities such as ecology, safety, comfort, etc. Details on the commercial usage of nanocomposites in automotives and future developments in this sector (including CNT-based nanocomposites) are now available[362]. For instance, there are reports on the current use of a number of nanocoatings in different parts of Audi, Evobus and Diamler Chrysler automobiles, as well as ongoing trials on fuel cells, porous filters (foams) and energy conversion components, which include nanoTiO_2-containing paints. Additionally, light weight bodies made of metal- or polymer-based nanocomposites with suitable reinforcements are reported to exhibit low density and very high strength (e.g. carbon Bucky fibers, with strength of 150 GPa and weight $\approx 1/5^{th}$ of steel). Also, two-phase heterogeneous nanodielectrics, generally termed dielectric nanocomposites, have wide applications in electric and electronic industries[338].

Metal and ceramic nanocomposites are expected to generate a great impact over a wide variety of industries, including the aerospace, electronic and military[305], while polymer nanocomposites major impacts will probably appear in battery cathodes[6,342], microelectronics[343], nonlinear optics[344], sensors[345], etc. Improved properties include significant enhancements in fracture strength (about 2 times) and toughness (about one half time); no time dependent wear transitions even at very low loads; higher high temperature strength and creep resistance; increased hardness with increasing heat treatment temperature; hardness values higher than those of existing commercial steel and alloys; possibility of synthesis of inexpensive materials; and significant increase in Young's modulus [about 105%], shear modulus and fracture strength (almost 3 times compared to microcomposites). These are brought out mainly by the nanosize reinforcements used, which result in an appropriate morphology for the products. Tables 21 and 22 summarize the possible developments associated with these materials in catalysts, sensors, structural materials, electronic, optical, magnetic, mechanical and energy conversion devices suggested by researchers in the field.

CNT-ceramic composites, on their turn, are reported[340] to be potential candidates for aerospace and sports goods, composite mirrors and automotive spares requiring electrostatic painting. Such materials have also been reported[341] to be useful for flat panel displays, gas storage devices, toxic gas sensors, Li^+ batteries, robust but lightweight parts and conducting paints. One example is the Al_2O_3-CNT composite, which shows high contact damage resistance without a corresponding increase in toughness and hardness. It is reported[92] to be a candidate for engineering and biomedical applications.

Despite these possibilities, there are only limited examples of industrial use of nanocomposite, mainly due to the challenges in processing and the cost involved, particularly for non-structural applications. In fact, one recent review[371] deals with various methods for the preparation of super hard coatings with merits and demerits of each method. However, the intense research in both metal- and ceramic-based nanocomposites suggests that the days are not far off when they will be actually in use. The cost factor may be a particularly serious problem for general engineering applications, while this may not be the case for specialized applications in electronics, aerospace, biomedical and other sectors, since the advantages might far outweigh costs and concerns in these sectors.

On the other hand, polymer-based nanocomposites are in the forefront of applications due to their more advanced development status compared to metal and ceramic counterparts, in addition to their unique properties. These include 2-3 fold strength property increase, even with low reinforcement content (1-4 wt. (%)) [*e.g.* 102.7% in Young's modulus] with complete elimination of voids/holes; gas barrier properties (about 200,000 times over oriented PP and about 2000 times that of Nylon-6 with tenfold requirements of expensive organic modifiers) [372], biodegradation and reduced flammability [about 60% reduction of heat release rate], etc. In addition, a good possibility of enhancing the shelf life of the existing MRE packaging and trays used in the UGR-H&S polymeric materials has also been reported[350]. This is due to the limitations of existing MRE packings, which do not meet the US military standards such as minimum shelf life of 6 and 12 months at about 322 K (120 °F) and 299 K (80 °F) respectively. In this case, nanocomposites,

which exhibit better gas barrier properties, can provide a longer shelf life. Such packaging, with different matrices and reinforcements, as well as different processing conditions, is being field tested by the US army since 2002 to arrive at an optimum combination. This is expected to reduce cost by 10-30% (nearly US$ 1-3 million) compared to the presently used materials, in addition to better performance.

Various types of polymer-based nanocomposites, containing insulating, semiconducting or metallic nanoparticles, have been developed to meet the requirements of specific applications. Recently, some PLS nanocomposites have become commercially available[18], being applied[237] as ablatives and as high performance biodegradable composites[265,267,280,343,346], as well as in electronic and food packaging industries[346,347]. These include Nylon-6 (e.g. Durethan LDPU60 by Bayer Food Packages)[18] and polypropylene for packaging and injection-molded articles, semi-crystalline nylon for ultra-high barrier containers and fuel systems, epoxy electrocoating primers and high voltage insulation, unsaturated polyester for watercraft lay-ups and outdoor advertising panels, and polyolefin fire-retardant cables, electrical enclosures and housings. Table 24 shows some examples of commercially available polymer nanocomposites. As an example, Nylon-6/surface-modified montmorillonite 2 wt. (%) nanocomposites are currently available from two commercial sources, Honeywell Engineered Polymers & Solutions and Bayer AG. Some of the products made from nanocomposites are shown in Figure 42.

Technological contributions in the areas of gas barrier, reinforcement and flame retardancy have also been extensively exploited[355,356]. For example, heat-resistant polymer nanocomposites are used to make fire fighter protective clothing and lightweight components suitable to work in situations of high temperature and stress. This includes hoods of automobiles and skins of jet aircrafts, as opposed to heavier and costlier metal alloys. They can also replace corrosion-prone metals in the building of bridges and other large structures with potentially lighter and stronger capabilities[357, 358]. Also, unsaturated polyester (UPE) nanocomposites can be employed in fibre-reinforced products used in marine, transportation and construction industries[359-361]. Currently, UPE/fibreglass nanocomposites, whose formulations are available from Polymeric Supply, Inc., are being used in boat accessories that are stronger and less prone to colour fading[362].

Regarding the variety of applications of polymer nanocomposites, prominent impacts over the automotive industry can be highlighted, including their use in tyres, fuel systems, gas separation membranes in fuel cells and seat textiles, mirror housings on various vehicle types, door handles, engine covers, intake manifolds and timing belt covers[363,364], with some of these already being exploited. For example, a thermoplastic nanocomposite containing nanoflake reinforcements (trade name Basell TPO-Nano) is being employed for the development of stiff and light exterior parts, like the step-assists by GM[348]. Also, porous polymer nanocomposites can be employed for the development of pollution filters[365]. Other promising technological application in the horizon is in air bag sensors, where nano-optical platelets are kept inside the polymer outer layer for transmitting signals at speed of light gaining milliseconds to bring down the level of possible impact injuries[373]. Finally, polymer/inorganic nanocomposites with improved conductivity, permeability, water management and interfacial resistance at the electrode are natural candidates for the replacement of traditional Nafion PEM in fuel cells, and are currently under trial[349].

Improvements in the mechanical properties of polymer nanocomposites have also resulted in their many general/industrial applications. These include impellers and blades for vacuum cleaners, power tool housings, and mower hoods and covers for portable electronic equipment, such as mobile phones and pagers[366]. Another example is the use of polymer nanocomposites in glues for the manufacturing of pressure moulds in the ceramic industry.

The development of environmentally friendly, non-foil and better packaging materials can reduce the amount of solid waste, improve package manufacturing capabilities, and reduce the overall logistics

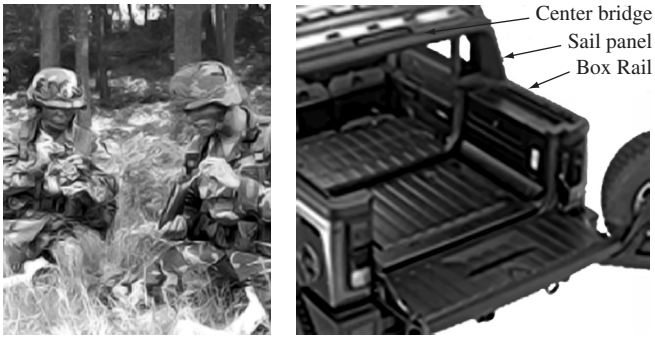

Figure 42. Nanocomposite-containing products [reproduced from references 347, 351, with the kind permission of US Army Natick Soldier Center, Plastics Technology, USA, AzoNano.com, PvtLtd., USA].

Table 24. Commercial polymer nanocomposites and their respective target markets (CNT = carbon nanotubes).

Supplier & Tradename	Matrix resin	Nano-filler	Target market
Bayer AG (Durethan LPDU)	Nylon 6	Organoclay	Barrier films
Clariant	PP	Organoclay	Packaging
Creanova (Vestamid)	Nylon 12	CNTs	Electrically conductive
GE Plastics (Noryl GTX)	PPO/Nylon	CNTs	Automotive painted parts
Honeywell (Aegis)	Nylon 6 Barrier Nylon	Organoclay Organoclay	Multi-purpose Bottles and film
Hyperion	PETG, PBT, PPS, PC, PP	CNTs	Electrically conductive
Kabelwerk Eupen of Belgium	EVA	Organoclay	Wire & cable
Nanocor (Imperm)	Nylon 6 PP Nylon MDX6	Organoclay Organoclay Organoclay	Multi-purpose moulding PET beer bottles
Showa Denko (Systemer)	Nylon 6 Acetal Clay	Mica Clay, mica	Flame retardancy Multi-purpose
Ube (Ecobesta)	Nylon 6, 12 Nylon 6, 66	Organoclay Organoclay	Multi-purpose Auto fuel systems
Antai Haili Ind. & Commerce of China	UHMWPE	Organoclay	Earthquake-resistant pipes

burden to users. In this context, the incorporation of nanoclay particles into thermoplastic resins has shown to be highly effective to improve barrier properties and package survivability[351]. Such excellent barrier characteristics have resulted in considerable interest in clay nanocomposites in food packaging applications, both flexible and rigid. Specific examples include packaging for processed meats, cheese, confectionery, cereals and boil-in-the-bag foods, also extrusion-coating applications in association with paperboard for fruit juice and dairy products, together with co-extrusion processes for the manufacture of beer and carbonated drinks bottles[367]. The use of nanocomposite formulations would be expected to enhance considerably the shelf life of many types of food. Honeywell industries have also been active in developing a combined active/passive oxygen barrier system for polyamide-6 materials[368]. It is mentioned here that Triton Systems and the US Army are conducting further work on barrier performance in a joint investigation, as mentioned earlier. They are trying to develop a non-refrigerated packaging system capable of maintaining food freshness for three years. Polymer/clay nanocomposites are currently showing considerable promise for this application.

The reduction of solvent transmission is another interesting aspect of polymer/clay nanocomposites. A study conducted by the UBE Industries has revealed[347] significant reductions in fuel transmission through polyamide-6/66 polymers by incorporation of a nanoclay filler. As a result, these materials are very attractive for the development of improved fuel tanks and fuel line components for cars. In addition, the reduced fuel transmission means significant cost reductions. The presence of filler incorporation at nanolevels has also been shown to have significant effects on the transparency and haze characteristics of films[369] in comparison to conventionally filled polymers. The ability to minimize the extent to which water is absorbed can be a major advantage for polymer materials that are degraded in moist environments[370].

Finally, CNT-polymer composites are reported[28] to be potential candidates for data storage media, photovoltaic cells and photo diodes, optical limiting devices, drums for printers, etc.

5. Perspectives

Outstanding potentials of nanocomposites can be exemplified by the massive investments from many companies and governments throughout the world. As a result, nanocomposites are expected to generate a great impact in world economy and business. This is very much evident from the publications pouring in, particularly on a variety of properties suited for different applications[350]. According to a report from Principia Partners, which is illustrated in Table 25, a market size of over than U$ 1,834 billion (USD) is estimated by 2009, considering only the different applications of polymer/clay nanocomposites[350]. The estimative may not be exaggerated, since many of the application areas already use these composites, with some of them being commercialized by many leading industries. Packaging, coating and automotive sectors are in the forefront for the use of these new materials.

Table 25. Estimated market size, by 2009, regarding different applications of polymer/clay nanocomposites [reproduced from reference 350 with the kind permission of the author and publishers]

Technology/Application	Estimated market size (by 2009) million US$
Polymer-Clay Nanocomposites	Over $183 billion US$
Packaging	671
Automotive	631
Building & Construction	276
Coatings	115
Industrial	87
Others	122

With increasing demand for high performance systems such as nanofillers and their composites and many sectors looking for them at low costs, optimistic estimates do not seem beyond reach[372]. A bright future is evident as many leading industrial laboratories, such as Argonne National Laboratory, are ready for commercialization of their nanoproducts [organoclays] and looking for industrial partners to develop and/or test them in a wide range of applications. Many of these are consumer products, and hence the envisaged market is expected to establish itself. For example, electroconductive polymers, nanosmart switches and sensors for automotives are already in use by GE and Cabot in USA, while since 2002 General Motors has successfully used nanocomposites containing clay and talc in their exterior structural components.

Further, as new power production and storage devices are attractive products, other nanotech revolutions expected to take place in the near future are reported[373] to be hydrogen storage, fuel cells, supercapacitors and batteries. In fact, it has been pointed out that the infrastructure cost of automotives would decrease by 10-100 times by the use of fuel cells alone, with other nanotechnologies having similar impact. Future areas of research, particularly for the automotive industry could be i) improved fire retardancy of nanocomposites, which can be used as interior parts, ii) improved weatherability for use as exterior parts, and iii) bipolarity, obtained by the use of nanocarbons, for the production of fuel cells. Similarly, the coating and internal structure of combustion engines may receive attention in the case of ceramic-based nanocomposites.

Nanoclays are expected to have 50% of the total nanomaterials market by 2020. Also, with the expected decrease in cost of CNTs, their nanocomposites are also expected to gain large share in the markets, thereby leading to the rapid commercialization of CNTs themselves[374]. It is also reported that two of the sectors, automotive and packaging, which will account for about 40% of demand by 2020, will be most important for the next decade or so. Then, the construction sector will probably dominate, while CNT-based nanocomposites will replace the presently used conducting materials in the electrical and electronic industries[375].

Considering the use of polymer-based nanocomposites during 2003 at 11,000 tons (11 million kg) at US$ 90.8 million, Business Communications Co. Inc., in its report on nanocomposites published in April 2004, has estimated this market to increase by nearly 3 times (35,960 tons) at US$ 211.1 during the current year (2008), with an annual growth rate (AAGR) of 18.4%[377]. Of this, thermoplastics, which were about 5.68 million kg at US$ 70.7 in 2003, would grow to 27.74 million kg with about 20.4% AAGR at US$ 178.9 million, while thermosets, with 5.45 million kg at US$ 20.1 million, would grow to 8.22 million kg with about 9.9 AAGR at US$ 32.2 million. Even if some difficulties are to be encountered for this, present applications of these materials are expected to grow higher than 20% of the total demand of polymer composites, with the fastest demand in engineered plastics and elastomers[374,376]. On the other hand, with thermoset-based nanocomposites being not so diverse compared to their thermoplastics counterparts, their market is expected to grow at the rate mentioned above based on the current uses of these composites in pre-finished wood flooring and other sectors.

There are other forecasts for US such as the ones from Freedonia Industry, which reports on the profiles of major industries in the area of nanocomposites in USA, market trends and indicators for these materials for every five years from 2010[375]. According to them, the demand for nanocomposites will be about 159 million kg by 2010 and about 3.2 billion kg, valued at US$ 15 billion, by 2020. The other estimate[376] for the global nanocomposite market rises to US$ 250 million with AAGR between 18-25% by 2008. It is also reported[374] that the packaging industry alone would use about 1.7 million kg of polymer

nanocomposites in the beverage and food industries by 2009, and that this will grow to about 45 million kg. All the above mentioned projections, though varying marginally, may not be exaggerated in view of the research options made by some of the developed countries, with USA leading with 400 research centres and industries with investments to the tune of US$ 3.4 billion, Europe with 175 organizations/industries with about US$ 1.7 billion and Japan with 100 organizations[350].

Some of the challenges to be faced for the success of the above projections, which will also give future research directions, include: suitable reinforcements such as nanofibres with or without spinning, which will have higher strength properties, being lighter than their micro counterparts and hence appearing as superior structural components; use of nanofibres in different areas such as biomedical, electrical and optical, for various functional devices; conducting polymer-based nanomaterials for electrochemical applications; modification of the mechanical behaviour of nanocomposites to get higher performances; surface modification of polymer nanofibres for their use in polymer matrices to overcome the poor interfacial bonding; modelling and simulation of mechanical properties of nanofibre-containing composites, etc.[377].

Other issues, which are also expected to get due attention, include various processing parameters in the case of the three types of nanocomposites, without which their wide spread commercialization would not come through. These include problems with compatibility and deagglomeration, which can be overcome through surface modification of reinforcements for homogeneous dispersion without agglomeration. The above, along with appropriate positioning of reinforcements [exfoliation and orientation] in the case of polymer-based composites are also issues to be solved.

Other promising area for future research on proper inexpensive reinforcements is the use of cheap and abundantly available polymeric (maybe recyclable) and reinforcing materials of natural origin for wide applications. If the latter can replace expensive carbon nanotubes, the cost of their nanocomposite products may be reduced to extend them to popular applications. Hence, concentrated efforts will be needed to find new formulations with materials from renewable resources (such as polymers derived from plasticized saccharides, polylactide (PLA), polyhydroxylalkanoates (PHAs), poly (ε-caprolactone), etc.), reinforced with easily available mineral/vegetal materials or synthetic reinforcements based on common elements like hydroxides, layered double hydroxides and layered hydroxide salts. The same procedure can also be used to improve the properties of synthetic biodegradable polymers. Research in these directions will be a certainty, keeping in view the increased attention on cleaner environment and ecology.

The study of nanocomposites is an interdisciplinary area, encompassing physics, chemistry, biology, materials science and engineering. Therefore, the knowledge arising from scientists with different backgrounds will undoubtedly create new science, and in particular new materials, with unforeseen technological possibilities such as creation of macroscopic engineered materials through nanoscale structures. It is therefore rightly pointed out that this calls for basic research on structure-property correlations in nanocomposites, leading to new challenges in the development of suitable fabrication techniques for dealing with nanoscale materials, for their characterization and mechanics, in order to understand interactions at such sizes[30]. Another exciting aspect is that nanocomposites will benefit many sectors of our society, including electronics and chemical, space and transportation industries, as well as medicine, health care and environmental protection. Because of this, nanocomposites are expected be of high impact in the improvement of our quality of life in the coming years.

As the properties of nanostructured composites are highly structure/size dependent, many research studies still have to be performed to provide a better understanding of the structure-property relationship in such systems. This is an essential requirement to allow the nanoscale design of multi-functional materials for engineering applications. In this regard, critical issues to be looked into include aspects of dispersion, alignment, volume and rate of fabrication and, finally, cost effectiveness. Some light has been thrown on these aspects[30]. Probably, processing-structure-properties maps similar to those developed for metals and alloys by Ashby[379] may further enhance the potentials of nanocomposites. This is because structure, which is dictated by the processing method, in turn dictates the properties of materials. Added to this is the engineering aspect of design.

For materials scientists, design could be one of the following[380]: i) design of materials having combinations of unique properties or ii) selection of materials having better characteristics for a specific purpose or iii) development of a new process for providing one of the above mentioned materials. Besides, in engineering a term called 'performance index' (P) is defined, which correlates the properties of materials for a given product, and helps in their selection for specific applications. The higher the value of P, the better will be the performance[380]. Further, another correlation generally used is between the relative cost and the performance index, whereby one can arrive at the economical material selection for a given product. The above concepts should also be applied in the case of nanocomposites, so that one could get the maximum benefit from them in any application.

Finally, as part of the social implications of this nascent and potential technology, there are some safety aspects to be considered while dealing with nanosized particles and their composites. For example, fabrics coated with nanoparticles are available, which can be configured to imbue the fabric with various attributes. Aerosolised chemical and biological agents are a clear threat that is likely to grow in the future. The release of nanoparticles into the environment is a major health and safety issue. Hence there is an increasing need for research into emission of nanocomposites and nanoparticles. Potentially harmful characteristics of nanotechnology products based on their large surface area, crystalline structure and reactivity may facilitate their easy transport into the environment or interaction with cell constituents, thus exacerbating many harmful effects related to their composition. One recent conference was devoted to the study of the safety and risks of nanoparticles[381], while the U.S. Environmental Protection Agency (EPA), as part of its Science to Achieve Results (STAR) program, is seeking applications that evaluate the potential impacts of manufactured nanomaterials on human health and the environment. This is important as new nanomaterials are constantly being manufactured; there is always a possibility of human and environmental exposure to waste streams, or other pathways entering the environment[382].

6. Conclusions

In conclusion, new technologies require materials showing novel properties and/or improved performance compared to conventionally processed components. In this context, nanocomposites are suitable materials to meet the emerging demands arising from scientific and technologic advances. Processing methods for different types of nanocomposites (CMNC, MMNC and PMNC) are available, but some of these pose challenges thus giving opportunities for researchers to overcome the problems being encluntered with nanosize materials. They offer improved performance over monolithic and microcomposite counterparts and are consequently suitable candidates to overcome the limitations of many currently existing materials and devices. A number of applications already exists, while many potentials are possible for these materials, which open new vistas for the future. In view of their unique properties such as very high mechanical properties even at low loading of reinforcements, gas barrier and flame related properties, many potential applications and hence the market for these materials have been projected in various sectors. Thus all the three types of nanocomposites provide opportunities and rewards creating new world wide interest in these new materials.

Acknowledgements

We are grateful to all authors of the papers, publishers of the journals from where tables and figures have been reproduced [The American Chemical Society, American Institute of Chemical Engineers, American Institute of Physics, Elsevier, Institute of Physics, Japan Society of Powder, Powder Metallurgy, John Wiley & Sons, Materials Research Society, Plastics Technology Magazine, Springer-Verlag, Wiley-VCH Verlag Gmbh & Co, web sites], for their courtesy and kind permission. The authors sincerely express their gratitude to Professor Jaisa F. Soares of Department of Chemistry, UFPR for her reading of the full manuscript, editing both technical and language aspects as well for her critical suggestions. We also acknowledge Mr. Gregorio Guadalupe Carbajal Arizaga, Department of Chemistry, UFPR, Mahesh Kestur Satya, USA, for their reading of the paper and useful suggestions.

References

1. Roy R, Roy RA, Roy DM. Alternative perspectives on "quasi-crystallinity": non-uniformity and nanocomposites. *Materials Letters*. 1986; 4(8-9):323-328.
2. Schmidt D, Shah D, Giannelis EP. New advances in polymer/layered silicate nanocomposites. *Current Opinion in Solid State & Materials Science*. 2002; 6(3):205-212.
3. Gleiter H. Materials with ultrafine microstructures: retrospectives and perspectives. *Nanostructured Materials*. 1992; 1(1):1-19.
4. Braun T, Schubert A, Sindelys Z. Nanoscience and nanotechnology on the balance. *Scientometrics*. 1997; 38(2):321-325.
5. Kamigaito O. What can be improved by nanometer composites? *Journal of Japan Society of Powder Metalurgy*. 1991; 38:315-321.
6. Iijima S. Helical microtubes of graphitic carbon. *Nature*. 1991; 354(6348):56-58.
7. Biercuk MJ, Llaguno MC, Radosvljevicm, HJ. Carbon nanotube composites for thermal management. *Appied Physics Letters*. 2002; 80(15):2767-2769.
8. Ounaies Z, Park C, Wise KE, Siochi EJ, Harrison JS. Electrical properties of single wall carbon nanotube reinforced polyimide composites. *Composites Science and Technology*. 2003; 63(11):1637-1646.
9. Weisenberger MC, Grulke EA, Jacques D, Ramtell T, Andrews R. Enhanced mechanical properties of polyacrylonitrile: multiwall carbon nanotube composite fibers. *Journal of Nanoscience and Nanotechnology*. 2003; 3(6):535-539.
10. Dalton AB, Coolins S, Muñoz E, Razal JM, Ebron VH, Ferraris JP et al. Super-tough carbon-nanotube fibres: these extraordinary composite fibres can be woven into electronic textiles. *Nature*. 2003; 423(6941):703-703.
11. Choa YH, Yang JK, Kim BH, Jeong YK, Lee JS, Nakayama T et al. Preparation and characterization of metal: ceramic nanoporous nanocomposite powders. *Journal of Magnetism and Magnetic Materials*. 2003; 266(1-2):12-19.
12. Wypych F, Seefeld N, Denicolo I. Preparation of nanocomposites based on the encapsulation of conducting polymers into 2H-MoS_2 and 1T-TiS_2. *Quimica Nova*. 1997; 20(4):356-360.
13. Aruna ST, Rajam KS. Synthesis, characterisation and properties of Ni/PSZ and Ni/YSZ nanocomposites. *Scripta Materialia*. 2003; 48(5):507-512.
14. Giannelis EP. Polymer layered silicate nanocomposites. *Advanced Materials*. 1996; 8(1):29-35.
15. Wypych F, Adad LB. Grothe MC: synthesis and characterisation of the nanocomposites K-0, $K_{0,1}(PEO)_xMoS_2$ (X = 0,5; 1,2). *Quimica Nova*. 1998; 21(6):687-692.
16. Sternitzke M. Review: structural ceramic nanocomposites. *Journal of European Ceramic Society*. 1997; 17(9):1061-1082.
17. Peigney A, Laurent CH, Flahaut E, Rousset A. Carbon nanotubes in novel ceramic matrix nanocomposites. *Ceramic International*. 2000; 26(6):677-683.
18. Alexandre M, Dubois P. Polymer-layered silicate nanocomposites: preparation, properties and uses of a new class of materials. *Materials Science & Engineering*. 2000; 28(1-2):1-63.
19. Gangopadhyay R, Amitabha D. Conducting polymer nanocomposites: a brief overview. *Chemistry of Materials*. 2000; 12(7): 608-622.
20. Thostenson ET, Ren Z, Chou TW. Advances in the science and technology of carbon nanotubes and their composites: a review. *Composites Science & Technology*. 2001; 61(13):1899-1912.
21. Pokropivnyi VV. Two-dimensional nanocomposites: photonic crystals and nanomembranes (review): Types and preparation. *Powder Metallurgy and Metal Ceramics*. 2002a; 41(5-6):264-272.
22. Pokropivnyi VV. Two-dimensional nanocomposites: photonic crystals and nanomembranes (review). II: Properties and applications. *Powder Metallurgy and Metal Ceramics*. 2002b; 41(7-8):369-381.
23. Gall K, Dunn ML, Liu Y, Finch D, Lake M, Munshi NA. Shape memory polymer nanocomposites. *Acta Materialia*. 2002; 50(20):5115-5126.
24. Kickelbick G. Concepts for the incorporation of inorganic building blocks into organic polymers on a nanoscale. *Progress in Polymer Science*. 2003; 28(1):83-114.
25. Fischer H. Polymer nanocomposites: from fundamental research to specific applications. *Materials Science and Engineering: C*. 2003; 23(6-8):763-772.
26. Ray SS, Okamoto M. Polymer - layered silicate nanocomposites: a review from preparation to processing. *Progress in Polymer Science*. 2003; 28(11):1539-1641.
27. Andrews R, Weisenberger MC. Carbon nanotube polymer composites. *Current Opinion in Solid State and Materials Science*. 2004; 8(1):31-37.
28. Wang C, Guo ZX, Fu S, Wu W, Zhu D. Polymers containing fullerene or carbon nanotube structures. *Progress in Polymer Science*. 2004; 29(11):1079-1141.
29. Pandey JK, Reddy KR, Kumar AP, Singh RP. An overview on the degradability of polymer nanocomposites. *Polymer Degradation and Stability*. 2005; 88(2):234-250.
30. Thostenson ET, Li C, Chou TW. Nanocomposites in context. *Composites Science and Technology*. 2005; 65(3-4):491-516.
31. Jordan J, Jacob KI, Tannenbaum R, Sharaf MA, Jasiuk I. Experimental trends in polymer nanocomposites: a review. *Materials Science and Engineering: A*. 2005; 393(1-2):1-11.
32. Choi SM, Awaji H. Nanocomposites: a new material design concept. *Science and Technology of Advanced Materials*. 2005; 6(1):2-10.
33. Xie XL, Mai YW, Zhou XP. Dispersion and alignment of carbon nanotubes in polymer matrix: a review. *Materials Science and Engineering: R*. 2005; 49(4):89-112.
34. Ray SS, Bousmina M. Biodegradable polymers and their layered silicate nanocomposites: in greening the 21st century materials world. *Progress in Matererials Science*. 2005; 50(8):962-1079.
35. Pandey JK, Kumar AP, Misra M, Mohanty AK, Drzal LT, Singh RP. Recent advances in biodegradable nanocomposites. *Journal of Nanoscience and Nanotechnology*. 2005; 5(4):497-526.
36. Awaji H, Choi SM., Yagi E. Mechanisms of toughening and strengthening in cermaic-based nanocomposites. *Mechanics of Materials* 2002; 34(7):411-422.
37. Niihara K. New design concept of strctural ceramics-ceramic nanocomposite. *Journal of the Ceramic Society of Japan (*Nippon Seramikkusu Kyokai Gakujutsu Ronbunshi). 1991; 99(6):974-982.
38. Nakahira A, Niihara K. Strctural ceramics-ceramic nanocomposites by sintering method: roles of nano-size particles. *Journal of the Ceramic Society of Japan*. 1992; 100(4):448-453.
39. Ferroni LP, Pezzotti G, Isshiki T, Kleebe HJ. Determination of amorphous interfacial phases in Al_2O_3/SiC nanocomposites by

computer-aided high-resolution electron microscopy. *Acta Materialia*. 2001; 49(11):2109-2113.

40. She J, Inoue T, Suzuki M, Sodeoka S, Ueno K. Mechanical properties and fracture behavior of fibrous Al_2O_3/Sic ceramics. *Journal of European Ceramic Society*. 2000; 20(12):1877-1881.
41. Tjong SC, Wang GS. High-cycle fatigue properties of Al-based composites reinforced with in situ TiB_2 and Al_2O_3 particulates. *Materials Science and Engineering: A*. 2004; 386(1-2):48-53.
42. Athawale AA, Bhagwat SV, Katre PP, Chandwadkar AJ, Karandikar P. Aniline as a stabilizer for metal nanoparticles. *Materials Letters*. 2003; 57(24-25):3889-3894.
43. Akita H, Hattori T. Studies on molecular composite. I. Processing of molecular composites using a precursor polymer for poly (P-Phenylene benzobisthiazole). *Journal of Polymer Science: Part B: Polymer Physics*. 1999; 37(3):189-197.
44. Akita H, Kobayashi H. Studies on molecular composite. III. Nano composites consisting of poly (P-phenylene benzobisthiazole) and thermoplastic polyamide. *Journal of European Ceramic Society*. 1999; 37(3):209-218.
45. Akita H, Kobayashi H, Hattori T, Kagawa K. Studies on molecular composite. II. Processing of molecular composites using copolymers consisting of a precursor of poly (P-phenylene benzobisthiazole) and aromatic polyamide. *Journal of European Ceramic Society*. 1999; 37(3):199-207.
46. Chang JH, An YU. Nanocomposites of polyurethane with various organoclays: thermomechanical properties, morphology, and gas permeability. *Journal of European Ceramic Society*. 2002; 40(7):670-677.
47. Zavyalov SA, Pivkina AN, Schoonman J. Formation and characterization of metal-polymer nanostructured composites. *Solid State Ionics*. 2002; 147(3-4):415-419.
48. Thompson CM, Herring HM, Gates TS, Connel JW. Preparation and characterization of metal oxide/polyimide nanocomposites. *Composites Science and Technology*. 2003; 63(11):1591-1598.
49. Liu TX, Phang IY, Shen L, Chow SY, Zhange WD. Morphology and mechanical properties of multiwalled carbon nanotubes reinforced nylon-6 composites. *Macromolecules*. 2004; 37(19):7214-7222.
50. Theng BKG. *The chemistry of clay-organic reactions.* New York: Wiley; 1974.
51. Ogawa M, Kuroda K. Preparation of inorganic composites through intercalation of organoammoniumions into layered silicates. *Bulletin of the Chemical Society of Japan*. 1997; 70(11):2593-2618.
52. Kojima Y, Usuki A, Kawasumi M, Okada A, Fukushima Y, Karauchi T, Kamigaito O. Mechanical properties of nylon-6-clay hybrid. *Journal of Materials Research*. 1993; 8(5):1185-1189.
53. Stearns LC, Zhao J, Martin P. Harmer Processing and microstructure development in Al_2O_3-SiC 'nanocomposites'. *Journal of European Ceramic Society*. 1992; 10(3):473-477.
54. Borsa CE, Brook RJ. Fabrication of Al_2O_3/SiC nanocomposites using a polymeric precursor for SiC. In: Hausner H, Messing GL, Horano S, editors. *Proceedings of the International Conference of Ceramic Processing Science and Technology*; Sept. 11-14, 1994, Friedrichshafen. Westerville, Germany: The American Ceramic Society; 1995. p. 653-658. (Ceramic Transactions. Vol. 51)
55. Riedel R, Strecker K, Petzow G. In situ polysilane-derived silicon-carbide particulates dispersed in silicon nitride composite. *Journal of the American Ceramic Society*. 1989; 72(11):2071-2077.
56. Riedel R, Seher M, Becker G. Sintering of amorphous polymer-derived Si, N and C containing composite powders. *Journal of European Ceramic Society*. 1989; 5(2):113-122.
57. Riedel R, Seher M, Mayer J, Szabo D. Polymer-derived Si-based bulk ceramics. Part I: Preparation, processing and properties. *Journal of European Ceramic Society*. 1995; 15(8):703-715.
58. Livage J. Sol-gel processes. *Current Opinon in Solid State and Materials Science*. 1997; 2(2):132-136.
59. Vorotilov KA, Yanovskaya MI, Turevskaya EP, Sigov AS. Sol-gel derived ferroelectric thin films: avenues for control of microstructural and electric properties. *Journal of Sol-Gel Science and Technology*. 1999; 16(2):109-118.
60. Hench LL, West JK. The sol-gel process. *Chemical Review*. 1990; 90(1):33-72.
61. Ennas G, Mei A, Musinu A, Piccaluga G, Pinna G, Solinas S. Sol-gel preparation and characterization of Ni-SiO_2 nanocomposites. *Journal of Non-Crystalline Solids.* 1998; 232-234:587-593.
62. Sen S, Choudharya RNP, Pramanik P. Synthesis and characterization of nanostructured ferroelectric compounds. *Materials Letters*. 2004; 58(27-28):3486-3490.
63. Viart N, Richard-Plouet M, Muller D, Pourroy G. Synthesis and characterization of Co/ZnO nanocomposites: towards new perspectives offered by metal/piezoelectric composite materials. *Thin Solid Films*. 2003; 437(1-2):1-9.
64. Kundu TK, Mukherjee M, Chakravorty D, Sinha TP. Growth of nano-alpha-Fe_2O_3 in a titania matrix by the sol gel route. *Journal of Matererials Science*. 1998; 33(7):1759-1763.
65. Baiju K, Sibu CP, Rajesh K, Pillai PK, Mukundan P, Warrier KGK, Wunderlich W. An aqueous sol-gel route to synthesize nanosized lanthana doped titania having an increased anatase phase stability for photocatalytic application. *Materials Chemistry and Physics*. 2005; 90(1):123-127.
66. Ananthakumar S, Prabhakaran AK, Hareesh US, Manoharan P, Warrier KGK. Gel casting process For Al_2O_3-SiC nanocomposites and its creep characteristics. *Materials Chemistry and Physics*. 2004; 85(1):151-157.
67. Sivakumar S, Sibu CP, Mukundan P, Pillai PK, Warrier KGK. Nanoporous titania-alumina mixed oxides: an alkoxide free sol-gel synthesis. *Materials Letters*. 2004; 58(21):2664-2669.
68. Warrier KGK, Anilkumar GM. Densification of mullite-SiC nanocomposite sol-gel precursors by pressureless sintering. *Materials Chemistry and Physics*. 2001; 67(1-3):263-266.
69. Wunderlich W, Padmaja P, Warrier KGK. TEM characterization of sol-gel-processed alumina–silica and alumina–titania nano-hybrid oxide catalysts. *Journal of European Ceramic Society*. 2004; 24(2):313-317.
70. Ghosh NN, Pramanik P. Aqueous sol–gel synthesis of nanosized ceramic composite powders with metal-formate precursors. *Materials Science and Engineering: C*. 2001; 16(1-2):113-117.
71. Camargo PHC, Nunes GG, Friedermann GR, Evans DJ, Leigh GJ, Tremiliosi-Filho GSEL, Zarbin AJG, Soares JF. Titanium and iron oxides produced by sol-gel processing of [FeCl{Ti-2(Opri)Q}]: structural, spectroscopic and morphological features. *Materials Research Bulletin*. 2003; 38(15):1915-1928.
72. Camargo PHC, Nunes GG, Friedermann GR, Evans DJ, LeighGJ, Tremiliosi-Filho GSEL, Zarbin AJG, Soares JF. Single-source precursor and homometal approaches to the sol–gel synthesis of iron and titanium oxides. Surface and Colloid Science. *Progress in Colloid and Polymer Science Series.* 2004; 128: 221'-226. DOI: 10.1007/b97089; ISBN: 978-3-540-21247-8.
73. Mathur S, Veith M, Shen H, Hufner S, Jilavi M. Structural and optical properties of $NdAlO_3$ nanocrystals embedded in an Al2O3 matrix. *Chemistry of Materials*. 2002; 14(2):568-582.
74. Ning J, Zhang J, Pan Y, Guo J. Fabrication and mechanical properties of SiO_2 matrix composites reinforced by carbon nanotube. *Materials Science and Engineering: A-Structural Materials Properties Microstructure and Processing*. 2003; 357(1-2):392-396.
75. Xia Z, Riester L, Curtin WA, Li H, Sheldon BW, Liang J, Chang B, Xu JM. Direct observation of toughening mechanisms in carbon nanotube ceramic matrix composites. *Acta Materialia*. 2004; 52(4):931-944.
76. An JW, You DH, Lima DS. Tribological properties of hot-pressed alumina–CNT composites. *Wear*. 2003; 255(1-6):677-681.

77. Kamalakaran R, Lupo F, Grobert N, Lozano-Castello D, Jin-Phillipp NY, Ruhle M. In-situ formation of carbon nanotubes in an alumina-nanotube composite by spray pyrolysis. *Carbon*. 2003; 41(14):2737-2741.

78. Jiang L, Gao L. Carbon nanotubes magnetite nanocomposites from solvothermal processes: formation, characterization, and enhanced electrical properties. *Chemistry of Materials*. 2003; 15(14):2848-2853.

79. Chaisan W, Yimnirun R, Ananta S. Preparation and characterization of ceramic: nanocomposites in the PZT–BT system. *Ceramics International*. 2009; 35(1):121-124.

80. Cha SI, Kim KT, Lee K, Mo CB, Hong SH. Strengthening and toughening of carbon nanotube reinforced alumina nanocomposite fabricated by molecular level mixing process. *Scripta Materialia*. 2005; 53(7):793-797.

81. Balázsi CS, Kónya Z, Wéber F, Biró LP, Arató P. Preparation and characterization of carbon nanotube reinforced silicon nitride composites. *Materials Science and Engineering*: *C*. 2003; 23(6-8):1133-1137.

82. Chung DDL. Cement-matrix structural nanocomposites. *Metals & Materials International*. 2004; 10(1):55-67.

83. Lim DS, You DH, Choi HJ, Lim SH, Jang H. Effect of CNT distribution on tribological behavior of alumina-CNT composites. *International Conference on Wear of Materials Special Issue*. 2005; 259(1-6):539-544.

84. Peigney A, Flahaut E, Lautent CH, Chastel F, Rousset A. Aligned carbon nanotubes in ceramic-matrix nanocomposites prepared by high-temperature extrusion. *Chemical Physics Letters*. 2002; 352(1-2):20-25.

85. Siegel RW, Chang SK, Ash BJ, Stone J, Ajayan PM, Doremus RW, Schadler LS. Mechanical behaviour of polymer and ceramic matrix nanocomposites. *Scripta Materialia*. 2001; 44(8-9):2061-2064.

86. Lee DY, Lee MH, Kim KJ, Heo S, Kim BY, Lee SJ. Effect of multiwalled carbon nanotube (M-CNT) loading on M-CNT distribution behavior and the related electromechanical properties of the M-CNT dispersed ionomeric nanocomposites. *Surface and Coating Technology*. 2005; 200(5-6):1920-1925.

87. Laurent C, Peigney A, Dumortier O, Rousset A. Carbon nanotubes Fe- alumina nanocomposites. Part II: microstructure and mechanical properties of the hot-pressed composites. *Journal of the European Ceramic Society*. 1998; 18(14):2005-2013.

88. Sinnott SB, Andrews R, Qian D, Rao AM, Mao Z, Dickey EC, Derbyshire F. Model of carbon nanotube growth through chemical vapor deposition. *Chemical Physics Letters*. 1999; 315(1-2):25-30.

89. Lim DS, An JW, Lee HJ. Effect of carbon nanotube addition on the tribological behavior of carbon/carbon composites. *Wear*. 2002; 252(5-6):512-517.

90. Bajwa S, Rainfoth WM, Lee WE. Sliding wear behaviour of SiC-Al2O3 nanocomposites. *International Conference on Wear of Materials.* 2005; 259(1-6):553-561.

91. Wang XT, Padture NP, Tanaka H. Contact-damage-resistant ceramic/ single-wall carbon nanotubes and ceramic/graphite composites. *Nature Materials*. 2004; 3(8):539-544.

92. Sealy C. Stronger by a hair - composites: glassy route to ultrahard ceramics: composites: uncommon behavior in ceramic composites: composites. *Materials Today*. 2004; 7(10):15-15.

93. Tai WP, Kim YS, Kim JG. Fabrication and magnetic properties of Al_2O_3/Co nanocomposites. *Materials Chemistry and Physics*. 2003; 82(2):396-400.

94. Li GJ, Huang XX, Guo JK. Fabrication, microstructure and mechanical properties of Al_2O_3/Ni nanocomposites by a chemical method. *Material Research Bulletin*. 2003; 38(11-12):1591-1600.

95. Goujon C, Goeuriot P. Solid state sintering and high temperature compression properties of Al-alloy5000/AlN nanocomposites. *Materials Science and Engineering: A.* 2001; 315(1-2):180-188.

96. Chen W, Zhang J, Cai W. Sonochemical preparation of Au, Ag, Pd/SiO_2 mesoporous nanocomposites. *Scripta Materialia*. 2003; 48(2):1061-1066.

97. Sawaguchi A, Toda K, Niihara K. Mechanical and electrical properties of silicon-silicon nitride-silicon carbide nanocomposite material. *Journal of the American Ceramic Society*. 1991; 74(2):1142-1144.

98. Suzuki Y, Sekino T, Niihara K. Effects of ZrO_2 addition on microstructure and mechanical properties of $MoSi_2$. *Scripta Metallurgica and Materialia*. 1995; 33(1):69-74.

99. Sasaki G, Suga T, Yanai T, Suganuma K, Niihara K. Microstructure of B_4C/TiB_2 composite fabricated by reaction sintering of B_4C and TiC. *Journal of the Ceramic Society of Japan* 1994; 102(1184):321-325.

100. Sakka Y, Bidinger DD, Aksay A. Processing of silicon carbide-mullite-alumina nanocomposites. *Journal of the American Ceramic Society*. 1995; 78(2):479-486.

101. Ge QL, Lei TC, Zhou Y. Microstructure and mechanical-properties of hot-pressed Al_2O_3-ZrO_2 ceramics prepared from ultrafine powders. *Materials Science and Technology*. 1991; 7(6):490-494.

102. Nawa M, Sekino T, Niihara K. Fabrication and mechanical-behavior of Al_2O_3/Mo nanocomposites. *Journal of Materials Science*. 1994; 29(12):3185-3192.

103. Anya CC. Microstructural nature of strengthening and toughening in Al_2O_3-SiC(P) nanocomposites. *Journal of Materials Science*. 1999; 34(22):5557-5567.

104. Baron B, Kumar CS, Le Gonidec G, Hampshire S. Comparison of different alumina powders for the aqueous processing and pressureless sintering of Al_2O_3-SiC nanocomposites. *Journal of the European Ceramic Society*. 2002; 22(9-10):1543-1552.

105. Timms LA, Ponton CB, Strangwood M. Processing of Al_2O_3/SiC nanocomposites - Part 2: green body formation and sintering. *Journal of the European Ceramic Society*. 2002; 22(9-10):1569-1586.

106. Mabuchi H, Tsuda H, Ohtsuka T, Matsui T, Morii K. In-situ synthesis of Si_3N_4-SiC composites by reactive hot-pressing high temperatures-high pressures. *High Temperatures-high Pressures*. 1999; 31(5):499-506.

107. Weimer AW, Bordia RK. Processing and properties of nanophase In-situ synthesis of SiC/ Si_3N_4 composites. *Composites Part B – Engineering*. 1999; 30(7):647-655.

108. Ma RZ, Wu J, Wei BQ, Liang J, Wu DH. Processing and properties of carbon nanotubes-nano-SiC ceramic. *Journal of Materials Science*. 1998; 33(21):5243-5246.

109. Zhan GD, Kuntz JD, Wan J, Mukherjee AK. Single-wall carbon nanotubes as attractive toughening agents in alumina-based nanocomposites. *Nature Materials*. 2003; 2(1):38-42.

110. Zhan GD, Kuntz JD, Wan J, Garay JE, Mukherjee AK. Electrical properties of nanoceramics reinforced with ropes of single-walled carbon nanotubes. *Applied Physical Letters*. 2003; 83(6):1228-1230.

111. Natile MM, Glisenti A. New NiO/Co_3O_4 and Fe_2O_3/ Co_3O_4 nanocomposite catalysts: synthesis and characterization. *Chemistry of Materials*. 2003; 15(13):2502-2510.

112. Balázsi CS, Shen Z, Kónya Z, Kaztovszky ZA, Wéber F, Vértesy Z, Biró LP, Kiricsi I, Arató P. Processing of carbon nanotube reinforced silicon nitride composites by spark plasma sintering. *Composites Science and Technology*. 2005; 65(5):727-733.

113. Baker C, Ismat Shah S, Hasanain SK. Magnetic behavior of iron and iron-oxide nanoparticle/polymer composites. *Journal of Magnetism and Magnetic Materials*. 2004; 280(2-3):412-418.

114. Yoon ES, Lee JS, Oh ST, Kim BK. Microstructure and sintering behavior of W–Cu nanocomposite powder produced by thermo-chemical process. *International Journal of Refractory Metals and Hard Materials*. 2002; 20(3):201-206.

115. Provenzano V, Louat NP, Imam MA, Sadananda K. Ultrafine superstrength materials. *Nanostructured Materials*. 1992; 1(1):89-94.

116. Contreras A, Lopez, Bedolla E. Mg/TiC composites manufactured by pressureless melt infiltration. *Scripta Materialia*. 2004; 51(3):249-253.

117. Khalid FA, Beffort O, Klotz UE, Keller BA, Gasser P, Vaucher S. Study of microstructure and interfaces in an aluminium–C_{60} composite material. *Acta Materialia*. 2003; 51(15):4575-4582.

118. Bhattacharya V, Chattopadhyay K. Microstructure and wear behaviour of aluminium alloys containing embedded nanoscaled lead dispersoids. *Acta Materialia*. 2004; 52(8):2293-2304.

119. Bhattacharya V, Chattopadhyay K. Microstructure and tribological behaviour of nano-embedded al-alloys. *Scripta Materialia*. 2001; 44(8-9):1677-1682.

120. Srinivasan D, Chattopadhyay K. Hardness of high strength nanocomposite Al–X–Zr (X=Si,Cu,Ni) alloys. *Materials Science and Engineering A-Structural Materials Properties Microstructure and Processing*. 2004; 375-377(Special Issue):1228-1234.

121. Branagan DJ. In: Alman DE, Newkirk JW, editors. *Powder metallurgy, particulate materials for industrial applications*. St. Louis: TMS Publication; 2000.

122. Branagan DJ, Tang Y. Developing extreme hardness (>15 GPa) in iron based nanocomposites. *Composites Part A – Applied Science and manufacturing*. 2002; 33(6):855-859.

123. Xiaochun Li, Yang Y, Cheng X. Ultrasonic-assisted fabrication of metal matrix nanocomposites. *Journal of Materials Science.* 2004; 39(9):3211-3212.

124. Ying DY, Zhang DL. Processing of Cu–Al_2O_3 metal matrix nanocomposite materials by using high energy ball milling. *Materials Science and Engineering*. 2000; 286(1):152-156.

125. Choy KL. Chemical vapour deposition of coatings. *Progress in Materials Science*. 2003; 48(2):57-170.

126. Joseph MC, Tsotsos C, Baker MA, Kench PJ, Rebholz C, Matthews A, Leyl A. Characterisation and tribological evaluation of nitrogen-containing molybdenum-copper pvd metallic nanocomposite films. *Surface and Coating Technology*. 2005; 190(2-3):345-356.

127. Chow GM, Holtz RL, Pattnaik A, Edelstein AS, Schlesinger TE, Cammarata RC. Alternative approach to nanocomposite synthesis by sputtering. *Applied Physical Letters*. 1990; 56(19):1853-1855.

128. Haubold T, Gertsman V. On the structure and properties of nanostructured copper-tungsten alloys. *Nanostructured Materials.* 1992; 1(4):303-312.

129. Holtzt RL, Provenzano V. Enhanced microhardness of copper-niobium nanocomposites. *Nanostructured Materials*. 1994; 4(2):241-256.

130. Cushing BL, Kolesnichenko VL. O'Connor CJ. Recent advances in the liquid-phase syntheses of inorganic nanoparticles. *Chemical Reviews*. 2004; 104(9):3893-3946.

131. West R, Wang Y, Goodson T. Nonlinear absorption properties in novel gold nanostructured topologies. *Journal of Physical Chemistry B*. 2003; 107(15):3419-3426.

132. Kamat PV, Flumiani M, Dawson A. Metal-metal and metal-semiconductor composite nanoclusters. *Colloid Surface A- Physicochemical and Engineering Aspects*. 2002; 202(2-3):269-279.

133. Roy SD, Chakravorty D, Agrawal DC. Magnetic properties of glass-metal nanocomposites prepared by the sol-gel route and hot pressing. *Journal of Applied Physics*. 1993; 74(7):4746-4749.

134. Carpenter EE, Kumbhar A, Wiemann JA, Srikanth Wiggins HJ, Zhou W, O'Connor CJ. Synthesis and magnetic properties of gold–iron–gold nanocomposites. *Materials Science and Engineering.* 2000; 286(1):81-86.

135. Chen X, Xia J, Peng J, Li W, Xie S. Carbon-nanotube metal-matrix composites prepared by electroless plating. *Composites Science and Technology*. 2000;60(2):301-306.

136. Chen WX, Lee JY, Liu Z. The nanocomposites of carbon nanotube with Sb and $SnSb_{0.5}$ as Li-ion battery anodes. *Carbon*. 2003; 41(5):959-966.

137. Chen WX, Lee JY, Liu Z. Electrochemical lithiation and de-lithiation of carbon nanotube-Sn_2Sb nanocomposites. *Electrochemical Communications*. 2002; 4(3):260-265.

138. Xu CL, Wei BQ, Ma RZ, Liang J, Ma XK, Wu DH. Fabrication of aluminium-carbon nanotube composites and their electrical properties. *Carbon*. 1999; 37(1):855-858.

139. Noguchi T, Magario A, Fuzukawa S, Shimizu S. Carbon nanotube/aluminium composites with uniform dispersion. *Materials Transactions*. 2004; 45(2):602-604.

140. Kuzumaki T, Miyazawa K, Ichinose H, Ito K. Processing of carbon nanotube reinforced aluminum composite. *Journal of Materials Research*. 1998; 13(9):2445-2449.

141. Yang J, Schaller R. Mechanical spectroscopy of mg reinforced with Al_2O_3 short fibers and carbon nanotubes. *Materials Science and Engineering*. 2004; 370(1-2):512-515.

142. Special feature: Tiny tubes boost for metal matrix composites. *Metal Powder Report*. 2004; 59(7):40-43.

143. Marchal Y, Delannay F, Froyen L. The essential work of fracture as a means for characterizing the influence of particle size and volume fraction on the fracture toughness of plates of Al/SiC composites. *Scripta Materialia*. 1996; 35(2):193-198.

144. Jang Y, Kim S, Lee S, Kim D, Um M. Fabrication of carbon nano-sized fiber reinforced copper composite using liquid infiltration process. *Composites Science and Technology*. 2005; 65(5):781-802.

145. Liu HH, Wang L, Wang A, Lou T, Ding B, Hu Z. Study of SiC/Al nanocomposites under high pressure. *Nanostructured Materials*. 1997; 9(1-8):225-228.

146. Venkatraman B, Sundararajan G. The sliding wear behaviour of Al-SiC particulate composites—I. Macrobehaviour. *Acta Materialia*. 1996; 44(2):451-460.

147. El-Eskandarany MS. Mechanical solid state mixing for synthesizing of SiCp/Al nanocomposites. *Journal of Alloys and Compounds.* 1998; 279(2):263-271.

148. Pathak JP, Tiwari SN, Malhotra SL. On the wear characteristics of leaded aluminum bearing alloys. *Wear*. 1986; 112(3-4):341-353.

149. Quin D, Dickey EC, Andrews R, Rantell T. Load transfer and deformation mechanisms in carbon nanotube-polystyrene composites. *Applied Physical Letters*. 2000; 76(20):2868-2870.

150. Schadler LS, Giannaris SC, Ajayan PM. Load transfer in carbon nanotube epoxy composites. *Applied Physical Letters*. 1998; 73(26):3842-3844.

151. Jimenez G, Ogata N, Kawai H, Ogihara T. Structure and thermal/mechanical properties of poly (ε-caprolactone) - clay blend. *Journal of Applied Polymer Science*. 1997; 64: 2211-2220.

152. Ogata N, Jimenez G, Kawai H, Ogihara T, Ogata N. Structure and thermal/mechanical properties of poly (l-lactide) – clay blend. *Journal of Polymer Science Part B: Polymer Physics*. 1997; 35(2):389-396.

153. Jeon HG, Jung HT, Lee SW, Hudson SD. Morphology of polymer silicate nanocomposites. *Polymer Bulletin*. 1998; 41(1):107-113.

154. Aranda P, Ruiz-Hitzky E. Poly (ethylene oxide) - silicate intercalation materials. *Chemistry of Materials*. 1992; 4(6):1395-1403.

155. Greenland DJ. Adsorption of polyvinylalcohols by montmorillonite. *Journal of Colloid Science*. 1963; 18(7):647-664.

156. Francis CW. Adsorption of polyvinylpyrrolidone on reference clay minerals. *Soil Science*. 1973; 115(1):40-54.

157. Zhao X, Urano K, Ogasawara S. Adsorption of polyethylene glycol from aqueous solutions on monmorillonite clays. *Colloid and Polymer Science*. 1989; 267(10):899-906.

158. Usuki A, Kojima Y, Kawasumi M, Okada A, Fukushima Y, Kurauchi T, Kamigaito O. Synthesis of Nylon-6-clay hybrid. *Journal of Materials Research*. 1993; 8(5):1179-1183.

159. Usuki A, Kawasumi M, Kojima Y, Okada A, Kurauchi T, Kamigaito O. Swelling behaviour of montmorrinollitecation exchanged for Ω-amino acid by ε–Caprolactum. *Journal of Materials Research*. 1993; 8(5):1174-1178.

160. Messersmith PB, Giannelis EP. Polymer Layered Silicate Nanocomposites: in situ intercalative polymerization of ε–caprolactone in layered silicates. *Chemistry of Materials*. 1993; 5(8):1064-1066.

161. Okamoto M, Morita S, Taguchi H, Kim YH, Kotaka T, Tateyama H. Synthesis and structure of smectic clay/poly(methyl methacrylate) and clay/polystyrene nanocomposites via in situ intercalative polymerization. *Polymer*. 2000; 41(10):3887-3890.

162. Okamoto M, Morita S, Kotaka T. Dispersed structure and ionic conductivity of smectic clay/polymer nanocomposites. *Polymer*. 2001; 42(6):2685-2688.

163. Yao KJ, Song M, Hourston DJ, Luo DZ. Polymer/layered clay nanocomposites: 2- polyurethane nanocomposites. *Polymer*. 2002; 43(3):1017-1020.

164. Messersmith PB, Giannelis EP. Synthesis and characterization of layered silicate-epoxy nanocomposites. *Chemistry of Materials*. 1994; 6(10):1719-1725.

165. Vaia RA, Giannelis EP. Lattice of polymer melt intercalation in organically modified layered silicates. *Macromolecules*. 1997; 30(25):7990-7999.

166. Gilmann JW. Flammability and thermal stability studies of polymer-layered –silicate (clay) nanocomposites. *Appied Clay Science*. 1999; 15(1-2):31-49.

167. Vaia RA, Vasudevan S, Krawiec W, Scanlon LG, Giannelis EP. New polymer electrolyte nanocomposites: melt intercalation of poly (ethylene oxide) in mica-type silicates. *Advanced Materials*. 1995; 7(2):154-156.

168. Kawasumi M, Hasegawa N, Kato M, Usuki A, Okada A. Preparation and mechanical properties of polypropylene-clay hybrids. *Macromolecules*. 1997; 30(20):6333-6338.

169. Vaia RA, Giannelis EP. Polymer melt intercalation in organically modified layered silicates: model predictions and experiment. *Macromolecules*. 1997; 30(25):8000-8009.

170. Tomasko DL, Han X, Liu DH, Gao W. Supercritical fluid applications in polymer nanocomposites. *Current Opinion in Solid State and Materials Science*. 2003; 7(4-5):407-412.

171. Watkins JJ, Mccarthy TJ. Polymerization in supercritical fluid-swollen polymers: a new route to polymer blends. *Macromolecules*. 1994; 27(17):4845-4847.

172. Watkins JJ, Mccarthy TJ. Polymer/metal nanocomposite synthesis in supercritical CO_2. *Chemistry of Materials*. 1995; 7(11):1991-1994.

173. Watkins JJ, Mccarthy TJ. Polymerization of styrene in supercritical CO2-swollen poly (chlorotrifluoroethylene). *Macromolecules*. 1995; 28(12):4067-4074.

174. Watkins JJ, Mccarthy TJ. Chemistry in supercritical fluid-swollen polymers: direct synthesis of metal-polymer nanocomposites: Part 2. *Abstract of Papers of the American Chemical Society*. 1995; 210:84-84.

175. Carrado KA, Xu LQ. In situ synthesis of polymer-clay nanocomposites from silicate gels. *Chemistry of Materials*. 1998; 10(5):1440-1445.

176. Fernando W, Satyanarayana KG. Functionalization of single layers and nanofibers: a new strategy to produce polymer nanaocomposites with optimized properties. *Journal of Colloid and Interface Science*. 2005; 285(1):532-543.

177. Park AY, Kwon H, Woo AJ, Kim SJ. Layered double hydroxide surface modified with (3-aminopropyl) triethoxysilane by covalent bonding. *Advanced Materials*. 2005; 17(1):106-109.

178. Mbhele ZH, Salemane MG, Van Sittert CGCE, Nedeljkovic JM, Djokovic V, Luyt AS. Fabrication and characterization of silver-polyvinyl alcohol nanocomposites. *Chemistry of Materials*. 2003; 15(26):5019-5024.

179. Aymonier C, Bortzmeyer D, Thomann R, Lhaupt RM. Poly (methyl methacrylate)/palladium nanocomposites: synthesis and characterization of the morphological, thermomechanical, and thermal properties. *Chemistry of Materials*. 2003; 15(25):4874-4878.

180. Evora VMF, Shukla A. Fabrication, characterization, and dynamic behavior of polyester/TiO_2 nanocomposites. *Materials Science and Engineering*. 2003; 361(1-2):358-366.

181. Di Lorenzo ML, Errico ME, Avella M. Thermal and morphological characterization of poly (ethylene terephthalate)/calcium carbonate nanocomposites. *Journal of Materials Science*. 2002; 37(11):2351-2358.

182. Park SS, Bernet N, De La Roche S, Hanh HT. Processing of iron oxide-epoxy vinyl ester nanocomposites. *Journal of Composite Materials*. 2003; 37(5):465-465.

183. Xu X, Yin Y, Ge X, Wu H, Zhang Z. Γ-radiation synthesis of poly (acrylic acid)–metal nanocomposites. *Materials Letters*. 1998; 37(6):354-358.

184. Liu J, Gao Y, Wang F, Li D, Xu J. Preparation and characteristic of a new class of silica/polyimide nanocomposites. *Journal of Materials Science*. 2002; 37(14):3085-3088.

185. Jackson CL, Bauer BJ, Nakatani AI, Barnes JD. Synthesis of hybrid organic-inorganic materials from interpenetrating polymer network chemistry. *Chemistry of Materials*. 1996; 8(3):727-733.

186. Avadhani CV, Chujo Y. Polyimide-silica gel hybrids containing metal salts: preparation via the sol-gel reaction. *Applied Organometalic Chemistry*. 1997; 11(2):153-161.

187. Sandler J, Shaffer MSP, Prasse T, Bauhofer W, Schulte K, Windle AH. Development of a dispersion process for carbon nanotubes in an epoxy matrix and the resulting electrical properties. *Polymer*. 1999; 40(21):5967-5971.

188. Qian D, Dickey EC, Andrews R, Rantell T. Load transfer and deformation mechanisms in carbon nanotube-polystyrene composites. *Applied Physical Letters*. 2000; 76(20):2868-2870.

189. Ding W, Eitan A, Fisher FT, Chen X, Dikin DA, Andrews R, Brinson LC, Schadler LS, Ruoff RS. Direct observation of polymer sheathing in carbon nanotube-polycarbonate composites. *Nano Letters* 2003; 3(11):1593-1597.

190. Lin Y, Zhou B, Fernando KAS, Liu P, Allard LF, Sun YP. Polymeric carbon nanocomposites from carbon nanotubes functionalized with matrix polymer. *Macromolecules*. 2003; 36(19):7199-7204.

191. Wong M, Paramsothy M, Xu XJ, Ren Y, Liao K. Physical interactions at carbon nanotube-polymer interface. *Polymer*. 2003; 44(25):7757-7764.

192. Koerner H, Price G, Pearce NA, Alexer M, Vaia RA. Remotely actuated polymer nanocomposites-stress-recovery of carbon-nanotube filled thermoplastic elastomers. *Nature Materials*. 2004; 3(2):115-119.

193. Kubayashi K, Hayashi S. *Woven fabric made of shape memory polymers*. United States. Patent 5, 128. 1992.

194. Tang W, Santare MH, Advani SG. Melt processing and mechanical property characterization of multi-walled carbon nanotube/high density polyethylene (MWNT/HDPE) composite films. *Carbon*. 2003; 41(14):2779-2785.

195. Andrews R, Jacques D, Minot M, Rantell T. Fabrication of carbon multiwall nanotube/polymer composites by shear mixing. *Macromolecular Materials and Engineering*. 2002; 287(6):395-403.

196. Park SJ, Cho MS, Lim LT, Choi HJ, Jhon MS. Synthesis and dispersion characteristics of multi-walled carbon nanotube composites with poly(methyl methacrylate) prepared by in-situ bulk polymerization. *Macromolecular Rapid Communications*. 2003; 24(18):1070-1073.

197. Maser WK, Benito AM, Callejas MA, Seeger T, Martínez MT, Schreiber J et al. Synthesis and characterization of new polyaniline/nanotube composites. *Materials Science and Engineering*. 2003; 23(1-2):87-91.

198. Park C, Ounaies Z, Watson KA, Crooks RE, Smith JJ, Lowther SE et al. Dispersion of single wall carbon nanotubes by in situ polymerization under sonication. *Chemical Physics Letters*. 2002; 364(3-4):303-308.

199. Philip B, Xie J, Abraham JK, Varadan VK. Polyaniline - carbon nanotube composites: starting with phenylamino functionalized carbon nanotubes. *Polymer Bulletin.* 2005; 53(2):127-138.

200. Velasco-Santos C, Martinez-Hernandez AL, Fisher FT, Rouff R, Castaño VM. Improvement of thermal and mechanical properties of carbon nanotube composites through chemical functionalization. *Chemistry of Materials*. 2003; 15(23):4470-4475.

201. Azioune A, Peck K, Soudi B, Chehimi MM, Mccarthy GP, Armes SP. Adsorption of human serum albumin onto polypyrrole powder and polypyrrole-silica nanocomposites. *Synthetic Metals*. 1999; 102(1-3):1419-1420.

202. Roslaniec Z, Broza G, Schulte K. Nanocomposites based on multiblock polyester elastomers (PEE) and carbon nanotubes (CNT). *Composite Interfaces*. 2003; 10(1):95-102.

203. Xia HS, Wang Q, Li KS, Hu GH. Preparation of polypropylene/carbon nanotube composite powder with a solid-state mechanochemical pulverization process. *Journal of Applied Polymer Science*. 2004; 93(1):378-386.

204. Kim JY, Kim M, Choi JH. Characterization of light emitting devices based on a single-walled carbon nanotube–polymer composite. *Synthetic Metals*. 2003; 139(3):565-568.

205. Valentini L, Biagiotti J, Kenny JJ, Santucci S. Morphological characterization of single-walled carbon nanotubes-PP composites. *Composites Science and Technology*. 2003; 63(8):1149-1153.

206. Ramamurthy PC, Malshe AM, Harrell WR, Gregory RV, McGuire K, Rao AM. Polyaniline/signle-walled carbon tube composite electronic devises. *Solid State Electrochemistry*. 2004; 48(10-11):2019-2024.

207. Bharadwaj RK. Modeling the barrier properties of polymer layered silicate nanocomposites. *Macromolecules*. 2001; 34(26):9189-9192.

208. Kojima Y, Usuki A, Kawasumi M, Okada A, Kurauchi T, Kamigaito O. Synthesis of nylon-6-clay hybrid by montmorillonite intercalated with ε-caprolactum. *Journal of Polymer Science and Polymer Chemistry*. 1993; 31(7):983-986.

209. Kojima Y, Usuki A, Kawasumi M, Okada A, Kurauchi T, Kamigaito O. One pot synthesis of nylon-6-clay hybrid. *Journal of Polymer Science and Polymer Chemistry*. 1993; 31(7):1755-1758

210. Bourbigot S, LeBras M, Dabrowski F, Gilman JW, Kashiwagi T. PA-6 clay nanocomposite hybrid as char forming agent in intumescent formulations. *Fire and Materials*. 2000; 24(4):201-208.

211. Ray SS, Yamada K, Okamoto M, Ueda K. New polylactide/layered silicate nanocomposite: a novel biodegradable material. *Nano Letters*. 2002; 2(10):1093-1096.

212. Okada A, Kawasumi M, Usuki A, Kojima Y, Kurauchi T, Kamigaito O. In: Schaefer DW, Mark JE, editors. Polymer-based molecular composites. *Proceedings of the MRS Symposium*; 1990; Pittsburgh. USA: [s.n]; 1990. p. 18-45.

213. Dabrowskii F, Bourbigot S, Delobel R, Lebras ML. Kinetic molding of the thermal degradation of polyamide-6 nanocomposite. *European Polymer Journal*. 2000; 36(2):273-284.

214. Lee JY, Baljon ARC, Loring RF, Panagiopoulos AZ. Simulation of polymer melt intercalation in layered nanocomposites. *Journal of Chemical Physics*. 1998; 109(23):10321-10330.

215. Balazs AC, Singh C, Zhulina E. Modeling the interactions between polymers and clay surfaces through self consistent field theory. *Macromolecules*. 1998; 31(23):8370-8381.

216. Fredrickson GH, Bicerano J. Barrier properties of oriented disk composites. *Journal of Chemical Physics*. 1999; 110(4):2181-2188.

217. Kuznetsov D, Balazs AC. Scaling theory for end-functionalized polymers confined between two surfaces: predictions for fabricating polymer nanocomposites. *Journal of Chemical Physics*. 2000; 112(9):4365-4375.

218. Manias E, Chen E, Krisnhamoorti R, Genzer J, Kramer EJ, Giannelis EP. Intercalation kinetics of long polymers in 2 nm confinements. *Macromolecules*. 2000; 33(21):7955-7966.

219. Herron N, Thorn DL. Nanoparticles: uses and relationships to molecular cluster compounds. *Advanced Materials*. 1998; 10(15):1173-1184.

220. Favier V, Canova GR, Shrivastava SC, Cavaille JV. Mechanical percolation in cellulose whisker nanocomposites. *Polymer Engineering Science.* 1997; 37(10):1732-1739.

221. Chazeau L, Cavaille JY, Canova G, Dendievel R, Boutherin B. Viscoelastic properties of plasticized PVC reinforced with cellulose whiskers. *Journal of Applied Polymer Science*. 1999; 71(11):1797-1808.

222. Ogawa M, Kuroda K. Preparation of inorganic–organic nanocomposites through intercalation of organoammonium ions into layered silicates. *Bulletinn of the Chemical Society of Japan*. 1997; 70(11):2593-2618.

223. Chen L, Yang WJ, Yang CZ. Preparation of nanoscale iron and Fe_3O_4 powders in a polymer matrix. *Journal of Materials Science*. 1997; 32(13):3571-3575.

224. Lu GT, Huang Y. Synthesis of polymaleimide/silica nanocomposites. *Journal of Materials Science*. 2002; 37(11):2305-2308.

225. Liu SH, Qian XF, Yuan JY, Yin J, He R, Zhu ZK. Synthesis of monodispersed CdSe nanocrystals in poly(styrene-alt-maleic anhydride) at room temperature. *Materials Research Bulletin*. 2003; 38(8):1359-1366.

226. Trindade T, O'Brien P. A single source approach to the synthesis of CdSe nanocrystallites. *Advanced Materials*. 1996; 8(2):161-163.

227. Trindade T, Neves MC, Barros AMV. Preparation and optical properties of CdSe/polymer nanocomposites. *Scripta Materialia*. 2000; 43(6):567-571.

228. Vaia RA, Wagner HD. Framework for nanocomposites. *Materials Today*. 2004; 7(11):32-37.

229. Curtin WA, Sheldon BW. CNT-reinforced ceramics and metals. *Materials Today*. 2004; 7(11):44-49.

230. Thostenson ET, Chou TW. On the elastic properties of carbon nanotube-based composites: modelling and characterization. *Journal of Physics D. Applied Physics*. 2003; 36(5):573-582.

231. Thostenson ET, Chou TW. Aligned multi-walled carbon nanotube-reinforced composites: processing and mechanical characterization. *Journal of Physics D. Applied Physics*. 2002; 35(16):L77-L80.

232. Tai NH, Yeh MK, Liu HH. Enhancement of the mechanical properties of carbon nano tube/phenolic composites using a carbon nanotube network as the reinforcement. *Carbon*. 2004; 42(12-13):2774-2777.

233. Gojny FH, Wichmann MHG, Kopke U, Fiedler B, Schulte K. Carbon nanotube-reinforced epoxy-composites: enhanced stiffness and fracture toughness at low nanotube content. *Composites Science and Technology*. 2004; 64(15):2363-2371.

234. Ogasawara T, Ishida Y, Ishikawa T, Yokota R. Characterization of multi-walled carbon nanotube/phenylethynyl terminated polyimide composites. *Composites part A - Applied Science*. 2004; 35(1):67-74.

235. Giannelis EP, Krishnamoorti R, Manias E. Polymer-silica nanocomposites: model systems for confined polymers and polymer blends. In: *Polymers in confined environments.* Book Series: Advances in polymer science. [S.L.]: [s.n.]; 1999. p. 107-147.

236. LeBaron PC, Wang Z, Pinnavaia TJ. Polymer-layered silicate nanocomposites: an overview. *Applied Clay Science*. 1999; 15(1-2):11-29.

237. Vaia RA, Price G, Ruth PN, Nguyen HT, Lichtenhan J. Polymer/layered silicate nanocompsosites as high performance ablative materials. *Applied Clay Science*. 1999; 15(1-2):67-92.

238. Biswas M, Ray SS. Recent progress in synthesis and evaluation of polymer–montmorillonite nanocomposites. *New polymerization techniques and synthetic methodologies*. Book series: Advances in polymer science. [S.L.]: [s.n.]; 2001. p. 167-221.

239. Giannelis EP. Polymer-layered silicate nanocomposites: synthesis, properties and applications. *Applied Organometalic Chemistry*. 1998; 12(10-11):675-680.

240. Xu R, Manias E, Snyder AJ, Runt J. New biomedical poly (urethane uera)-layered silicate nanocomposites. *Macromolecules*. 2001; 34(2):337-339.

241. Messersmith PB, Giannelis EP. Synthesis and barrier properties of poly (ε-caprolactone)-layered silicate nanocomposites. *Journal of Polymer Science Part A- Polymer Chemistry*. 1995; 33(7):1047-1057.

242. Yano K, Usuki A, Okada A, Kurauchi T, Kamigaito O. Synthesis and properties of polimidie-clay hybrid. *Journal of Polymer Science Part A- Polymer Chemistry*.1993; 31(10):2493-2498.

243. Gilman JW, Jackson CL, Morgan AB, Harris Jr. R, Manias E, Giannelis EP et al. Flammability properties of polymer-layered silicate nanocomposites: propylene and polystyrene nanocomposites. *Chemistry of Materials*. 2000; 12(7):1866-1873.

244. Hori T, Kuramoto N, Tayagaya H, Karasu M, Kadokawa JI, Chiba K. Preparation of conducting film composed of polyaniline and metal oxide by sol-gel method. *Journal of Materials Research*. 1999; 14(1):5-7.

245. Blumstein A. Polymerization of adsorbed monolayers. II. Thermal degradation of the inserted polymers. *Journal of Polymer Science Part A-General papers*. 1965; 3(7PA):2665-2673.

246. Theng BKG. *Formation, properties of clay–polymer complexes*. Amsterdam: Elsevier; 1979.

247. Vaia RA, Ishii H, Giannelis EP. Synthesis and properties two-dimensional nanostructures by direct intercalation of polymer melts in layered silicates. *Chemistry of Materials*. 1993; 5(12):1694-1696.

248. Passaglia E, Bertoldo M, Ciardelli F, Prevosto D, Lucchesi M. Evidences of macromolecular chains confinement of ethylene-propylene copolymer in organophilic montmorillonite nanocomposites. *European Polymer Journal*. 2008; 44(5):1296-1308.

249. Krishnamoorti R, Vaia RA, Giannelis EP. Structure and dynamics of polymer- layered silicate nanocomposites. *Chemistry of Materials*. 1996; 8(8):1728-1734.

250. Hasegawa N, Kawasumi M, Kato M, Usuki A, Okada A. Preparation and mechanical properties of polypropylene-clay hybrids using a maleic anhydride-modified polypropylene oligomer. *Journal of Applied Polymer Science*. 1998; 67(1):87-92.

251. Lee DC, Jang LW. Preparation and characterization of PMMA–clay composite by emulsion polymerization. *Journal of Applied Polymer Science*. 1996; 61(7):1117-1122.

252. Noh MW, Lee DC. Synthesis and characterization of ps-clay nanocomposite by emulsion polymerization. *Polymer Bulletin*. 1999; 42(5):619-626.

253. Wang Z, Pinnavaia TJ. Nanolayer reinforcement of elastomeric polyurethane. *Chemistry of Materials*. 1998; 10(12):3769-3771.

254. Wang Z, Pinnavaia TJ. Hybrid organic-inorganic nanocomposites: exfoliation of magadiite nanolayers in an elastomeric epoxy polymer. *Chemistry of Materials*. 1998; 10(7):1820-1826.

255. Yano K, Usuki A, Okada A. Synthesis and properties of polyimide-clay hybrid films. *Journal of Polymer Science and Polymer Chemistry*. 1997; 35(11):2289-2294.

256. Liu LM, Qi ZN, Zhu XG. Studies on nylon 6/clay nanocomposites by melt-intercalation process. *Journal of Applied Polymer Science*. 1999; 71(7):1133-1138.

257. Fornes TD, Yoon PJ, Keskkula H, Paul DR. Nylon 6 nanocomposites: the effect of matrix molecular weight. *Polymer*. 2001; 42(25):9929-9940.

258. Oakada A, Usuki A. The chemistry of polymer-clay hybrids. *Materials Science and Engineering*. 1995; 3(2):109-115.

259. Laus M, Francesangeli O, Sandrolini F. New hybrid nanocomposites based on an organophilic clay and poly (styrene-*b-butadiene)* copolymers. *Journal of Materials Research*. 1997; 12(11):3134-3139.

260. Becker O, Varley R, Simon G. Morphology, thermal relaxations and mechanical properties of layered silicate nanocomposites based upon high-functionality epoxy resins. *Polymer*. 2002; 43(16):4365-4373.

261. Wang S, Long C, Wang X, Li Q, Qi Z. Synthesis and properties of silicone rubber/organomontmorillonite hybrid nanocomposites. *Journal of Applied Polymer Science*. 1998; 63(8):1557-1561.

262. Zhu J, Morgan AB, Lamelas FJ, Wilkie CA. Fire properties of polystyrene-clay nanocomposites. *Chemistry of Materials*. 2001; 13(10):3774-3780.

263. Ray SS, Yamada K, Okamoto M, Ogami A, Ueda K. New polylactide / layered silicate nanocomposites. 3. High-performance biodegradable materials. *Chemistry of Materials*. 2003; 15(7):1456-1465.

264. Nielsen LE. Models for the permeability of filled polymer systems. *Journal of Macromolecular Science Part A: Pure and Applied Chemistry*. 1967; 1(5):929-942.

265. Ray SS, Yamada K, Okamoto M, Ueda K. New polylactide-layered silicate nanocomposites. 2. Concurrent improvements of material properties, biodegradability and melt rheology. *Polymer*. 2003; 44(3):857-866.

266. Lee SR, Park HM, Lim HL, Kang T, Li X, Cho WJ, Ha CS. Microstructure, tensile properties, and biodegradability of aliphatic polyester/clay nanocomposites. *Polymer*. 2002; 43(8):2495-2500.

267. Ray SS, Okamoto M. Biodegradable polylactide and its nanocomposites: opening a new dimension for plastics and composites. *Macromolecular Rapid Communications*. 2003; 24(14):815-840.

268. Okada A, Kawasumi M, Kurauchi T, Kamigaito O. Synthesis and characterization of a nylon 6-clay hybrid. *Polymer Preprints*. 1987; 28(2):447-448.

269. Lwan BR. Ceramic-based layer structures for biomechanical applications. *Current Opinion in Solid State and Materials Science*. 2002; 8(3):229-235.

270. Oriakhi CO, Farr IV, Lerner MM. Thermal characterization of poly (styrene sulfonate)/layered double hydroxide nanocomposites. *Clays and Clay Minerals*. 1997; 45(2):194-202.

271. Wilson OC, Olorunyolemi T, Jaworski A, Borum L, Young D, Siriwat A et al. Surface and interfacial properties of polymer-intercalated layered double hydroxide nanocomposites. *Appied Clay Science*. 1999; 15(1-2):265-279.

272. Do Nascimento GM, Constantino VRL, Temperini MLA. Spectroscopic characterization of a new type of conducting polymer-clay nanocomposite. *Macromolecules*. 2002; 35(20):7535-7537.

273. Yang Y, Zhu ZK, Yin J, Wang XY, Qi ZE. Preparation and properties of hybrids of organo-soluble polyimide and montmorillonite with various chemical surface modification methods. *Polymer*. 1999; 40(15):4407-4414.

274. Lee J, Takekoshi T, Giannelis EP. Fire retardant polyetherimide nanocomposites. *Materials Research Soceity Symposium Proccedings*. 1997; 457:513-518.

275. Ray SS, Bousmina M, Okamoto K. Structure and properties of nanocomposites based on poly (butylene succinate-co-adipate) and organically modified montmorillonite. *Macromolecular Materials and Engineering*. 2005; 290(8):759-768.

276. Morgan AB, Harris RH, Kashiwagi T, Chyall LJ, Gilman JW. Flammability of Polystyrene Layered Silicate (Clay) Nanocomposites: Carbonaceous Char Formation. *Fire and Materials* 2002; 26 (6):247-253.

277. Scherer C. PA film grade with improved barrier properties for flexible food packaging applications. *Proceedings of the 99th New Plastics;* 1999 Feb 2-4; London.

278. Kim JW, Kim SG, Choi JH, Jhon MS. Synthesis and electrorheological properties of polyaniline-na+-montmorillonite suspensions. *Macromolecular Rapid Communications*. 1999; 20(8):450-452.

279. Lan T, Kavitatna PD, Pinnavia TJ. On the nature of polyimide clay hybrid composites. *Chemistry of Materials*. 1994; 6(5):573-575.

280. Mohanty AK, Drzal LT, Misra M. Nano reinforcement of Bio-based polymers - The Hope and The Reality. (Presented at 225th ACS National Meeting, New Orleans, March 2003, U665-665, Abstract: 33-PMSE). Polymeric *Materials Science & Engineering*. 2003; 88: 60-61.

281. Dutta A, Das D, Grilli ML, Di Bartolomeo E, Traversa E, Chakravorty D. Preparation of sol-gel nano-composites containing copper oxide and their gas sensing properties. *Journal of Sol - Gel Science and Technology*. 2003; 26(1-3):1085-1094.

282. Ghose S, Watson KA, Delozier DM, Working DC, Siochi EJ, Connell JW. Incorporation of multi-walled carbon nanotubes into high

temperature resin using dry mixing techniques. *Composites part A - Applied Science and Manufacturing*. 2006; 37(3):465-475.

283. Lijie CI, Jinbo B. The reinforcement role of carbon nanotubes in epoxy composites with different matrix stiffness. *Composites Science and Technology*. 2006; 66(3-4):599-603.
284. Xu YS, Ray G, Abdel-Magid B. Thermal behavior of single-walled carbon nanotube polymer–matrix composites. *Composites part A - Applied Science and Manufacturing*. 2006; 37(1):114-121.
285. Lucas M, Young RJ. Raman spectroscopic study of the effect of strain on the radial breathing modes of carbon nanotubes in epoxy/ SWNT composites. *Composites Science and Technology*. 2004; 64(15):2297-2302.
286. Shofner ML, Rodríguez –Macías FJ, Vaidyanathan R, Barrera EV. Single wall nanotube and vapor grown carbon fiber reinforced polymers processed by extrusion freeform fabrication. *Composites Part A – Applied Science and manufacturing*. 2003; 34(12):1207-1217.
287. Bai JB, Allaoui A. Effect of the length and the aggregate size of mwnts on the improvement efficiency of the mechanical and electrical properties of nanocomposites: experimental investigation. *Composites Part A – Applied Science and manufacturing*. 2003; 34(8):689-694.
288. Hu Y, Jang I, Sinnott SB. Modification of carbon nanotube-polystyrene matrix composites through polyatomic-ion beam deposition: predictions from molecular dynamics simulations. *Composites Science and Technology*. 2003; 63(11):1663-1669.
289. Hussain M, Simon GP. Fabrication of phosphorus-clay polymer nanocomposites for fire performance. *Journal of Materials Science Letters*. 2003; 22(21):1471-1475.
290. Frankl SJV, Harik VM, Odegard GM, Brenner DW, Gates TS. The stress–strain behavior of polymer–nanotube composites from molecular dynamics simulation. *Composites Science and Technology*. 2003; 63(11):1655-1661.
291. Haque A, Ramasetty A. Theoretical study of stress transfer in carbon nanotube reinforced polymer matrix composites. *Composites Structure*. 2005; 71(1):68-77.
292. Karger-Kocsis J, Zhang Z. In: Palta Calleja JF, Michler G, editors. *Mechanical properties of polymers based nano structure morphology*. New York: Marcel Dekker; 2004.
293. Merkulov VI, Lowndes DH, Wei YY, Eres G, Voelkl E. Patterned growth of individual and multiple vertically aligned carbon nanofibers. *Applied Physical Letters*. 2000; 76(24):3555-3557.
294. Endo M, Kim YA, Hayashi T, Fukai Y, Oshida K, Terronnes M et al. Structural characterization of cup-stacked-type carbon nanofibers with an entirely hollow core. *Applied Physical Letters*. 2002; 80(7):1267-1269.
295. Endo M, Kim YA, Ezaka M, Oshida K, Yanagisawa T, Dresselhaus MS. Selective and efficient impregnation of metal nanoparticles on cup-stacked-type carbon nanofibers. *Nano Letters.* 2003; 3(6):723-726.
296. Finegan IC, Tibbetts GG, Glasgow DG. Surface treatment for improving the mechanical properties of carbon nanofiber/thermoplastic composites. *Journal of Materials Science.* 2003; 38(16):3485-3490.
297. Finegan IC, Tibbetts GG, Gibson RF. Modeling and characterization of damping in carbon nanofiber/polypropylene composites. *Composites Science and Technology*. 2003; 63(11):1629-1635.
298. Ma HA, Zeng JJ, Realff ML, Kumar S, Schiraldi DA. Processing, structure, and properties of fibers from polyester/carbon nanofiber composites. *Composites Science and Technology*. 2003; 63(11):1617-1628.
299. Sandler J, Windle AH, Werner P, Altstädt V, Es MV, Shaffer MSP. Carbon-nanofibre-reinforced poly (ether ether ketone) fibres. *Journal of Materials Science*. 2003; 38(10):2135-2141.
300. Valentini L, Puglia D, Frulloni E, Armentano I, Kenny JM, Santucci S. Dielectric behavior of epoxy matrix/single-walled carbon nanotube composites. *Composites Science and Technology*. 2004; 64(1):23-33.
301. Qian D, Wagner GJ, Liu WK, Yu MF, Ruoff RS. Mechanics of carbon nanotubes. *Applied Mechanics Review*. 2002; 55(6):495-533.
302. Srivastava D, Wei C, Cho K. Nanomechanics of carbon nanotubes and composites. *Applied Mechanics Review*. 2003; 56(2):215-230.
303. Veith M, Mathur S, Lecerf N, Bartz K, Heintz M, Huch V. Synthesis of a $NdAlO_3/Al_2O_3$ ceramic-ceramic composite by single-source precursor CVD. *Chemistry of Materials*. 2000; 12(2):271-274.
304. Veith M, Mathur S, Shen H, Lecerf N, Huffner S, Jilavi M. Single-step preparation of oxide-oxide nanocomposites: chemical vapor synthesis of $LnAlO_3/Al_2O_3$ (Ln = Pr, Nd) thin films. *Chemistry of Materials*. 2001; 13(11):4041-4052.
305. Voevodin AA, Zabinski JS. Nanocomposite and nanostructured tribological materials for space applications. *Composites Science and Technology*. 2005; 65(5):741-748.
306. Meda L, Marra G, Galfetti L, Inchingalo S, Severini F, De Luca L. Nano-composites for rocket solid propellants. *Composites Science and Technology*. 2005; 65(5):769-773.
307. Bafna A, Beaucage G, Mirabella F, Mehta S. 3D hierarchical orientation in polymer-clay nanocomposite films. *Polymer*. 2003; 44(4):1103-1115.
308. Bafna A, Beaucage G, Mirabella F, Mehta S. Shear induced orientation and associated property enhancement in polymer/clay nanocomposites. *Proceedings Nanocomposites.* 2002 Sept. 23-25; San Diego. USA: ECM Publication.
309. Lange FF. Effect of microstructure on strength of si3n4-sic composite system. *Journal of the American Ceramic Society*. 1973; 56(9):445-450.
310. Becher PF. Microstructural design of toughened ceramics. *Journal of the American Ceramic Society*. 1991; 74(2):255-269.
311. Harmer M, Chan HM, Miller GA. Unique opportunities for microstructural engineering with duplex and laminar ceramic composites. *Journal of the American Ceramic Society*. 1992; 75(2):1715-1728
312. *Nanotechnology information by application.* Available from: <http:// www.azonano.com/Applications.asp>. Access in: 20 Nov. 2008.
313. Dresselhaus MS, Dresslhaus G, Eklund PC. *Science of fullerenes*: carbon nanotubes. San Diego: Academic Press; 1996.
314. Nalwa HS. *Handbook of nanostructured materials and technology*. New York: Academic Press; 2000.
315. Dresselhaus MS, Dresslhaus G, Avouris P. *Carbon nanotubes*: synthesis, structure, properties and applications. Berlin: Springer Verlag; 2001.
316. Ajayan PM, Schadler L, Braun PV. *Nanocomposite science and technology*. Weinheim: Wiley-VCH, Verlag Gmbh & Co. KgaA; 2003.
317. Alpha Gary. Nanotubes of advanced polymer products. *Plastics, Additives and Compounding*. 2003; 5(4):12.
318. Agnihotri S, Rostam-Abadi M, Rood MJ. Temporal changes in nitrogen adsorption properties of single-walled carbon nanotubes. *Carbon*. 2004; 42(12-13):2699-2710.
319. Belin T, Epron F. Characterization methods of carbon nanotubes: a review. *Materials Science and Engineering*. 2005; 119(2):105-118.
320. Dresselhaus MS, Dresselhaus G, Saito R, Jorio A. Raman spectroscopy of carbon nanotubes. *Physics Report - Review Section of Physics Letters*. 2005; 409(2):47-99.
321. Serp P, Corrias M, Kalck P. Carbon nanotubes and nanofibers in catalysis. *Appied Catalysis. A-General*. 2003; 253(2):337-58.
322. Penn SG, He L, Natan MJ. Nanoparticles for bioanalysis. *Current Opinion in Chemical Biology*. 2003; 7(5):609-615.
323. Darkrim FL, Malbrunot P, Tartaglia GP. Review of hydrogen storage by adsorption in carbon nanotubes. *Internation Journal of Hydrogen energy*. 2002; 27(2):193-202.
324. Kupfer M. Electronic properties of carbon nanostructures. *Surface Science Reports*. 2001; 42(1-2):1-74.
325. Roche S. Carbon nanotubes: exceptional mechanical and electronic properties. *Annales de Chimie – Science des Materiaux*. 2000; 25(7):529-532.

326. Rao CNR, Seshadri R, Govindaraj A, Sen R. Fullerenes, nanotubes, onions and related carbon structures. *Materials Science and Engineering*. 1995; 15(6):209-262.

327. Hammel E, Tang X, Trampert M, Schmitt T, Mauthner K, Eder A, Pötschke P. Carbon nanofibers for composite applications. *Carbon*. 2004; 42(5-6):1153-1158.

328a. Byron Pipes R, Hubert P. Helical carbon nanotube arrays: mechanical properties. *Composites Science and Technology*. 2002; 62(3): 419-428.

328b. Byron Pipes R, Hubert P. Helical carbon nanotube arrays: thermal expansion. *Composites Science and Technology*. 2003; 63(11):1571-1579.

329. Salvetat-Delmotte JP, Rubio A. Mechanical properties of carbon nanotubes: a fiber digest for beginners. *Carbon*. 2002; 40(10):1729-1734.

330. Terrones M, Jorio A, Endo M, Rao AM, Kim YA, Hayashi T et al. New direction in nanotube science. *Materials Today*. 2004; 7(10):30-45.

331. Sinnott SB, Andrews R. Carbon nanotubes: synthesis, properties, and applications. *Critical Reviews in Solid State and Materials Science*. 2001; 26(3):145-249.

332. Cohen ML. Nanotubes, nanoscience, and nanotechnology. *Materials Science and Engineering*. 2001; 15(1-2):1-11.

333. Ajayan PM. Carbon nanotubes: novel architecture in nanometer space. *Progress of Crystal Growth and Characterization of Materials*. 1997; 34(1-4):37-51.

334. Chirila V, Marginean G, Brandl W. Effect of the oxygen plasma treatment parameters on the carbon nanotubes surface properties. *Surface and Coating Technology*. 2005; 200(1-4):548-555.

335. Gupta VK, Pangannaya NB. Carbon nanotubes: bibliometric analysis of patents. *World Patent Information*. 2000; 22(3):185-189.

336. Wypych F. In: Wypych F, Satyanarayana KG, editors. *Clay surfaces*: fundamentals, applications. Amsterdam: Academic Press; 2004.

337. Verpek S. Superhard and functional nanocomposites formed by self-organization in comparison with hardening of coatings by energetic ion bombardment during their deposition (Invited Paper Int. Conf on Nanomaterials and Nanotechnologies). *Reviews on Advanced Materials Science*. 2003; 5(1):6-16.

338. Cao Y, Irwin PC, Younsi K. The future of nanodielectrics in the electrical power industry. *IEEE Transactions on Dielectrics and Electrical Insulation*. 2004; 11(5):797-807.

339. Jilek M, Cselle T, Holubar P, Mosrtein M, Verpek-Huijman MCJ, Verpek S. Development of novel coating technology by vacuum arc with rotating cathodes for industrial production of Nc-($Al_{1-x}Ti_x$) N/A-Si_3N_4 super hard nanocomposite coatings for dry, hard machining. *Plasma Chemistry and, Plasma Processing*. 2004; 24(4):493-510.

340. Breuer O, Sunderraj U. Big returns from small fibers: a review of polymer/carbon nanotube composites. *Polymer Composites.* 2004; 25(6):630-645.

341. Terrones M. Science and technology of the twenty-first century: synthesis, properties, and applications of carbon nanotubes. *Annual Review of Materials Research*. 2003; 33:419-501. DOI: 10.1146/annurev.matsci.33.012802.100255.

342. Nazar LF, Zhang Z, Zinkweg D. Insertion of poly (para phenylenevinylene) in layered MoO_3. *Journal of the American Chemical Society*. 1992; 114(15):6239-6240.

343. Vassilliou JK, Ziebarth RP, Disalvo FJ. Preparation of a novel polymer blend of poly (ethylene oxide) and the inorganic polymer (Mo_3Se_3-)-infinity - infrared-absorption of thin-films. *Chemistry of Materials*. 1990; 2(6):738-741.

344. Beecroft LL, Ober CK. Nanocomposite materials for optical applications. *Chemistry of Materials*. 1997; 9(6):1302-1307.

345. Cão G, Garcia MF, Aleala M, Burgess LF, Mallouk TE. Chiral molecular recognition in intercalated zirconium phospate. *Journal of the American Chemical Society.* 1992; 114(19):7574-7575.

346. Garces JM, Moll DJ, Bicerano J, Fibiger R, McLeod DG. Polymeric nanocomposites for automotive applications. *Advanced Materials*. 2000; 12(23):1835-1839.

347. Leaversuch R. *Nanocomposites Broaden Roles in Automotive, Barrier Packaging*. Available from: <http://www.plastictechnology.com>. [Online Feature article from Plastics technology]. Access in: 20 Nov. 2008.

348. Patrick Ponticel. *Material innovations:* GM the big winner in plastics. Automotive Engineering International Online: Material Innovations. Available from: http://www.sae.org/automag/material/01-2002/. Access in: 10 March 2009.

349. *Nanocomposites:* enhancing value in the global plastics industry 2005. Available from: http://www.principia consulting.com/ publishing/PDF/brochure_Nanocomposites.pdf. Access in: 10 March 2009.

350. *Polymer nanocomposites for packaging applications.* Available from: http://www.natick.army.mil soldier/media /fact/food/PolyNano.htm. Access in: 10 March 2009.

351. *Nanocomposite*. Available from: www.fortunecity.com/oasis/labreya/163/nanocomposite.html. Access in: 10 March 2009.

352. Holehonnur H. Private communication. (Oct. 2006).

353. Malinauskas A, Malinauskiene J, Ramanavicius A. Conducting polymer-based nanostructurized materials: electrochemical aspects. *Nanotechnology.* 2005; 16(10):R51-R62.

354. Ke Z, Bai YP. Improve the gas barrier property of pet film with montmorillonite by in situ interlayer polymerization. *Materials Letters*. 2005; 59(27):3348-3351.

355. Marosfoi B, Matko S, Anna P, Marosi G. Fire retarded polymer nanocomposites. *Current Applied Physics*. 2006; 6(2):259-261.

356. Zammarano M, Franeschi M, Bellayer S, Gilman JW, Mriani S. Preparation and flame resistance properties of revolutionary self-extinguishing epoxy nanocomposites based on layered double hydroxides. *Polymer*. 2005; 46(22):9314-9328.

357. Bourbigot S, Devaux E, Flambard X. Flammability of polyamide-6/clay hybrid nanocomposite textiles. *Polymer Degradation and Stability*. 2002; 75(2):397-402.

358. Schubel PJ, Johnson MS, Warrior NA, Rudd CD. Characterisation of thermoset laminates for cosmetic automotive applications. Part III: Shrinkage control via nanoscale reinforcement. *Composites Part A – Applied Science and manufacturing*. 2006; 37(10):1757-1772.

359. Schubel PJ, Warrior NA, Kendall KN, Rudd CD. Part III: Shrinkage control via nanoscale reinforcement. *Composites Part A – Applied Science and manufacturing*. 2006; 37(10):1734-1746.

360. Schubel PJ, Parsons AJ, Lester EH, Warrior NA, Rudd CD. Characterisation of thermoset laminates for cosmetic automotive applications. Part I – Surface Characterisation. *Composites Part A – Applied Science and manufacturing*. 2006; 37(10):1747-1756.

361. Lan T, Cho J, Liang Y, Qian J, Peter M. *Applications of nanomer in nanocomposites*: from concept to reality. Available from: <http://www.nanocor.com / tech_papers/ nanocomposite2001.pdf>. Access in: 20 Nov. 2008

362. Presting H, Konig U. Future nanotechnology developments for automotive applications. *Materials Science and Engineering: C*. 2003; 23(6-8):737-741.

363. Caroline E. Auto applications drive commercialization of nanocomposites. *Plastics, Additives, Compounding*. 2002; 4(11):30-33.

364. Swearingen C, Macha S, Fitch A. Leashed ferrocenes at clay surfaces: potential applications for environmental catalysis. *Journal of Molecular Catalysis A - Chemical*. 2003; 199(1-2):149-160.

365. Fischer H. Polymer nanocomposites: from fundamental research to specific applications. *Materials Science and Engineering: C*. 2003; 23(6-8):763-772.

366. Avella M, De Vlieger JJ, Errico ME, Fischer S, Vacca P, Volpe MG. Biodegradable starch/clay nanocomposite films for food packaging. *Applications Food Chemistry*. 2005; 93(3):467-474.

367. Hay JN, Shaw SJ. *Nanocomposites*: properties and applications. Available from: <http://www.azom.com/details.asp?articleid=921>. Access in: 20 Nov. 2008.

368. Hedicke K, Wittich H, Mehler C, Gruber F, Altstädt V. Crystallisation behaviour of polyamide-6 and polyamide-66 nanocomposites. *Composites Science and Technology*. 2006; 66(3-4):571-575.

369. Vlasveld DPN, Groenewold J, Bersee HEN, Picken SJ. Moisture absorption in polyamide-6 silicate nanocomposites and its influence on the mechanical properties. *Polymer*. 2005; 46(26):12567-12576.

370. Veprek S, Martiza GJ, Veprek-Heijman MGJ, Karvankova P, Prochazka J. Different approaches to superhard coatings and nanocomposites. *Thin Soild Films*. 2005; 476(1):1-29.

371. Argonne National Laboratory. *Nanocomposites and organoclays*. Chicago: The University of Chicago; 2003. Available from: http://www.anl.gov/techtransfer/pdf/Nanocomposite4-7-03.pdf. Access in: 10 March 2009.

372. Lownsdale G. *Nanocomposites in the automotive industry* - November 2004. Available from: Nanocomposites/Market Trends.htm Access in: 8 June 2005.

373. Sourcebook: High-Performance Composites: Composites Technology: Publisher Info. Available from: <http://www.compositesworld.com/hpc/issues/2004/November/619>.

374. Downing-Perrault A. *Polymer nanocomposites are the future*. Available from: <http://www.iopp.org/ files/nanostructures.pdf?pageid= pageid>. Access in: 20 Nov. 2001.

375. Alan Ross Machinery Corporation. [Online]. Available from: <http://www.americanrecycler.com/0606 Polymer.shtml>. Access in: 2008 Nov. 20.

376. South East Asia leads global polymer markets. In: South East Asian Plastics Industry Report. *Additives for Polymers*. 2004; 5(12):10-12.

377. *Nanocomposites to 2011* - Market Research, Market Share, Market . Available from: http:// www.freedoniagroup.com /Nanocomposites. html - 26k. Access in: 10 March 2009.

378. Huang ZM, Zhang YZ, Kotaki M, Ramakrishnan S. A review on polymer nanofibers by electrospinning and their applications in nanocomposites. *Composites Science and Technology*. 2003; 63(15):2223-2253.

379. Ashby MF. *Materials selection in mechanical design*. Oxford: Pergamon Press; 1992.

380. Callister WD. *Materials science & engineering*: an introduction. New York: John Wiley & Sons, Inc.; 1997-2004.

381. *FEI Sponsors 2006 Safer Nano Conference*. Available from: http://www.cpd.ogi.edu/coursespecific.asp?pam=2003. Access in: 10 March 2009.

382. *Impacts of Manufactured Nanomaterials on Human Health and the Environment*. Available from: <http://es.epa.gov/ncer/rfa/current/2003_nano.html>. Access in: 20 Nov. 2008.